Fisheries and Oceans Canada | Pêches et Océans Canada
Science | Sciences

CSAS | **SCCS**

Canadian Science Advisory Secretariat | **Secrétariat canadien de consultation scientifique**

Research Document 2012/036 | **Document de recherche 2012/036**

Newfoundland and Labrador Region | **Région de Terre-Neuve et Labrador**

Bayesian Surplus Production modelling for American Plaice (*Hippoglossoides platessoides*)

Modèle bayésien de production excédentaire pour la plie canadienne (*Hippoglossoides platessoides*)

J.A. Bailey

Fisheries and Oceans Canada
Science Branch
PO Box 5667
St. John's NL A1C 5X1

This series documents the scientific basis for the evaluation of aquatic resources and ecosystems in Canada. As such, it addresses the issues of the day in the time frames required and the documents it contains are not intended as definitive statements on the subjects addressed but rather as progress reports on ongoing investigations.

La présente série documente les fondements scientifiques des évaluations des ressources et des écosystèmes aquatiques du Canada. Elle traite des problèmes courants selon les échéanciers dictés. Les documents qu'elle contient ne doivent pas être considérés comme des énoncés définitifs sur les sujets traités, mais plutôt comme des rapports d'étape sur les études en cours.

Research documents are produced in the official language in which they are provided to the Secretariat.

Les documents de recherche sont publiés dans la langue officielle utilisée dans le manuscrit envoyé au Secrétariat.

This document is available on the Internet at: www.dfo-mpo.gc.ca/csas-sccs

Ce document est disponible sur l'Internet à:

ISSN 1499-3848 (Printed / Imprimé)
ISSN 1919-5044 (Online / En ligne)
© Her Majesty the Queen in Right of Canada, 2012
© Sa Majesté la Reine du Chef du Canada, 2012

Canada

Correct citation for this publication:

Bailey, JA. 2012. Bayesian Surplus Production modelling for American Plaice (*Hippoglossoides platessoides*). DFO Can. Sci. Advis. Sec. Res. Doc. 2012/036 ii + 144 p.

ABSTRACT

Using a Bayesian modelling approach, a Schaefer surplus-production (SP) curve was fit to commercial landings and indices of population biomass of each of three populations of American Plaice (*Hippoglossoides platessoides*). The curve was then projected forward under various scenarios using Bayesian probability modeling in order to assess expected population trajectories over a biologically reasonable time frame for this species (48 years).

In order to examine the possibility that productivity may have changed between 1960-2009, several models were examined for each stock which divided the time series into 1 to 3 periods of productivity.

The paper describes the process and methodology used to fit a Bayesian Surplus Production Model to American Plaice biomass. Results indicated that such models could be useful in the Recovery Potential Assessment of American plaice. The results were consistent with stock assessments of these populations and showed that all three remain well below the estimated biomass level at the beginning of their respective time series.

RÉSUMÉ

En fonction d'une approche fondée sur le modèle bayésien, une courbe de production excédentaire Schaefer a été adaptée aux débarquements commerciaux et aux indices de la biomasse de chacune des trois populations de plie canadienne (*Hippoglossoides platessoides*). La courbe a ensuite fait l'objet de prévisions selon divers scénarios reposant sur un modèle bayésien de probabilité. On souhaitait ainsi évaluer les trajectoires prévue des populations sur une période raisonnable sur le plan biologique pour cette espèce (48 ans).

Afin d'étudier la possibilité que la productivité ait changé de 1960 à 2009, on a examiné plusieurs modèles pour chacun des stocks, ce qui a réparti les séries chronologiques en une à trois périodes de productivité.

Le document décrit le processus et la méthode utilisés pour adapter un modèle bayésien de production excédentaire à une biomasse de plie canadienne. Selon les résultats obtenus, de tels modèles pourraient s'avérer utiles dans l'évaluation du potentiel de rétablissement de la plie canadienne. Les résultats, qui concordaient avec l'évaluation des stocks pour ces populations, démontrent que les trois populations demeurent bien en deçà du niveau de biomasse estimé au début de leurs séries chronologiques respectives.

INTRODUCTION

In order to present a recovery action plan for a species at risk, it is essential to develop an understanding of the current state of the population, along with past dynamics. A working model covering the biomass trajectories of the past will be vital in forecasting future biomass trends and the effect of scenarios based on fishery mortality which might be implemented to aid recovery while minimizing socio-economic impacts.

The Committee On the Status of Endangered Wildlife In Canada (COSEWIC) has designated the American plaice (*Hippoglossoides platessoides)*, Newfoundland and Labrador DU (2009) as threatened. Fisheries and Oceans instituted a process r to assess the probability of recovery under different management scenarios. In order to aid in this process this paper explores the potential use of Bayesian state-space implementation of the Schaefer Surplus-Production (SP) models of the population dynamics of American Plaice for stocks in NAFO divisions 3LNO, 3Ps, and 2J3K using survey and catch data from 1960-2009. The aim is to determine an adequate model formulation for use in the recovery potential assessment for the Newfoundland designated unit of this species.

PART I: ANALYSIS OF POPULATION BIOMASS TRENDS USING BAYESIAN STATISTICS

The surplus production model works on the assumption that fish produce more than enough offspring for the population to be maintained. A maximal sustainable yield (MSY), then, would be the surplus quantity of fish that could theoretically be removed from that population without leading to a decline. In a SP model, the parameters for recruitment, growth, and natural mortality are combined in the single parameter *r*, the intrinsic rate of population growth.

The Schaefer (Schaefer 1954) form of a surplus production model used here is:

$$P_t=[P_{t-1}+ r\cdot P_{t-1}\ (1 - P_{t-1})- C_{t-1}/K]\cdot \eta_t$$

where P_{t-1} and C_{t-1} denote exploitable biomass (as a proportion of carrying capacity) and catch, respectively, for year *t-1* (Meyer and Millar, 1999a, 1999b). Carrying capacity, *K*, is the level of stock biomass at equilibrium prior to commencement of a fishery, *r* is the intrinsic rate of population growth, and ηt is a random variable describing stochasticity in the population dynamics (process error). The model utilizes biomass proportional to an estimate of *K* in order to aid mixing of the Markov Chain Monte Carlo (MCMC) samples and to help minimize autocorrelation between each state and *K* (Meyer and Millar, 1999a, 1999b).

An observation equation is used to relate the unobserved biomass, P_t, to the observations that have been made (*e.g.* through research vessel surveys), I_t.

$$I_t=q\cdot P_t\cdot \varepsilon_t$$

where *q* is the catchability parameter, P_t is an estimate of the biomass proportional to *K* at time *t*, and ε_t is observation error.

Biomass was modeled historically using estimated priors for *K*, *r*, and *q* (see Tables 1 and 2). Catch, stock biomass estimates from Canadian RV surveys, as well as data from European and

USSR surveys for 3LNO, were incorporated into the model as observed data with error. Models were examined for convergence and population parameters were forecast 48 years (3 generations) forward using scenarios of fishing mortality based on *F* for 3LNO, 3Ps, and 2J3K. These were:

1. No Fishing mortality, $F = 0$

2. Fishing mortality, *Fcurrent* = mean of F for past 3 years
   a. Fcurrent 3LNO = 0.048
   b. Fcurrent 3Ps = 0.0247
   c. Fcurrent 2J3K = 0.00055

3. For 3Ps, F was also increased incrementally until no increase in biomass was observed over the 50-year projection period
   a. F=0.1
   b. F=0.15

The freely available software, WinBUGS (v.1.4.3), was used for all Bayesian Markov Chain Monte Carlo with Gibbs sampling models. WinBUGS was called from R (v.2.12.1) using the R2WinBUGS package (http://cran.r-project.org). Convergence and model diagnostics were all run from R using the Bayesian Output Analysis (BOA) library. Models were run using 150000 iterations and a burn-in period of 50000 with thinning at 10 to reduce the possibility of autocorrelation within the series.

DATA

3LNO

The following data were used from NAFO divisions 3LNO.

(1) Landings – 1960-2009
(2) Canadian RV Survey Indices: Yankee Trawl – 1975-1982
(3) Canadian RV Survey Indices: Spring Converted Series – 1984-2009 (excluding 2006)
(4) Canadian RV Survey Indices: Fall Converted Series – 1990-2009 (excluding 2004)
(5) EU (Spain) RV Survey – 1997-2008
(6) USSR Surveys– 1972-1991

3Ps

The following data were used for NAFO division 3Ps. Surveys were conducted in the Spring.

(1) Landings – 1960-2009
(2) Canadian RV Survey Indices: Engels Trawl – 1972-1995
(3) Canadian RV Survey Indices: Campelen Trawl – 1996-2009

2J3K

The following data were used for NAFO divisions 2J3K. All surveys were conducted in the fall of the year, with most taking place in November-December.

(1) Landings – 1960-2009
(2) Canadian RV Survey Indices: Engels Trawl – 1978-1994
(3) Canadian RV Survey Indices: Campelen Trawl – 1995-2009

PRIOR DISTRIBUTIONS

In Bayesian modeling, priors are placed on each parameter in the model and these, combined with the dataset, produce posterior estimates. Bayesian modeling differs from likelihood modeling such that the likelihood values are weighted by prior probabilities to give posterior probabilities. One of the advantages of Bayes methods is the ability to use prior knowledge, if available, and to apply models to data-poor species. Concern arises only when posteriors rely heavily on the priors used (for example in very data-poor species where informative priors are used). In other words, the modeler is essentially providing the result, which will be the same as the input prior.

Non-informative priors were used for catchability (q) and for observation and process errors. Priors for observation error were limited to a lower bound equal to the coefficient of variation (CV) of each index. The upper bound was set at 3 times this CV (Swain et al. 2009). Vague priors were used for carrying capacity (K) and the intrinsic rate of population increase (r).

Typically, K is set to the stock biomass in the year prior to the onset of fishing (P_0; see Meyer and Millar 1999a). However, in the models used here, the stock biomass in 1960 was not assumed to be the virgin biomass. This may have been the case but, since it is impossible to know for certain, P_0 was allowed to vary between 0.5 and 1 (*i.e.* initial biomass was allowed to vary between $K/2$ and K).

A lognormal distribution for K was specified here with a mean of 900 ('000t) and a standard deviation of 1000 ('000t) for NAFO areas 3LNO. The mean was estimated at approximately twice the maximum stock estimation over the entire Canadian survey time series but was allowed to vary considerably. The upper and lower boundaries were established to encompass well beyond this estimate in order to reduce the possibility of limiting K to an erroneously low level. Although this prior contained an estimate for the value of K with a very wide distribution about the mean, it was limited such that the parameter could remain biologically plausible while covering a broad range of possible values. Similarly, K priors for 3Ps and 2J3K were both set at μ=300 ('000t) and std=1000 ('000t).

The prior for r was based on past work with this species and expert opinion. Like the priors for K, r was only vaguely informative, utilizing a mean with a very wide lognormal distribution about the mean. For all 3 stocks examined r was set at μ=0.15 and std=1 and restricted to values between 0.0001 and 3. All prior distributions are given in Tables 1 and 2.

RESULTS

Bayesian surplus production models (BSP) were fit to data from NAFO divisions 3LNO, 3Ps and 2J3K. Posterior results are provided in Tables 3-5 respectively, representing the 3 stocks examined.

3LNO is the largest, both in biomass and area covered. With respect to estimated carrying capacity, 3LNO is about 5x larger than the next largest stock (2J3K) and about 7-8x that of 3Ps (Table 6). This is similar to what has been observed in the RV surveys carried out in these areas, with estimated stock biomass of 3LNO being much larger than both 3Ps and 2J3K.

Being the largest and, hence, the most commercially valuable stock, it is also the stock upon which most research has been conducted. Age-based data is available for this stock, allowing a VPA to be run and used for comparison. In addition, surveys conducted by the EU and USSR vessels are available for this stock.

As mentioned, 3Ps has the lowest biomass of the 3 stocks examined here, with 2J3K slightly larger than 3Ps. The estimated parameters, then, for *K, BMSY, and MSY*, presented in Table 6 seem to be consistent with previous knowledge on these stocks. It has also been suggested (Morgan et al. 2002) that catch has not been the driving force in population decline, especially for 2J3K and that perhaps other sources of mortality (*i.e. M*, natural mortality) has played a large role in this decline. In the BSP model, natural mortality would be incorporated into *r*. This is reflected in the very low productivity parameter estimate (*r*) for this stock (2J3K - Table 6).

MODEL FIT

3LNO

The BSP model, based on data from 3LNO (1960-2009), is shown in figure 1. A fit obtained from a virtual population analysis (VPA) of age-based data (Biomass ages 5-15+) is provided for comparison. As shown, the surplus production model follows the VPA biomass estimates with relative accuracy, decreasing during the 60s and 70s, with a period of stability between the mid-70s and mid-80s, followed by a second period of decreasing biomass during the mid-80s, early 90s. Since the mid-90s there has been a slight tendency of a slow increase in biomass and this is picked up in both the VPA and the BSP. Note, however, that the current estimations of biomass for 3LNO are nowhere near historical levels.

Other parameters of interest are provided in figures 2-4 (B/B_{MSY},(B_{ratio}) and F/F_{MSY}, (F_{Ratio})). B_{ratio} is well below 1 and has been so since the early 70s. Figure 4 (F_{ratio}) indicates that F has been above F_{MSY} since the mid-60s, essentially since a fishery was begun for this species.

Posterior distributions of parameters are shown in figures 5-8 with values given in Table 3. As shown in the figures, prior distributions for each parameter were set using completely uninformative or vague distributions. This was done in an attempt to let the data from the surveys be used to estimate each of the parameters in the model.

Estimated catchabilities (*q*) for the Spring and Fall Campelen series, as well as the European Union series, appear to be similar between that calculated using a VPA and the posterior estimates for the same parameters in the BSP (Table 7).

Model fit to the survey data used are given in figures 9-13. Fit is shown with 95 % credible intervals. Standardized residuals, calculated by taking the difference between each observed data point and its value in each MCMC (Markov Chain Monte Carlo) sampling step are also given. In most cases, fit to the indices appears to be good. Some series with high variability (*e.g.* first few years of the Yankee series, figure 12; or USSR series, figure 13) are more difficult to fit and show wider credible intervals or points outside the 95 % credible intervals (Figure 13), but, in general, the model follows trends in the indices used.

Some of the tests used to evaluate convergence are given in figures 14-16 for 3 chosen parameters (*K, r,* and *Sigma*). Kernel density estimates of the posterior distributions, Gelman and Rubin shrink factors, sampler running means, and a time series plot of the sampled points in both chains are shown.

Kernel densities for posterior estimates for both chains are provided to examine how well estimates from each chain overlap one another. Gelman & Rubin shrink factors examine the reduction in bias in estimation. The shrink factor approaches 1 when the pooled within-chain variance dominates the between-chain variance. At that point, all chains have escaped the influence of their starting points. Both chains in the figure showing sampler running means are expected to converge from their starting points. The figures indicate acceptable convergence for the parameters shown.

3Ps

The BSP model, based on data from 3Ps (1960-2009), is shown in figure 17. No VPA has been performed on this stock and so could not be used for comparison. As shown, the surplus production model follows a similar trend to that seen in 3LNO, decreasing during the 60s and 70s, with a period of stability between the mid-70s and mid-80s, and even a slight increase in biomass during the early 80s. This is followed by a second period of decreasing biomass during the mid-80s and early 90s. Since the mid-90s there has been a slight tendency of a slow increase in biomass (Figure 17). Note again, however, that the current estimations of biomass for 3Ps are nowhere near historical levels.

Other parameters of interest are provided in figures 18-20 (B/B_{MSY}, F, F_{Ratio}). B_{ratio} is below 1 and has been since the early 70s. The series is marked by two increases in F (Figure 19), coinciding with the decreases in biomass shown in Figure 17. Figure 20 (F_{ratio}) indicates that F has been above F_{MSY} for much of the time series but especially during the periods when decreases in biomass are observed.

Posterior distributions of parameters are shown in figures 21-23 with values given in Table 4. As shown in the figures, prior distributions for each parameter were set using completely uninformative or vague distributions. This was done in an attempt to let the data from the surveys be used to estimate each of the parameters in the model.

Model fit to the survey data used are given in figures 24-25. Fit is shown with 95 % credible intervals and residuals are provided. In most cases, fit to the indices appears to be good. In the early years of the Engels series there was high variability between years and this is reflected in the corresponding residuals.

Some of the tests used to evaluate convergence are given in figures 26-28 for 3 chosen parameters (*K, r,* and *Sigma*). Kernel density estimates of the posterior distributions, Gelman and Rubin shrink factors, sampler running means, and a time series plot of the sampled points in both chains are shown.

Kernel densities for posterior estimates for both chains are provided to examine how well estimates from each chain overlap one another. Gelman and Rubin shrink factors, sampler running means, and a time series plot of the sampled points in both chains are shown. The figures indicate acceptable convergence for the parameters shown.

2J3K

The BSP model, based on data from 2J3K (1960-2009), is shown in figure 29. No VPA has been performed on this stock and so could not be used for comparison. As shown, the surplus production model follows a slightly different trend to that seen in 3LNO and 3Ps. There was a

steady decline in biomass from the mid-60s through to the 90s. This was followed by a low, yet stable, biomass estimate to the present time with very little increase or decrease. This stock shows very low production with an estimate of *r* at ~0.05 (Table 5). There has been no real increase since the start of the series in this stock and current estimates are not near the ~160kt estimated carrying capacity of this area.

Other parameters of interest are provided in figures 30-32 (B/B_{MSY}, F, F_{Ratio}). B_{ratio} is below 1 and has been since the early 70s (Figure 30). Figure 32 (F_{ratio}) indicates that F has been above F_{MSY} for much of the time series with high variation and uncertainty in the estimates.

Posterior distributions of parameters are shown in figures 33-35 with values given in Table 4. As shown in the figures, prior distributions for each parameter were set using completely uninformative or vague distributions. This was done in an attempt to let the data from the surveys be used to estimate each of the parameters in the model. Posterior estimates of the catchability parameters do not show perfectly defined peaks, and cover a relatively broad range of values. The posterior estimate of sigma also shows a bump in the distribution. It seems that for at least part of the series, the model is making use of low process error, giving the bump in the distribution on the low side. It should be pointed out that the survey series for this stock were much shorter than the other two stocks. Surveys started in 1978, while biomass was estimated based on landings back to 1960. This has undoubtedly caused more difficulty in estimating parameters in the model and has resulted in increased uncertainty, especially during the early part of the series.

Model fit to the survey data used are given in figures 36-37. Fit is shown with 95 % credible intervals and residuals are provided. It can be seen in the figures that the model follows the Engels and Campelen series relatively well, with no residuals outside the 95 % CI.

Some of the tests used to evaluate convergence are given in figures 38-40 for 3 chosen parameters (*K, r,* and *Sigma*). Kernel density estimates of the posterior distributions, Gelman and Rubin shrink factors, sampler running means, and a time series plot of the sampled points in both chains are shown. The issue mentioned above with the posterior distribution of sigma can be more easily seen in Figure 40a. One of the chains is showing a strong second peak on the kernel density estimate, likely an effect of the long period in the beginning of the model where estimates were being made without any observation data (*i.e.* the period between 1960-1977). The other convergence diagnostics shown all indicate convergence in this parameter.

PROJECTIONS

3LNO

Model projections using F=0 and $F_{current}$ are shown in figures 41-42. $F_{current}$ is calculated using the mean F of the latest 3 years (2007-2009) = 0.048. The figures appear to show promise for the future using current values of F with increases almost immediately in the projection period. However, the reader should be encouraged to interpret the figures carefully. The area encompassed by the dotted lines covers the 95 % credible interval, and a very broad range of possible values. After a very short period of time, the interval width increase at an almost exponential rate. The lower limit in these intervals takes as much as 15 years to reach ~50 ('000t), which is the current 2009 median estimate. In the same period of time, the upper limit expands from 57 ('000t) to 577('000t). We can, therefore, be 95 % certain that the actual biomass will be somewhere between 50,000t and 577,000t in 15 years, assuming we continue fishing at $F_{current}$ = 0.048. Viewing the estimates in this manner, one undoubtedly appreciates

that caution must be taken in using these projections for predicting biomass beyond a few years hence.

3Ps

Given the above for a data-rich stock such as that found in 3LNO, long-term predictions on stocks with less data will be more uncertain. Neither 3Ps nor 2J3K stocks have been surveyed to the same extent as 3LNO, nor do they have biomass estimates to compare this model to (*e.g.* VPA) as does 3LNO. A precautionary approach when predicting beyond a few years then, apply here as well. However, the BSP model is especially helpful under circumstances where there is little data and it is therefore that this kind of model was selected here. Age-based data on catch is not available for these stocks and so biomass estimates using a SP model and Bayesian methodology at least allows these estimates to be performed.

Figures 43-46 outline four scenarios of fisheries mortality for this stock: F=0, $F_{current}$= 0.0247, F=0.1, and F=0.15. All scenarios with the exception of F=0.15 (Figure 46) indicate growth in the median stock biomass; But, consider the caution above. All four scenarios show a lower 95 % credible interval near the current estimate or increasing slowly. At $F_{current}$, the lower 95 % credible interval increases at a slow rate during the next 50 years (to ~17,000t). However, we can make statements about the probability of events based on current estimates. For example, there is a 50 % probability that the stock will be between 19,500t and 47,000t (median 31,000t) in 10 years if fished at $F_{current}$. In order to be 95 % certain, the range must include 5,000t-128,000t. This illustrates the peril of using model estimates beyond even 5 years and further illustrates the need to regularly update the model with new data as yearly surveys are performed.

2J3K

It goes without saying that, for this stock, as for the others, care must be taken in interpreting the projection figures. Projections were made using F=0 and $F_{current}$, where $F_{current}$ in this stock is essentially the same as F=0, given that it is 0.00055. In both situations (Figures 47 and 48) there is a very slow increase in biomass with a sharp increase in the upper 95 % credible limit. There is much uncertainty in this stock and the model estimates very little increase, even at F=0. The dark mass of 5 % isolines near the x-axis indicates that the most likely scenario for the future, based on historical trends, is no increase in this population. There has been no increase observed in the stock since the early 90s. Based on past data, then, and erring on the side of caution, we cannot predict a significant increase in the stock over the near future.

PART II: MODELS INCORPORTAING MULTIPLE PERIODS WITH CHANGING POPULATION GROWTH RATES

The models described above use survey indices of biomass and landings data to estimate population growth rate, *r*, through a surplus production function. The posterior distribution of *r*, *K*, and *sigma* are then used to project future yearly biomass.

As mentioned, a VPA has been applied to the 3LNO stock of American plaice. It has been shown that the best fit for the VPA was obtained when natural mortality, *M*, was increased to 0.53 for all ages of plaice (from the normally-used value of 0.2) during the period 1989-1996 (Morgan and Brodie 2001). During this period there was a marked increase in mortality that could not be attributed to fishing. The same trend is seen in the biomass estimates here for 3LNO, but also for 3Ps and, to a lesser extent, 2J3K. Decreasing biomass for each stock is seen between the mid-80s to the mid-90s for 3LNO and 3Ps but simply continue a consistent decline starting at the beginning of the series in 2J3K (Figures 1, 17, and 29).

Prior to this decrease, there was a period of stability, and small increases in biomass even though landings were relatively high (Figures 1 and 17). It is suggested that these periods might possibly be confounding the posterior estimates for *r*, giving higher population growth rates than would be expected considering the relatively low period of production since the mid-90s. During this period there have been very low landings, yet biomass has not increased to the extent that would be expected. It may be possible under the Bayesian surplus-production framework, that, in order to fit the survey indices, the model is using judicious amounts of process error to force the biomass predictions to follow the survey indices. In other words, what has been observed through surveys since the mid 90s is not what would be expected given the rate of population growth predicted by the model.

In order to conduct a rudimentary 'check' of this, the last 10 years of the indices were removed from the series and the model run using these shortened series. The model was used to 'predict' the period between 2000-09 and predictions were compared to actual observations from the surveys. Figure 49 shows the results of this projection for 3LNO. It can be seen that biomass estimates deviate sharply from that predicted by the VPA Yet the VPA remains within the 95 % credible intervals of the prediction. The result is not surprising considering that, by removing 10 years of observation data where levels of productivity appear to be quite low, the estimate of *r* consequently increases. The median (and 95 % credible intervals) estimate of *r* using this model is 0.32 (0.15-0.60). This can be compared to 0.20 (0.11-0.31) when the posterior of *r* is predicted using the complete series. No surprise then that biomass increase is faster over this period. Figure 50 compares the "original" Campelen Spring index to that predicted by the SP model. The prediction is higher than what has been observed and credible intervals expand immediately as the values are predicted. The actual value still is encompassed by the 95 % credible intervals, which is what should be expected, yet the medians are considerably higher.

Removing data at the end of the series may give some indication of whether the model is forecasting as should be expected. However, because simply removing data also changes the posterior estimates of all other parameters in the model, including *r*, other models must be examined that include separate periods of productivity, allowing for suspected changes and estimating current productivity based on recent data.

As mentioned, using the VPA, higher than normal mortality was assumed to have occurred between 1989-1996. Thus it seems appropriate that the same period of increased natural

mortality be incorporated and assessed in new SP models evaluating changes in productivity levels. Since, in a SP model, the parameters for recruitment, growth, and natural mortality are combined in the single parameter *r*, the intrinsic rate of population growth, the time series was divided to include 1, 2 and 3 periods of productivity where *r* was estimated separately for each period. Four different models were run for the stock in 3LNO using several permutations on this theme.

(1) One period with one estimate of *r* based on data between 1960-2009 (*i.e.* the model outlined above)
(2) Two periods with two estimates of *r*, where *r1* is based on data between 1960-1988; and *r2* is based on data between 1989-2009.
(3) Three periods with two estimates of *r*, where *r1* is based on data between 1960-1988 and 1997-2009; and *r2* is based on data between 1989-1996.
(4) Three periods with three estimates of *r*, where *r1* is based on data between 1960-1988, *r2* is based on data between 1989-1996, and *r3* is based on data between 1997-2009.

Similarly, two separate models were run for each of the stocks in 3Ps and 2J3K. For 3Ps, the models examined included:

(1) One period with one estimate of *r* based on data between 1960-2009
(2) Two periods with two estimates of *r*, where *r1* is based on data between 1960-1984; and *r2* is based on data between 1985-2009.

For 2J3K, the models examined were:

(1) One period with one estimate of *r* based on data between 1960-2009
(2) Two periods with two estimates of *r*, where *r1* is based on data between 1960-1984; and *r2* is based on data between 1985-2009.

Cut-offs for the periods used for the 3Ps and 2J3K stocks were chosen through discussion with personnel at DFO and through an examination of the biomass survey estimates.

Each of these models is presented briefly here for comparative purposes in order to assess which is most appropriate for biomass projections.

MODELING

As described previously, biomass was modeled historically using estimated priors for *K*, *r* (and where appropriate *r1*, *r2*, and *r3*), and *q* (catchability coefficient) (see Tables 1 and 2). Catch, stock biomass estimates from Canadian RV surveys, as well as data from European and USSR surveys (for 3LNO), were incorporated into the models as observed data with error.

The freely available software, WinBUGS (v.1.4.3), was used for all Bayesian Markov Chain Monte Carlo with Gibbs sampling models. WinBUGS was called from R (v.2.10.1) using the R2WinBUGS package. Convergence and model diagnostics were also run from R using the Bayesian Output Analysis (BOA) library. Models were run using 150000 iterations and a burn-in period of 50000 with thinning at 10 to reduce the possibility of autocorrelation within the series.

PRIOR DISTRIBUTIONS

As above, non-informative priors were used for catchabilities and for observation and process errors. Vague priors were used for carrying capacity (*K*) and the intrinsic rate of population increase (*r*).

The prior for *K* was set with a slightly narrower distribution but can still be considered considerably vague. For 3LNO, *K* was described as a lognormal distribution with a mean of 900 ('000t) and a standard deviation of 400 ('000t). For 3Ps and 2J3K, *K* were both set at μ=300 ('000t) and std=400 ('000t). For all 3 stocks examined, and where one period of productivity was used in the model, *r* was set at μ=0.15 and std=1 and was restricted to values between 0.0001 and 3. Where more than one period of productivity was used, r2 and r3 were set at μ=0.1 and std=1 as it was assumed that productivity was lower in more recent periods. Prior distributions are given in Tables 1 and 2.

RESULTS

Bayesian surplus production models (BSP) were fit to data from NAFO divisions 3LNO, 3Ps and 2J3K. Posterior results are provided in Tables 8-10 respectively for each model, representing the 3 stocks examined.

Concentration will be placed mostly on 3LNO. As mentioned, this is the population where the most data is available and where a comparison is available for an accepted population model (VPA). The 4 models presented here all show similar fit with respect to the indices used (see figures 60-64), and so it is suggested that the choice of process or model used to describe the 3LNO stock will be based on what is believed to have happened in the population. Either of the models presented, it can be argued, fit the historical data, and while one can use the Deviance Information Criteria (DIC) alone to "select" the model, it is advisable to include our understanding of the species/population in making a final decision. This should be kept in mind when reading the brief description of the results for each model below.

3LNO – Models 1-4

The BSP model, based on data from 3LNO (1960-2009), is shown in figures 51a-d corresponding to each of the 4 models. A fit obtained from a virtual population analysis (VPA) of age-based data (Biomass ages 5-15+) is provided for comparison. As shown, the surplus production model follows the VPA biomass estimates with relative accuracy, decreasing during the 60s and 70s, with a period of stability between the mid-70s and mid-80s, followed by a second period of decreasing biomass during the mid-80s, early 90s. Since the mid-90s there has been a tendency to a slow increase in biomass and this is picked up in both the VPA and the BSP (Figures 1a-d). Note, however, that the current estimations of biomass for 3LNO are nowhere near historical levels.

Figure 52a-d (F_{ratio}) indicates that F has been above F_{MSY} for much of the time series since the mid-60s, essentially since a fishery was begun for this species. In all models, the period between 1989-1996 shows obvious increased levels of estimated fishing mortality. Models that separate out this period (especially models 2-3) show more uncertainty in this estimate of fishing mortality, indicated by the large bounds on the credible intervals. At the same time, these models estimate extremely low levels of productivity for this period, and are thereby likely including higher levels of natural mortality in the estimates of *r*.

Posterior distributions for *sigma*, deviance, *K*, and *r* are shown in figures 53-56 with values given in Table 8. As shown in the figures, prior distributions for each parameter were set using completely uninformative or vague distributions. This was done in an attempt to let the data from the surveys be used to estimate each of the parameters in the model.

Model fit to the survey data used are given in figures 60-64 for Models 2 and 3. Fit for models 1 and 4 look the same and, with the aim of keeping the number of figures down, they are not shown here. Suffice to say, however, that they showed very similar patterns. Fit is shown with 95 % credible intervals. Standardized residuals, calculated by taking the difference between each observed data point and its value in each MCMC (Markov Chain Monte Carlo) sampling step are also given. Fit is good when compared to the observed data and residuals show no real pattern. Most residuals fall within 95 % confidence intervals with only a single point outside in some cases (*e.g.* first years of the Yankee, EU and USSR series, figures 62-64).

Some of the tests used to evaluate convergence are given in figures 65-67. For comparison, the figures are provided for *K* in each model. Kernel density estimates of the posterior distributions, Gelman and Rubin shrink factors, and sampler running means in both chains are shown. The figures indicate acceptable convergence for the parameters shown.

3LNO – Model 1 (One period, One estimate of productivity, *r1*)

As mentioned above, this model fits the available data and corresponds to what would be expected based on VPA estimates and what is known about this population. Model 1 has the lowest DIC of the 4 tested here at 929.8 but also includes the least number of parameter estimates (*i.e.* one estimate of *r, MSY* and *FMSY*). In accepting this model one would be suggesting that the level of productivity has not changed in the population throughout the time series between 1960-2009, and that this level of population productivity will not change in the foreseeable future. Projections would be based on a model utilizing a carrying capacity of 784.7 (472.0-1485.0) (median ('000t) and 95 % credible intervals) and an *r* of 0.20 (0.11-0.31).

3LNO – Model 2 (Two periods, Two estimates of productivity, *r1* & *r2*)

Again, as mentioned above, this model fits the available data and corresponds to what would be expected based on the VPA. Model 2 has the next lowest DIC of the 4 tested here at 941.7. In accepting this model one would be suggesting that the level of productivity has changed since the early part of this time series. There was higher productivity during the period including years 1960-1988, when something happened in the population and productivity dropped and has remained low since 1989. It is not within the capacity of this modeling exercise to speculate on what may have caused this drop in productivity or whether or not this productivity will increase to historical levels. Projections would be based on a model utilizing a carrying capacity of 681.0 (514.0-1168.0) (median ('000t) and 95 % credible intervals) and an *r* of 0.12 (0.07-0.18).

3LNO – Model 3 (Three periods, Two estimates of productivity, *r1* & *r2*)

As for the others, this model fits the available data and corresponds to what would be expected based on the VPA. Model 3 has the third lowest DIC of the 4 tested here at 944.6, very similar to Model 2. In accepting this model one would be suggesting that the level of productivity changed during a short period between 1989-1996. During this period, productivity dropped as there was a large increase in natural mortality, possibly caused by abnormally cold water in the area (Morgan and Brodie 2001). This model attempts to remove this period from the estimation of population productivity by using the periods before (1960-1988) and after (1997-2009) to

estimate the *r* with which projection will be made. However, by excluding this "anomaly" from the parameter estimate, we are also suggesting that the event will not recur within the prediction period. Projections using this model would be based on a carrying capacity of 830.0 (536.2-1458.0) (median ('000t) and 95 % credible intervals) and an *r* of 0.19 (0.12-0.30). This productivity estimate is, in fact, very similar to the one for model 1 (0.20 (0.11-0.31)).

3LNO – Model 4 (One Three periods, Three estimates of productivity, *r1,r2,r3*)

This model fits the available data and corresponds to what would be expected based on the VPA. Model 4 has the highest DIC of the 4 tested here at 950.6, but also contains the most number of parameter estimates. In accepting this model one would be suggesting that the level of productivity has changed several times between 1960-2009. There was a period of relatively high productivity between 1960-1988, followed by a short period of high levels of natural mortality and a correspondingly low level of productivity (1989-1996), and finally a third period (1997-2009) where productivity has recovered somewhat, but not necessarily to historical levels. This model attempts to estimate current productivity based on the series between 1997-2009 but utilizes previous historical data to estimate all other parameters in the model (*e.g. K, indices fits, q, etc.*). This model is slightly different than Model 3, however, in that it does not utilize the data between 1960-1988 in the parameter estimate of the *r* which will be used for projection. Here we are suggesting that *r* has changed and that this change is random and cannot be predicted if/when it will recur. Projection, then, is based on a carrying capacity of 604.3 (503.9-1047.0) (median ('000t) and 95 % credible intervals) and an *r* of 0.15 (0.056-0.23).

3Ps

The BSP model results for both models based on data from area 3Ps (1960-2009), is shown in figure 68a-b. As illustrated, biomass estimates from the surplus production model shows a similar trend to that seen in 3LNO. Biomass decreased during the late 60s and early 70s, and was followed by a period of stability between and slight increase in biomass during the mid-70s to mid-80s. This was, in turn, followed by a decrease in biomass during from the mid-80s to early 90s where population has remained relatively low, but has shown a very slow increase since this time. Again, as in 3LNO, it should be pointed out that the rate of increase since the early 90s has been very slow and that current estimates place the population at levels well-below historical estimates.

Figure 69a-b (F_{ratio}) indicates that F has been above F_{MSY} for the periods where large decreases in biomass estimates are seen. For Model 2, there is more uncertainty (indicated by larger 95 % credible intervals) in estimates of the F_{ratio} since the mid 80s. This may suggest that F alone may not be solely responsible for the trends seen in the population during this period.

Posterior distributions for *sigma*, deviance, *K*, and *r* are shown in figures 70-74 with values given in Table 9. As shown in the figures, prior distributions for each parameter were set using completely uninformative or semi-informative distributions. Most of the distributions for both models, while giving different values (*e.g. K* in Figure 72), look smooth. There seems to be a broader utilization of process error in Model 1 (Figure 70). The posterior distribution for *r1* in Model 2 (Figure 74) shows a somewhat flat, irregular peak. The median of this distribution is given as 0.78, a value highly unlikely or near impossible for this species.

Model fit to the survey data used are given in figures 75-76 for Models 1 and 2 and is shown with 95 % credible intervals. Standardized residuals, calculated by taking the difference between each observed data point and its value in each MCMC (Markov Chain Monte Carlo)

sampling step are also given. Fit is very good when compared to the observed data and residuals show no real pattern. Most residuals fall within the 95 % confidence intervals with only a single point outside in the Engels series of Model 1.

Some of the tests used to evaluate convergence are given in figures 77-79. For comparison, the figures are provided for *K* in each model. Kernel density estimates of the posterior distributions, Gelman and Rubin shrink factors, and sampler running means in both chains are shown. The figures indicate acceptable convergence for the parameters shown.

3Ps – Model 1 (One period, One estimate of productivity, *r1*)

As mentioned above, both models fit the available data. The DIC for this model is lower than that found for Model 2 but, as with some of the models mentioned above for the 3LNO stock, Model 2 has more parameters to estimate and so one would expect a slightly higher DIC. As with Model 1 for the 3LNO stock, in accepting this model one would be suggesting that the level of productivity has not changed in the population throughout the time series between 1960-2009, and that this level of population productivity will not change in the foreseeable future. Perhaps fluctuations have occurred in the past but the mean productivity level remains the same. Projections would be based on a model utilizing a carrying capacity of 117.4 (100.6-322.6) (median ('000t) and 95 % credible intervals). Productivity, *r*, would be at 0.15 (0.07-0.28).

3Ps – Model 2 (Two periods, Two estimates of productivity, *r1* & *r2*)

The parameter estimate for *Sigma* has a slightly narrower distribution than that seen in Model 1. Model 2 also has a lower DIC (277) than Model 1 (285). However, the posterior estimate for *r1* in model 2 is extremely high and some would say impossible for this species. If this model were accepted, one would be suggesting that the level of productivity has changed since the early part of this time series. The change occurred sometime in the mid-80s. Again, it is not within the capacity of this modeling exercise to speculate on what may have caused this drop in productivity, or whether or not this productivity will increase to historical levels. Using this model, carrying capacity is estimated to be much lower at 37.94 (26.36-74.44) (median ('000t) and 95 % credible intervals). Productivity is, however, slightly higher than Model 1 at 0.17 (0.062-0.31).

2J3K

The BSP models, based on data from 2J3K (1960-2009), are shown in figures 80a-b. No VPA was performed on this stock and so could not be used for comparison. As shown, the surplus production model follows a slightly different trend to that seen in 3LNO and 3Ps. There was a steady decline in biomass from the mid-60s to the early 90s. This was followed by a low, yet stable, biomass estimate since the early 90s to the present time. This stock shows very low production with an estimate of *r* at ~0.05 (Table 10) for Model 1 (entire series, 1960-2009). There has been no real increase since the mid-90s in this stock and current estimates are not near the estimated carrying capacity of this area found using Model 1 (159kt) or Model 2 (151kt).

Figure 81a-b (F_{ratio}) indicates an F_{ratio} above 1 for much of the series but with large variation and wide credible intervals. For Model 2, there is more uncertainty in estimates of the F_{ratio}, especially during the period when other stocks showed significant declines (*i.e.* 1989-1996). This may again suggest that F alone may not be solely responsible for the trends seen in the population during this period.

Posterior distributions for *sigma*, deviance, *K*, and *r* are shown in figures 82-86 with values given in Table 10. As shown in the figures, prior distributions for each parameter were set using completely uninformative or vague distributions. The estimate for *sigma* in Model 1 shows a bump on the left of the distribution, indicating that the model is using a slightly wider range of process error. The bump in the distribution is seen to a much lesser extent in Model 2 and may indicate the difficulty with using consistent process error across the entire time series.

Model fit to the survey data used are given in figures 87-88 for Models 1 and 2 and is shown with 95 % credible intervals. Standardized residuals, calculated by taking the difference between each observed data point and its value in each MCMC sampling step are also given. Fit is very good when compared to the observed data and residuals lie on the line about 0. No pattern is seen for either of the models.

Some of the tests used to evaluate convergence are given in figures 89-91. For comparison, the figures are provided for *K* in each model. Kernel density estimates of the posterior distributions, Gelman and Rubin shrink factors, and sampler running means in both chains are shown. Both chains in the figure showing sampler running means are expected to converge from their starting points. The figures indicate convergence for both models.

2J3K – Model 1 (One period, One estimate of productivity, *r1*)

As mentioned above, both models fit the available data. The DIC for Model 1 (247) is only slightly higher than that found for Model 2 (242). As with Model 1 for 3LNO and 3Ps stocks, in accepting this model one would be suggesting that the level of productivity may have varied but has not permanently changed in the population throughout the time series between 1960-2009, and will not change in the foreseeable future. Projections would be based on a model utilizing a carrying capacity of 159.0 (102.0-712.0) (median ('000t) and 95 % credible intervals) and productivity, *r*, of 0.053 (0.013-0.15).

2J3K – Model 2 (Two periods, Two estimates of productivity, *r1* & *r2*)

Again, as mentioned above, this model fits the available data. In accepting this model one would be suggesting that the level of productivity has changed since the early part of this time series. There was higher productivity during the period including years 1960-1984 (r=0.09), when something happened in the population and productivity dropped slightly and has remained low since 1985 (r=0.046). Projections would be based on a model utilizing a carrying capacity of 151.90 (101.60-685.5) (median ('000t) and 95 % credible intervals) and an *r* of 0.046 (0.009-0.15).

PROJECTIONS

Projections were made using two scenarios for fishing mortality based on F=0 and F=0.1. These are provided to illustrate what the projections might look like for the chosen model for each stock.

3LNO

Model projections using the scenarios outlined above are shown in figures 92a-d and 93a-d. Models 1 and 3 provide similar projections. Recall that Model 1 is projecting using an estimation of *r* based on the entire time series (*r*=0.20) while Model 3 uses an estimate of *r* from the first (1960-1988) and third (1997-2009) periods (*r*=0.19). The posteriors for *r* in both of these models are very similar and so it is not surprising that the projections resemble one another.

As expected, projections using Model 2 (*r*=0.12) and Model 4 (*r*=0.15) are also similar and projected biomass increase is slower than that seen for Models 1 and 3 above. There is less uncertainty in these projections, indicated by the 95 % credible intervals, compared to Models 1 or 3.

3Ps

Model projections using the scenarios outlined above are shown in figures 94a-b and 95a-b. Model 1 is projecting using an estimation of *r* based on the entire time series (*r*=0.15) while Model 2 uses an estimate of *r* from the second period in the series (1985-2009) (*r*=0.17). The differences in population growth rate, then, are a little surprising at first considering the relatively small difference in the posterior for *r* upon which projection is based. The projection makes more sense when one examines the amount of error around the estimate. There is more uncertainty in the projections for Model 1 than Model 2. Since the width of the 95 % credible intervals is increasing at a more rapid rate in Model 1 than in Model 2, the median of these intervals follows and increases accordingly. A further explanation may be that this slight increase in population growth rate is enough to get the population some sort of threshold to allow more rapid growth. Following the 'isolines' on the figures, however, the highest probability (area where lines are most densely situated on the figure) for each model trajectory is more similar. This once more illustrates the need for careful interpretation of long-term projections.

2J3K

Model projections using the scenarios outlined above are shown in figures 96a-b and 97a-b. Biomass increase is extremely slow in both models. Model 1 is projecting using an estimation of *r* based on the entire time series (*r*=0.053) while Model 2 uses an estimate of *r* from the second period in the series (1985-2009) (*r*=0.046). The differences in population growth rate, then, are not surprising considering the relatively insignificant difference in the posterior for *r* from each model. Model 1 shows a very slightly increased rate of population growth compared to that expected from Model 2. Once fishing mortality is added to the predictions for each model at F=0.1, we can be fairly certain that the population will not increase and that it will most likely fall to near 0 biomass. Due to the low level of productivity, even at an extremely low level of F, ($F_{current}$=0.00055), this population shows almost no increase in biomass (Figure 48).

MODAL SELECTION

As has been pointed out, all models tested here fit the data similarly. None of the models utilizing multiple periods were shown to be significantly better than models using the entire time series to estimate a posterior for *r*, nor could they provide new insight into what may have happened or will likely happen with respect to population biomass trajectory. To the contrary for 3Ps, the estimates of *r*, especially for period 1, are not consistent with what is possible for this species.

In order to suggest that levels of productivity have changed in the time series (at least for the periods chosen here), significant evidence is needed leading to this conclusion. The models tested above do not seem to provide this evidence. In most cases the estimates of productivity, while different for each period and model, overlap at their 95 % intervals suggesting that they are not entirely different from one another. Without the evidence to suggest otherwise, the law of parsimony prevails and the model utilizing the least number of parameter estimates should be used.

REFERENCES

Meyer, R. and Millar, R.B. 1999a. BUGS in Bayesian stock assessments. Can. J. Fish. Aquat. Sci. 56: 1078-1086.

Meyer, R. and Millar, R.B.. 1999b. Bayesian stock assessment using a state–space implementation of the delay difference model. Can. J. Fish. Aquat. Sci. 56: 37-52.

Morgan, M.J. and Brodie, W.B. 2001. An exploration of virtual population analyses for Divisions 3LNO American plaice. NAFO. SCR. Doc. 01/04.

Morgan, M.J., Brodie, W.B., and Kulka, D.W. 2002. Was over-exploitation the cause of the decline of the American plaice stock off Labrador and northeast Newfoundland. Fish. Research 57: 39-49.

Schaefer, M.B. 1954. Some aspects of the dynamics of populations important to the management of commercial marine fisheries. Bull. Int..-Am. Trop. Tuna Com. 1: *25-56.*

Swain, D.P., Jonsen, I.D., Simon, J.E., and Myers, R.A. 2009. Assessing threats to stage-structured state–space models: mortality trends in skate Populations. Ecological Applications 19:1347–1364.

Appendix 1. Sample WinBUGS script for American Plaice surplus production model

3Ps

```
model
{
# Prior for intrinsic rate of increase(r),
r ~ dlnorm(-3.81,0.262)I(0.0001,3)

# prior distribution of q's
q.eng~dunif(0,20)
q.cam~dunif(0,20)

# prior distribution of K
K~dlnorm(4.46,0.40)I(100,3000)

# Prior for process noise, sigma
sigma ~ dunif(0,10)
isigma2 <- pow(sigma, -2)

# Prior for observation errors, tau.
tau.eng~dunif(0.79,2.38)
itau2.eng <- pow(tau.eng, -2)
tau.cam~dunif(0.39,1.17)
itau2.cam <- pow(tau.cam, -2)

# Prior for initial population size as proportion of K, P[1]
Pin~dunif(0.1, 1)
Pm[1] <- log(Pin)
P[1] ~ dlnorm(Pm[1], isigma2)I(0.001,5)

# State equation - SP Model.
for (t in 2:(N))  {
Pm[t] <- log(max(P[t-1] + r*P[t-1]*(1-P[t-1]) - L[t-1]/K, 0.0001))
P[t] ~ dlnorm(Pm[t], isigma2)I(0.001,5)
}

# Observation equations
for (t in 1:(24)) {
Iengm[t] <- log(q.eng*K * P[t])
Ieng[t] ~ dlnorm(Iengm[t], itau2.eng)
}
for (t in 25: N) {
Icamm[t] <- log(q.cam*K * P[t])
Icam[t] ~ dlnorm(Icamm[t], itau2.cam)
}
```

```
# Output. Using the proportion and K to estimate biomass, B.
for(t in 1:N) {
B[t] <- P[t] * K
F[t] <- L[t]/B[t]
Fratio[t] <- F[t]/FMSY
Bratio[t] <- B[t]/BMSY
}

# further management parameters and predictions:
MSY <- r*K/4
FMSY<-r/2
BMSY<-K/2

#generate replicate data sets
for (i in 1:24){
        leng.rep[i] ~ dlnorm(lengm[i],itau2.eng)
        #residuals of log values of replicate data
        res.leng.rep[i] <- log(leng.rep[i])-log(leng[i])
        #prob. of a more extreme observation
        p.smallerleng[i] <- step(leng[i]-leng.rep[i])
}
for (i in 25:N){
        lcam.rep[i] ~ dlnorm(lcamm[i],itau2.cam)
        #residuals of log values of replicate data
        res.lcam.rep[i] <- log(lcam.rep[i])-log(lcam[i])
        #prob. of a more extreme observation
        p.smallerlcam[i] <- step(lcam[i]-lcam.rep[i])
}} ## END

#Inits
list(list(P=c(0.08, 0.08, 0.08, 0.08, 0.08, 0.08, 0.08, 0.08, 0.08, 0.08, 0.08, 0.08, 0.08, 0.08, 0.03, 0.03,
0.005, 0.09, 0.02, 0.01, 0.02, 0.09, 0.07, 0.10, 0.11, 0.06, 0.16, 0.08, 0.08, 0.07, 0.04, 0.01, 0.03,
0.02, 0.01, 0.01, 0.01, 0.03, 0.02, 0.04, 0.04, 0.05, 0.05, 0.04, 0.04, 0.04, 0.06, 0.06, 0.06, 0.09,
0.04), r=0.3, K=400, logq.eng=0.001, logq.cam=0.7, sigma=0.1, tau.eng=1, tau.cam=0.6),
list(P=c(0.17, 0.17, 0.17, 0.17, 0.17, 0.17, 0.17, 0.17, 0.17, 0.17, 0.17, 0.17, 0.17, 0.17, 0.07, 0.07,
0.01, 0.19, 0.05, 0.02, 0.04, 0.18, 0.13, 0.20, 0.23, 0.11, 0.32, 0.15, 0.17, 0.14, 0.09, 0.03, 0.06,
0.03, 0.02, 0.02, 0.02, 0.06, 0.04, 0.07, 0.07, 0.11, 0.09, 0.08, 0.09, 0.07, 0.12, 0.12, 0.11, 0.18,
0.07), r=0.1, K=200, logq.eng=0.005, logq.cam=1, sigma=0.1, tau.eng=0.8, tau.cam=0.4))
```

Table 1: Priors for parameters used in the 3LNO surplus production model.

NAFO	Parameter	Description	Prior Distribution
3LNO	K	Carrying Capacity	LN (μ=900kt, std=1000kt)
	r (r1)	Population growth rate (Models 1-4)	LN (μ=0.15, std=1)
	r2	Population growth rate (Models 2-4)	LN (μ=0.10, std=1)
	r3	Population growth rate (Models 3-4)	LN (μ=0.10, std=1)
	q.s.cam	Catchability, Canadian Spring Campelen Trawl Series	U(0,10)
	q.ynke	Catchability, Canadian Yankee Trawl Series	U(0,10)
	q.f.cam	Catchability, Canadian Fall Campelen Trawl Series	U(0,10)
	q.eu	Catchability, European Union Series	U(0,10)
	q.ussr	Catchability, USSR Series	U(0,10)
	Sigma	Process error	U(0,10)
	tau.ynke	Observation error, Canadian Yankee Trawl	U(0,0.77)
	tau.s.cam	Observation error, Canadian Spring Campelen Trawl	U(0,1.2)
	tau.f.cam	Observation error, Canadian Fall Campelen Trawl	U(0,0.88)
	tau.eu	Observation error, European Union Series	U(0,1.55)
	tau.ussr	Observation error, USSR Series	U(0,2.13)

Table 2: Priors for parameters used in surplus production models for 3Ps and 2J3K.

NAFO	Parameter	Description	Prior Distribution
3Ps	K	Carrying Capacity	LN (μ=300kt, std=1000kt)
	r (r1)	Population growth rate (Model 1-2)	LN (μ=0.15, std=1)
	r2	Population growth rate (Model 2)	LN (μ=0.10, std=1)
	q.eng	Catchability, Canadian Engels Trawl Series	U(0,10)
	q.cam	Catchability, Canadian Campelen Trawl Series	U (0,10)
	sigma	Process error	U (0,10)
	tau.eng	Observation error, Canadian Engels Trawl	U (0.79,2.38)
	tau.cam	Observation error, Canadian Campelen Trawl	U (0.39,1.17)
2J3K	K	Carrying Capacity	LN (μ=300kt, std=1000kt)
	r (r1)	Population growth rate (Model 1-2)	LN (μ=0.25, std=0.32)
	r2	Population growth rate (Model 2)	LN (μ=0.10, std=1)
	q.eng	Catchability, Canadian Engels Trawl Series	U (0,10)
	q.cam	Catchability, Canadian Campelen Trawl Series	U (0,10)
	sigma	Process error	U (0,10)
	tau.eng	Observation error, Canadian Engels Trawl	U (0.68,2.03)
	tau.cam	Observation error, Canadian Campelen Trawl	U (0.41,1.24)

Table 3: Summary of parameter estimates using a Bayesian surplus production model for 3LNO American plaice.

NAFO Div.	Parameter	Description	Posterior (median, 95 % CI)
	K	Carrying Capacity	784.7 (472.0-1485.0)
	r	Population growth rate	0.20 (0.11-0.31)
	logq.ynke	Log Catchability, Canadian Yankee	0.098 (0.004-0.38)
	logq.s.cam	Log Catchability, Canadian Spring Campelen	1.54 (1.22-1.83)
	logq.f.cam	Log Catchability, Canadian Fall Campelen	1.99 (1.67-2.29)
	logq.eu	Log Catchability, European Union	1.15 (0.73-1.56)
	logq.ussr	Log Catchability, USSR	1.53 (1.26-1.82)
	sigma	Process error	0.16 (0.042-0.26)
	tau.ynke	Observation error, Canadian Yankee	0.15 (0.01-0.44)
	tau.s.cam	Observation error, Canadian Spring Campelen	0.25 (0.17-0.36)
	tau.f.cam	Observation error, Canadian Fall Campelen	0.11 (0.028-0.20)
	tau.eu	Observation error, European Union Series	0.46 (0.31-0.78)
	tau.ussr	Observation error, USSR Series	0.35 (0.24-0.55)
	MSY	Maximum Sustainable Yield	38.86 (22.84-65.70)
	FMSY	F at MSY	0.098 (0.056-0.16)
	BMSY	Biomass at Maximum Sustainable Yield	392.3 (236.0-742.4)
	DIC	Deviance Information Criteria	929.8

Table 4: Summary of parameter estimates using a Bayesian surplus production model for 3Ps American plaice.

NAFO Div.	Parameter	Description	Posterior (median, 95 % CI)
3Ps	K	Carrying Capacity	117.4 (100.6-322.6)
	r	Population growth rate	0.15 (0.07-0.28)
	logq.eng	Catchability, Canadian Engels Trawl	0.09 (0.003-0.40)
	logq.cam	Catchability, Canadian Campelen Trawl	0.57 (0.034-1.45)
	sigma	Process error	0.16 (0.007-0.46)
	tau.eng	Observation error, Canadian Engels Trawl	0.95 (0.80-1.36)
	tau.cam	Observation error, Canadian Campelen Trawl	0.44 (0.39-0.67)
	MSY	Maximum Sustainable Yield	4.55 (2.52-13.18)
	FMSY	F at MSY	0.07 (0.04-0.14)
	BMSY	Biomass at Maximum Sustainable Yield	58.69 (50.31-161.31)
	DIC	Deviance Information Criteria	285

Table 5: Summary of parameter estimates using a Bayesian surplus production model for 2J3K American plaice.

NAFO Div.	Parameter	Description	Posterior (median, 95 % CI)
2J3K	K	Carrying Capacity	159.0 (102.0-712.0)
	r	Population growth rate	0.053 (0.013-0.15)
	logq.eng	Catchability, Canadian Engels Trawl	1.38 (0.15-2.08)
	logq.cam	Catchability, Canadian Campelen Trawl	1.95 (0.38-3.23)
	sigma	Process error	0.21 (0.12-0.48)
	tau.eng	Observation error, Canadian Engels Trawl	0.73 (0.68-0.97)
	tau.cam	Observation error, Canadian Campelen Trawl	0.46 (0.41-0.68)
	MSY	Maximum Sustaniable Yield	2.25 (0.56-11.1)
	FMSY	F at MSY	0.026 (0.006-0.075)
	BMSY	Biomass at Maximum Sustainable Yield	79.70 (51.20-356.00)
	DIC	Deviance Information Criteria	247

Table 6: Comparison of some parameter estimates (median and 95 % credible intervals) using a Bayesian surplus production model for American plaice.

Parameter	3LNO	3Ps	2J3K
K	784.7 (472.0-1485.0)	117.4 (100.6-322.6)	159.0 (102.0-712.0)
r	0.20 (0.11-0.31)	0.15 (0.07-0.28)	0.053 (0.013-0.15)
MSY	38.86 (22.84-65.70)	4.55 (2.52-13.18)	2.25 (0.56-11.1)
FMSY	0.098 (0.056-0.16)	0.07 (0.04-0.14)	0.026 (0.006-0.075)
BMSY	392.3 (236.0-742.4)	58.69 (50.31-161.31)	79.70 (51.20-356.00)

Table 7: Estimates of catchability (q) for several series used in a virtual population analysis (VPA) and a Bayesian surplus production model (BSP) for American plaice. The ranges of VPA estimates for catchability are provided.

Catchability (q)	BSP (median, 95 % Credible Intervals)	VPA (Range)
Spring Campelen	4.48 (2.32-7.64)	5.94 - 9.51
Fall Campelen q	6.69 (3.67-11.43)	3.18 - 6.11
EU q	2.72 (1.42-5.21)	1.85 - 5.02

Table 8: Summary of posterior parameter estimates using a Bayesian surplus production model for 3LNO American plaice.

Parameter	1 Period – 1r (median, 95 % CI)	2 Periods – 2r (median, 95 % CI)	3 Periods – 2r (median, 95 % CI)	3 Periods – 3r (median, 95 % CI)
K	784.7 (472.0-1485.0)	681.0 (514.0-1168.0)	830.0 (536.2-1458.0)	604.3 (503.9-1047.0)
r1	0.20 (0.11-0.31)	0.25 (0.15-0.38)	0.19 (0.12-0.30)	0.32 (0.16-0.49)
r2	-	0.12 (0.07-0.18)	0.08 (0.02-0.24)	0.069 (0.013-0.21)
r3	-	-	-	0.15 (0.056-0.23)
logq.ynkc	0.098 (0.004-0.38)	0.09 (0.001-0.37)	0.07 (0.001-0.31)	0.097 (0.004-0.42)
logq.s.cam	1.54 (1.22-1.83)	1.38 (1.10-1.64)	1.36 (1.07-1.69)	1.30 (1.00-1.63)
logq.f.cam	1.99 (1.67-2.29)	1.83 (1.54-2.08)	1.82 (1.52-2.15)	1.75 (1.45-2.08)
logq.eu	1.15 (0.73-1.56)	0.98 (0.60-1.36)	0.99 (0.57-1.40)	0.91 (0.49-1.34)
logq.ussr	1.53 (1.26-1.82)	1.48 (1.23-1.74)	1.43 (1.13-1.71)	1.45 (1.17-1.74)
sigma	0.16 (0.042-0.26)	0.14 (0.06-0.24)	0.13 (0.02-0.25)	0.12 (0.018-0.23)
tau.ynkc	0.15 (0.01-0.44)	0.15 (0.01-0.42)	0.19 (0.02-0.51)	0.17 (0.02-0.45)
tau.s.cam	0.25 (0.17-0.36)	0.24 (0.17-0.35)	0.25 (0.17-0.36)	0.24 (0.17-0.35)
tau.f.cam	0.11 (0.028-0.20)	0.11 (0.04-0.19)	0.11 (0.04-0.19)	0.11 (0.049-0.19)
tau.eu	0.46 (0.31-0.78)	0.46 (0.31-0.77)	0.47 (0.31-0.78)	0.47 (0.31-0.77)
tau.ussr	0.35 (0.24-0.55)	0.36 (0.24-0.55)	0.38 (0.25-0.58)	0.38 (0.25-0.60)
MSY1	38.86 (22.84-65.70)	43.10 (27.93-63.47)	39.60 (25.53-64.58)	48.31 (32.86-68.78)
MSY2	-	20.20 (10.85-37.53)	17.60 (3.52-50.92)	10.92 (2.07-34.59)
MSY3	-	-	-	22.84 (8.37-44.07)
FMSY1	0.098 (0.056-0.16)	0.12 (0.07-0.19)	0.10 (0.06-0.15)	0.16 (0.081-0.24)
FMSY2	-	0.06 (0.03-0.09)	0.04 (0.01-0.12)	0.035 (0.01-0.11)
FMSY3	-	-	-	0.074 (0.028-0.12)
BMSY	392.3 (236.0-742.4)	341.0 (257.0-584.01)	415.0 (268.1-729.2)	302.1 (252.0-523.6)
DIC	929.8	941.7	944.6	950.6

Table 9: Summary of parameter estimates using a Bayesian surplus production model for 3Ps American plaice.

Parameter	Description	Model 1 Posterior (median, 95 % CI)	Model 2 Posterior (median, 95 % CI)
K	Carrying Capacity	117.4 (100.6-322.6)	37.94 (26.36-74.44)
r1	Population growth rate (Model 1-2)	0.15 (0.07-0.28)	0.78 (0.30-1.38)
r2	Population growth rate (Model 2)	-	0.17 (0.062-0.31)
logq.eng	Log Catchability, Cdn Engels	0.09 (0.004-0.43)	0.14 (0.006-0.54)
logq.cam	Log Catchability, Cdn Campelen	0.65 (0.039-1.57)	0.56 (0.037-1.13)
sigma	Process error	0.25 (0.011-0.54)	0.075 (0.004-0.28)
tau.eng	Observation error, Cdn Engels	0.82 (0.55-1.24)	0.86 (0.79-1.13)
tau.cam	Observation error, Cdn Campelen	0.27 (0.045-0.53)	0.44 (0.39-0.66)
MSY1	Maximum Sustainable Yield (Per 1)	4.55 (2.52-13.18)	7.42 (5.02-9.88)
MSY2	Maximum Sustainable Yield (Per 2)	-	1.60 (0.69-2.99)
FMSY1	F at MSY (Period 1)	0.07 (0.04-0.14)	0.39 (0.15-0.69)
FMSY2	F at MSY (Period 2)	-	0.082 (0.031-0.16)
BMSY	Biomass at Maximum Sustainable Yield	58.69 (50.31-161.31)	18.97 (13.18-37.22)
DIC	Deviance Information Criteria	285	277

Table 10: Summary of parameter estimates using a Bayesian surplus production model for 2J3K American plaice.

Parameter	Description	Model 1 Posterior (median, 95 % CI)	Model 2 Posterior (median, 95 % CI)
K	Carrying Capacity	159.0 (102.0-712.0)	151.90 (101.60-685.5)
r1	Population growth rate (Period 1)	0.053 (0.013-0.15)	0.09 (0.017-0.42)
r2	Population growth rate (Period 2)	-	0.046 (0.009-0.15)
logq.eng	Log Catchability, Cdn Engels	0.09 (0.003-0.40)	1.26 (0.08-2.06)
logq.cam	Log Catchability, Cdn Campelen	0.57 (0.034-1.45)	1.87 (0.29-3.21)
sigma	Process error	0.16 (0.007-0.46)	0.26 (0.032-0.51)
tau.eng	Observation error, Cdn Engels	0.95 (0.80-1.36)	0.73 (0.68-0.96)
tau.cam	Observation error, Cdn Campelen	0.44 (0.39-0.67)	0.46 (0.41-0.68)
MSY1	Maximum Sustainable Yield (Period 1)	0.09 (0.003-0.40)	3.95 (0.75-21.23)
MSY2	Maximum Sustainable Yield (Period 2)	-	1.91 (0.32-11.11)
FMSY1	F at MSY1	0.026 (0.006-0.075)	0.047 (0.009-0.21)
FMSY2	F at MSY2	-	0.023 (0.004-0.072)
BMSY	Biomass at Maximum Sustainable Yield	79.70 (51.20-356.00)	75.96 (50.81-342.81)
DIC	Deviance Information Criteria	247	242

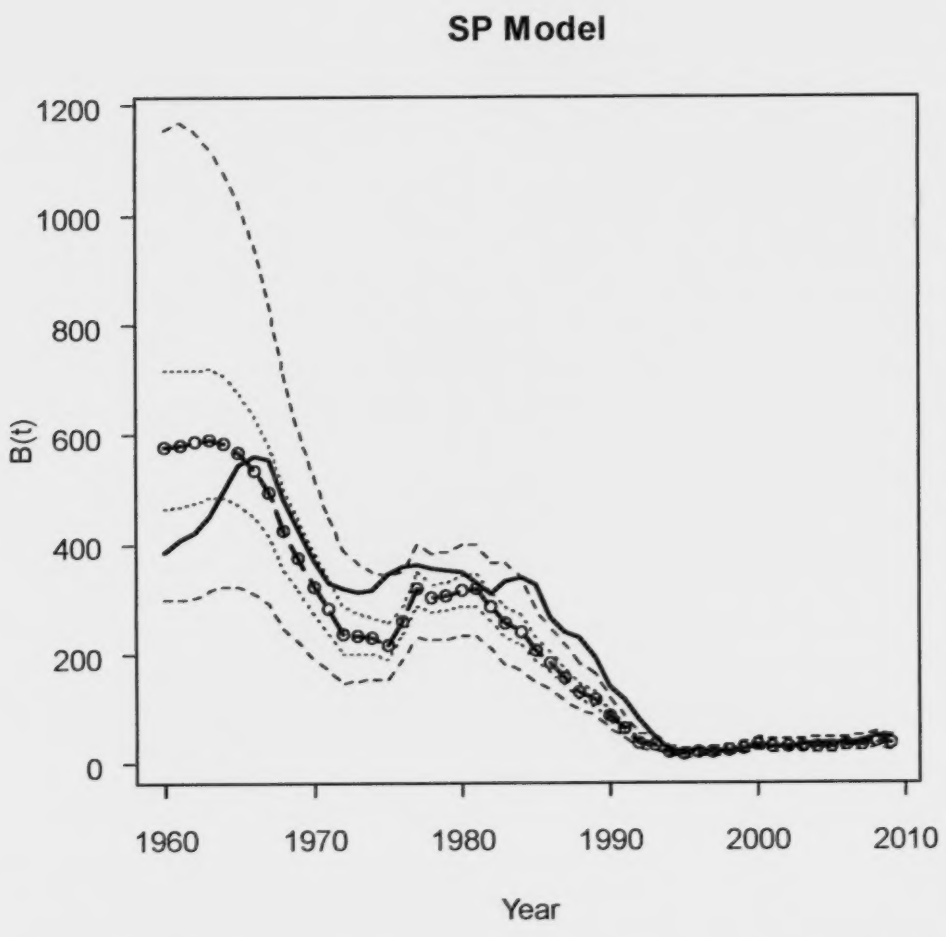

Figure 1: Schaefer surplus production model of biomass ('000t) from 1960-2009 (dashed line) for 3LNO American plaice. Dotted lines represent 50 % and 95 % credible intervals while the solid line is an age-based virtual population analysis (VPA) displayed here for comparison.

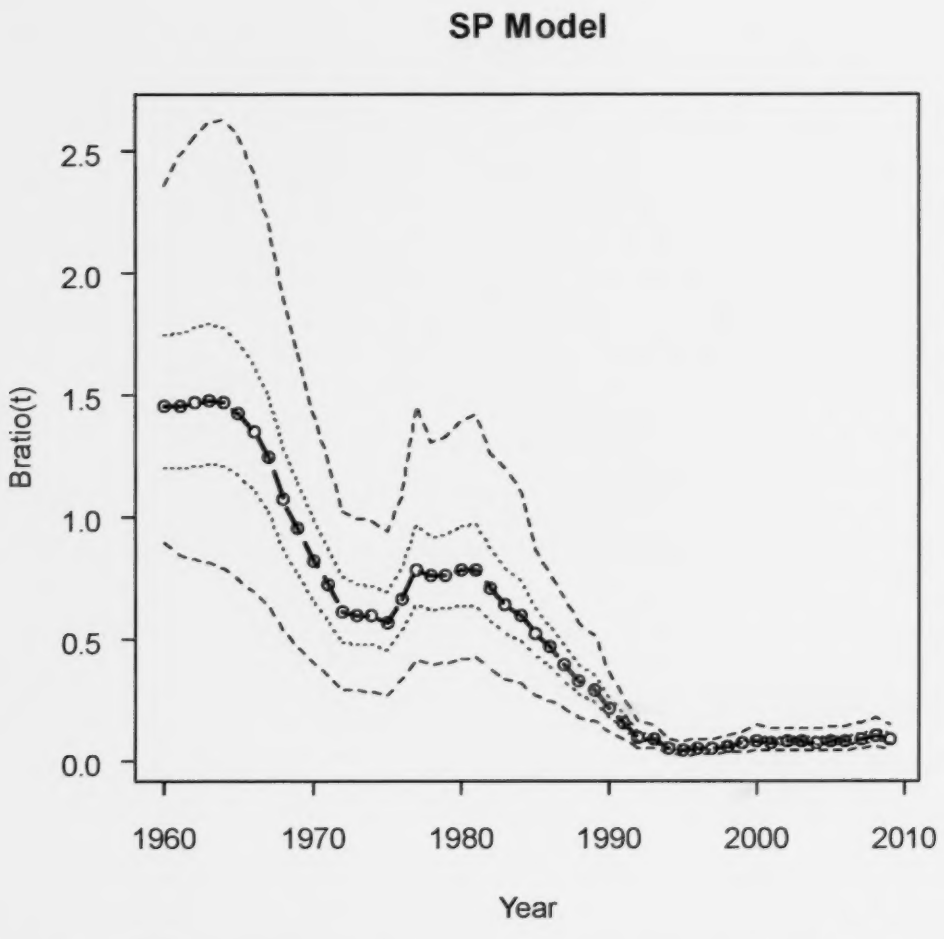

Figure 2: Schaefer surplus production model of B_{ratio} (B/B_{MSY}) from 1960-2009 (dashed line) for 3LNO American plaice. Dotted lines represent 50 % and 95 % credible intervals.

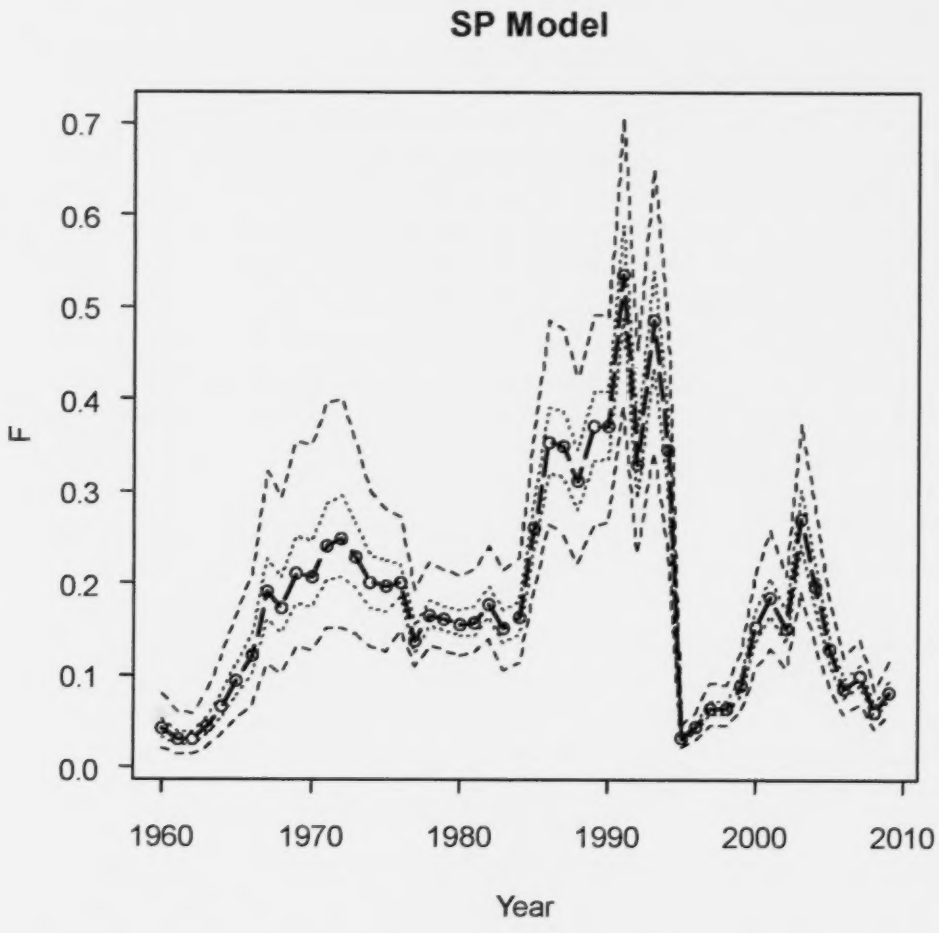

Figure 3: Modeled values for F, fisheries mortality, from 1960-2009 (dashed line) for 3LNO American plaice. Dotted lines represent 50 % and 95 % credible intervals.

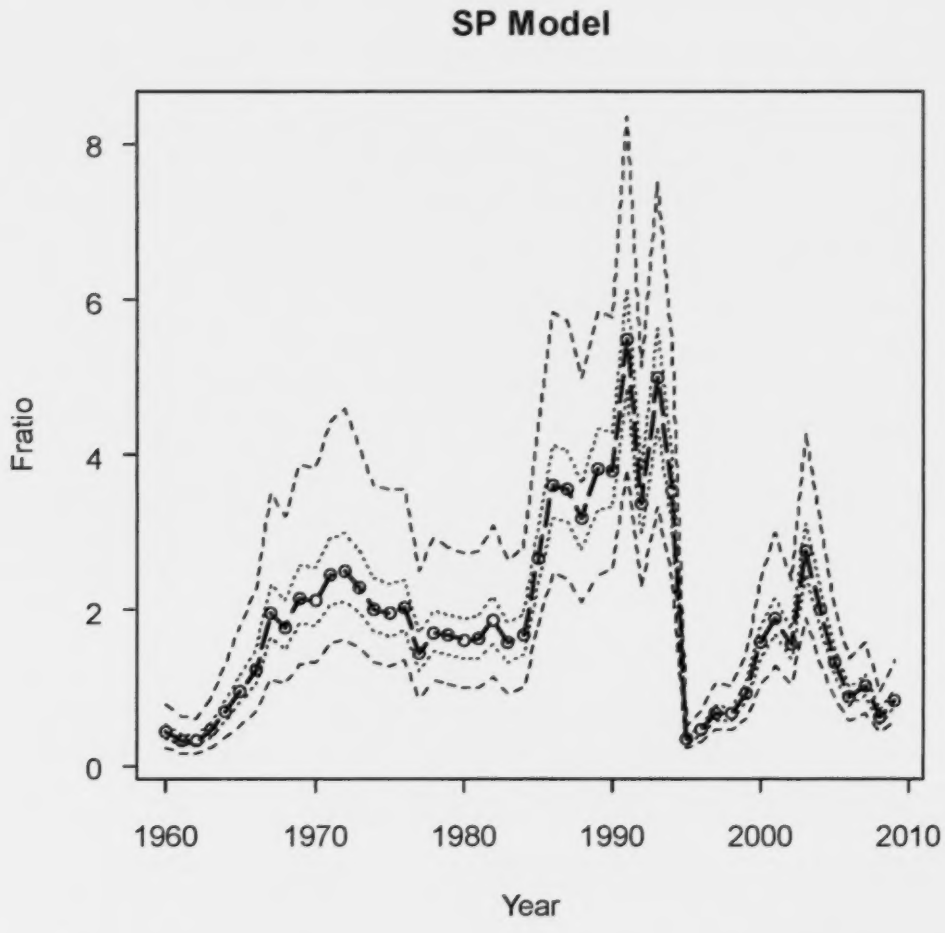

Figure 4: Modeled values for F_{ratio}, the ratio of fishing mortality to that estimated for F_{MSY}, from 1960-2009 (dashed line) for 3LNO American plaice. Dotted lines represent 50 % and 95 % credible intervals.

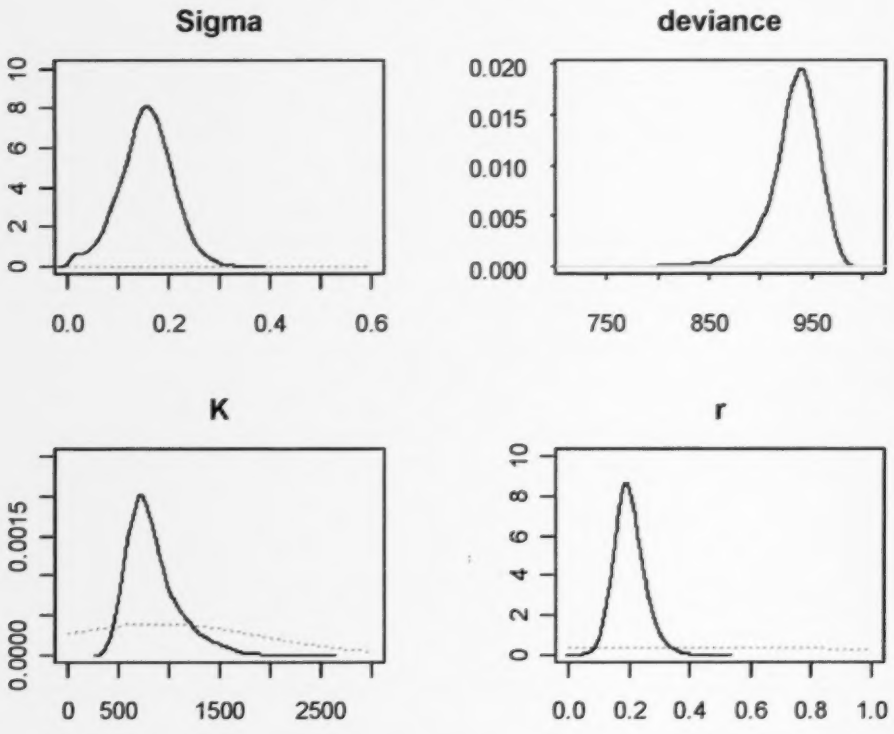

Figure 5: Posterior distributions for process error precision (Sigma), deviance, carrying capacity (K) and the intrinsic rate of population growth (r) for 3LNO American plaice. Vague prior distributions are shown for K, r, and sigma (red dotted lines).

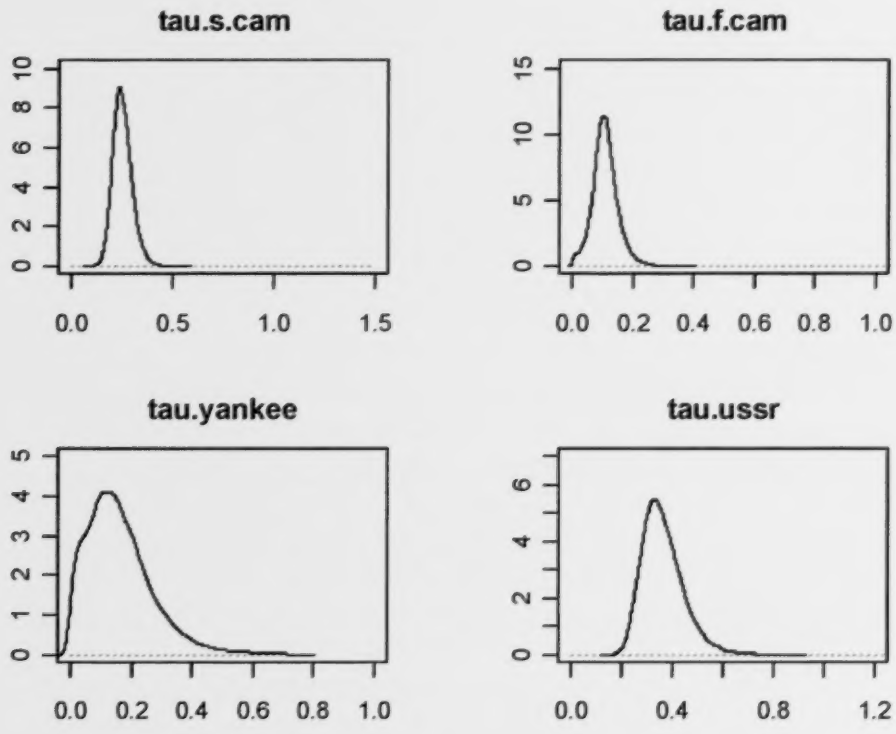

Figure 6: Posterior (solid line) and prior (red dotted lines) distributions for observation error precision (tau) for the Spring converted Campelen series, the Fall converted Campelen series, the Yankee series, and the USSR series for 3LNO American plaice BSP model.

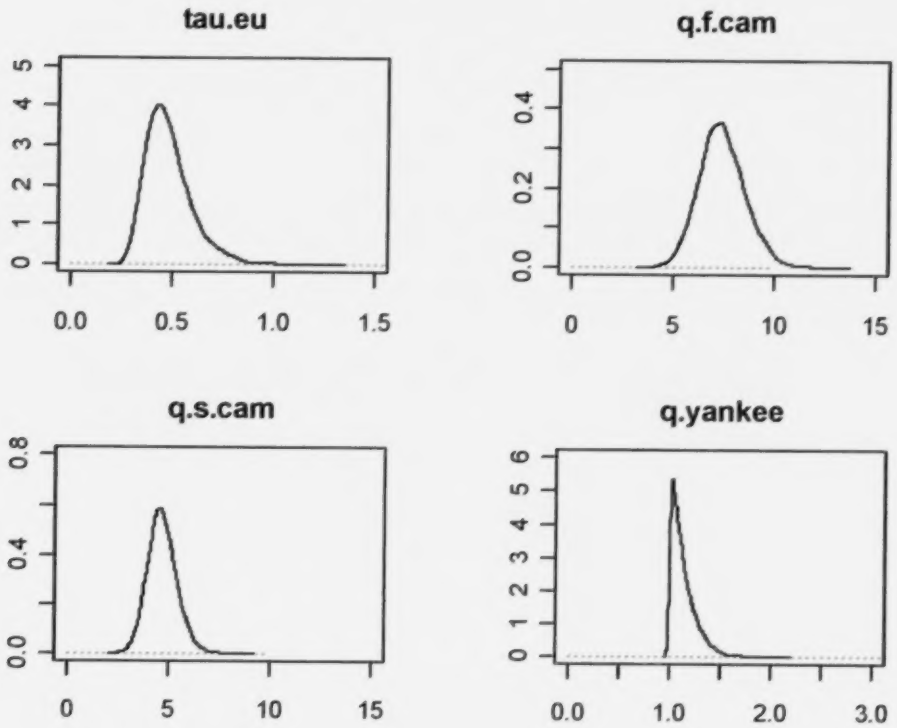

Figure 7: Posterior (solid line) and prior (red dotted lines) distributions for observation error (tau) of the EU series, catchability parameters (q) of Spring converted Campelen, Fall converted Campelen, and Yankee surveys for 3LNO American plaice.

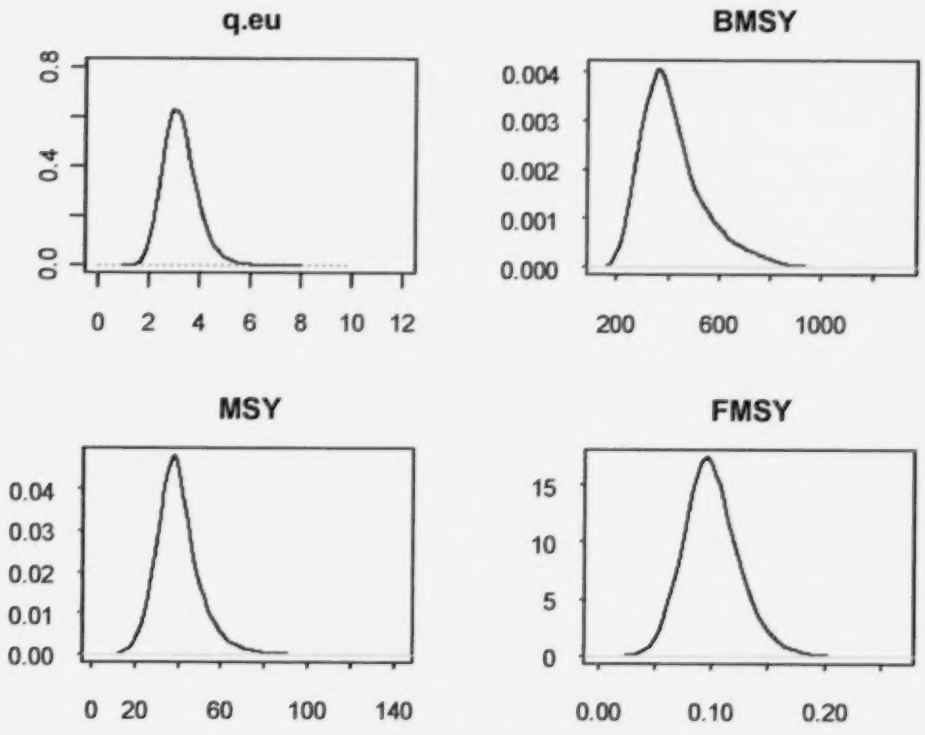

Figure 8: Posterior (solid line) and prior (red dotted lines) distributions for EU series catchability (q), BMSY, MSY, and FMSY for 3LNO American plaice.

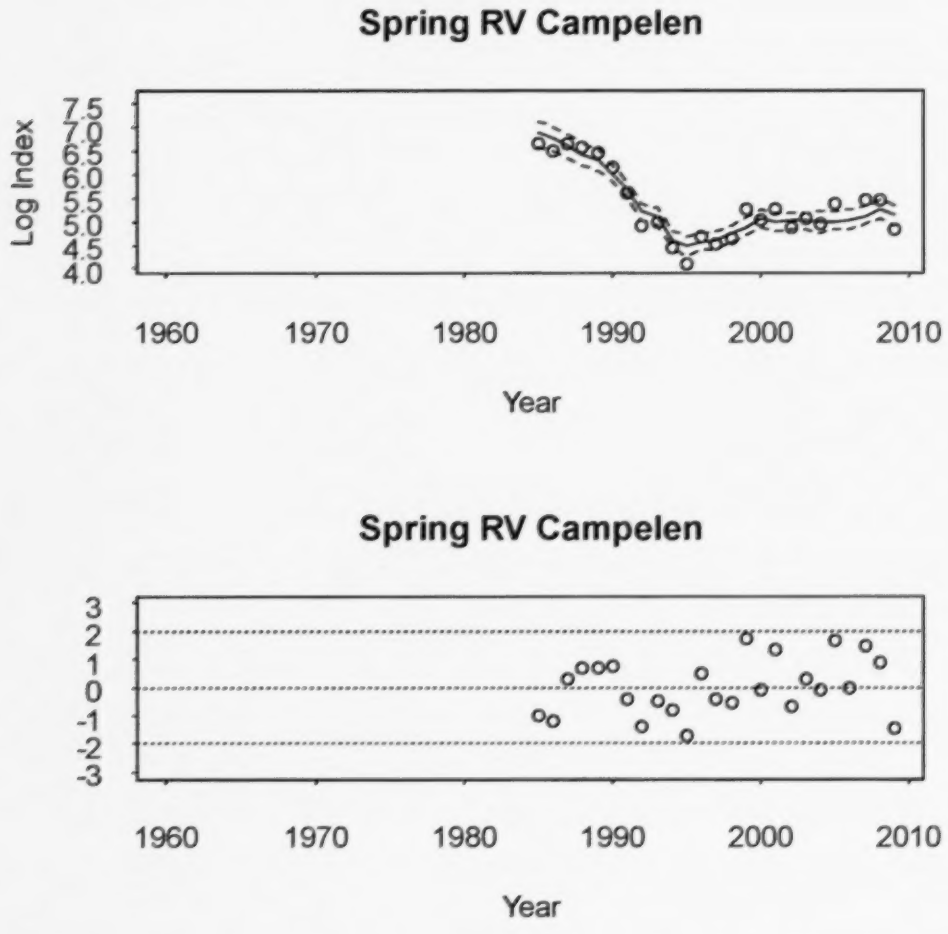

Figure 9: Spring converted Campelen series estimates with 95 % credible intervals (top) and residuals (bottom) for 3LNO American plaice.

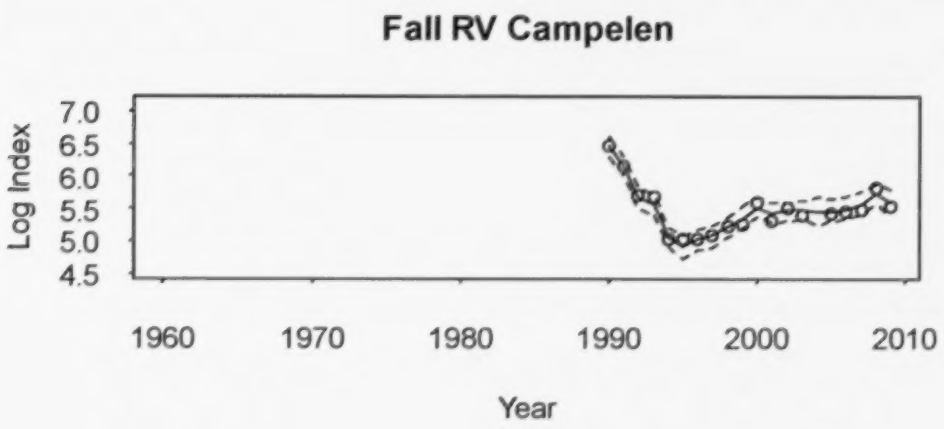

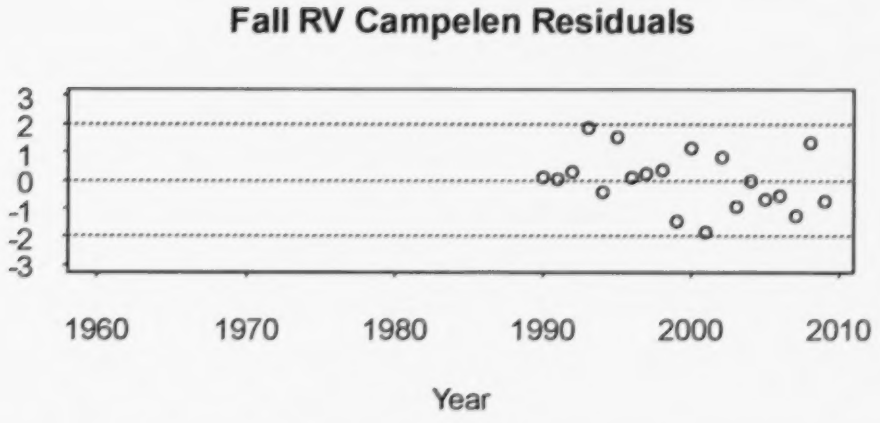

Figure 10: Fall converted Campelen series estimates with 95 % credible intervals (top) and residuals (bottom) for 3LNO American plaice.

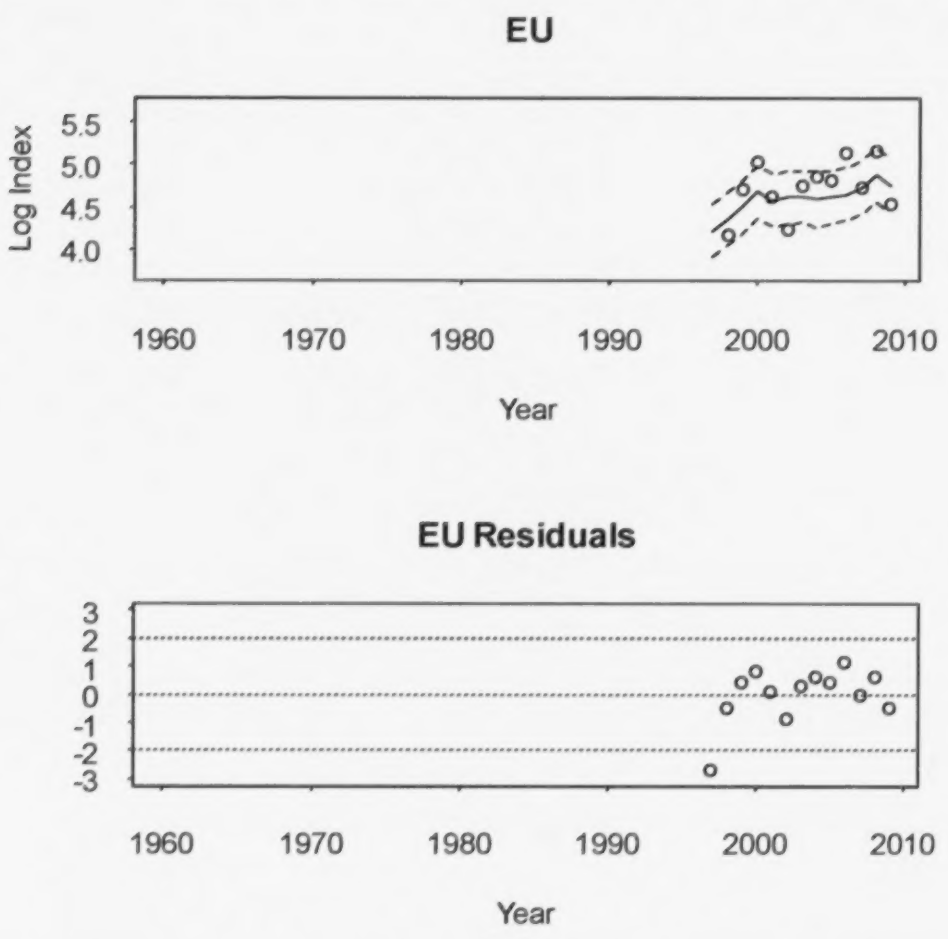

Figure 11: European Union series estimates with 95 % credible intervals (top) and residuals (bottom) for 3LNO American plaice.

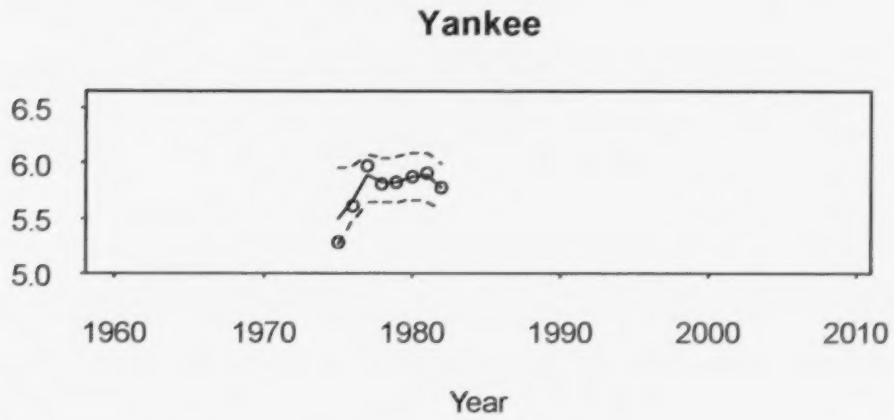

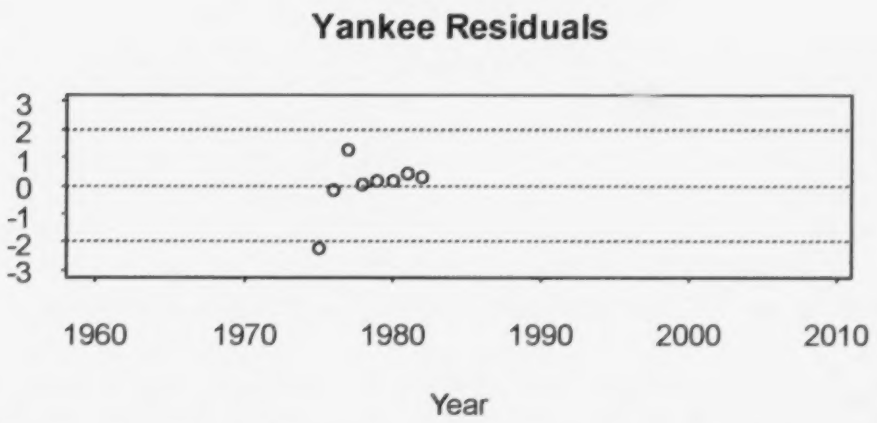

Figure 12: Yankee series estimates with 95 % credible intervals (top) and residuals (bottom) for 3LNO American plaice.

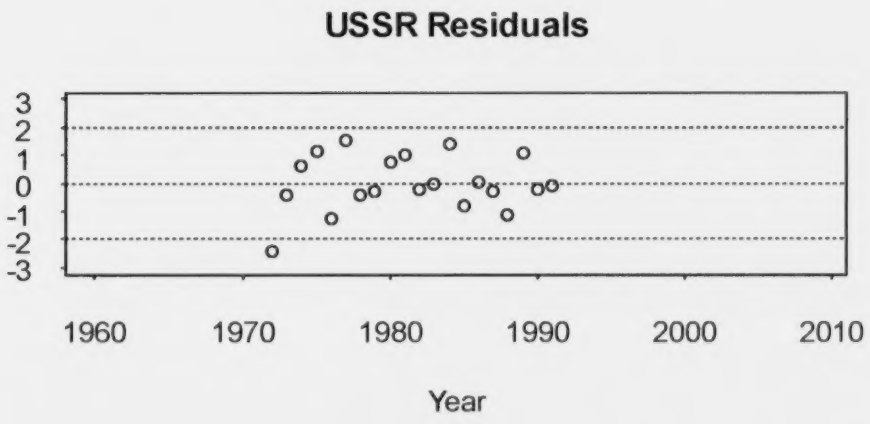

Figure 13: USSR series estimates with 95 % credible intervals (top) and residuals (bottom) for 3LNO American plaice.

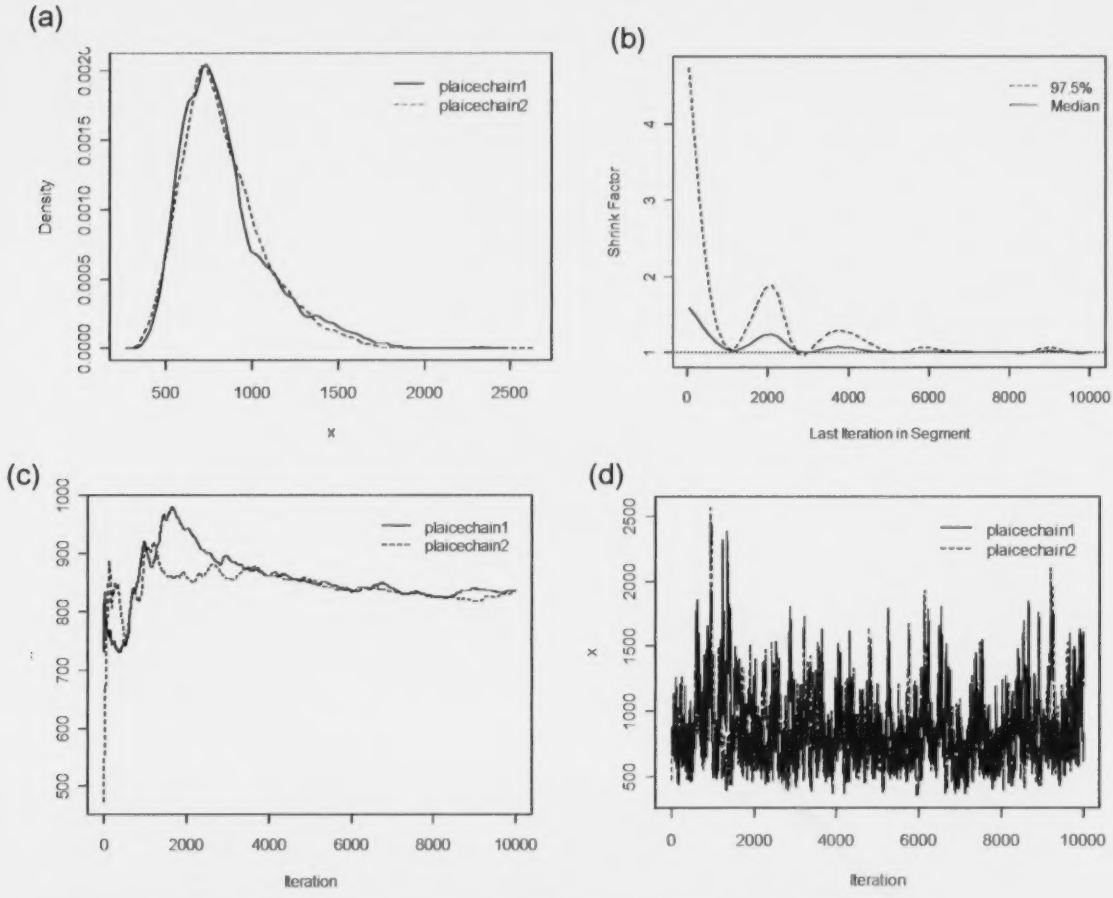

Figure 14: (a) Kernel density estimates of the posterior distribution of K for both chains. (b) Gelman and Rubin shrink factors for K. Gelman & Rubin shrink factors examining the reduction in bias in estimation. The shrink factor approaches 1 when the pooled within-chain variance dominates the between-chain variance. At that point, all chains have escaped the influence of their starting points. (c) Sampler running mean for K. (d) A time series trace of the sampled points for K in both chains.

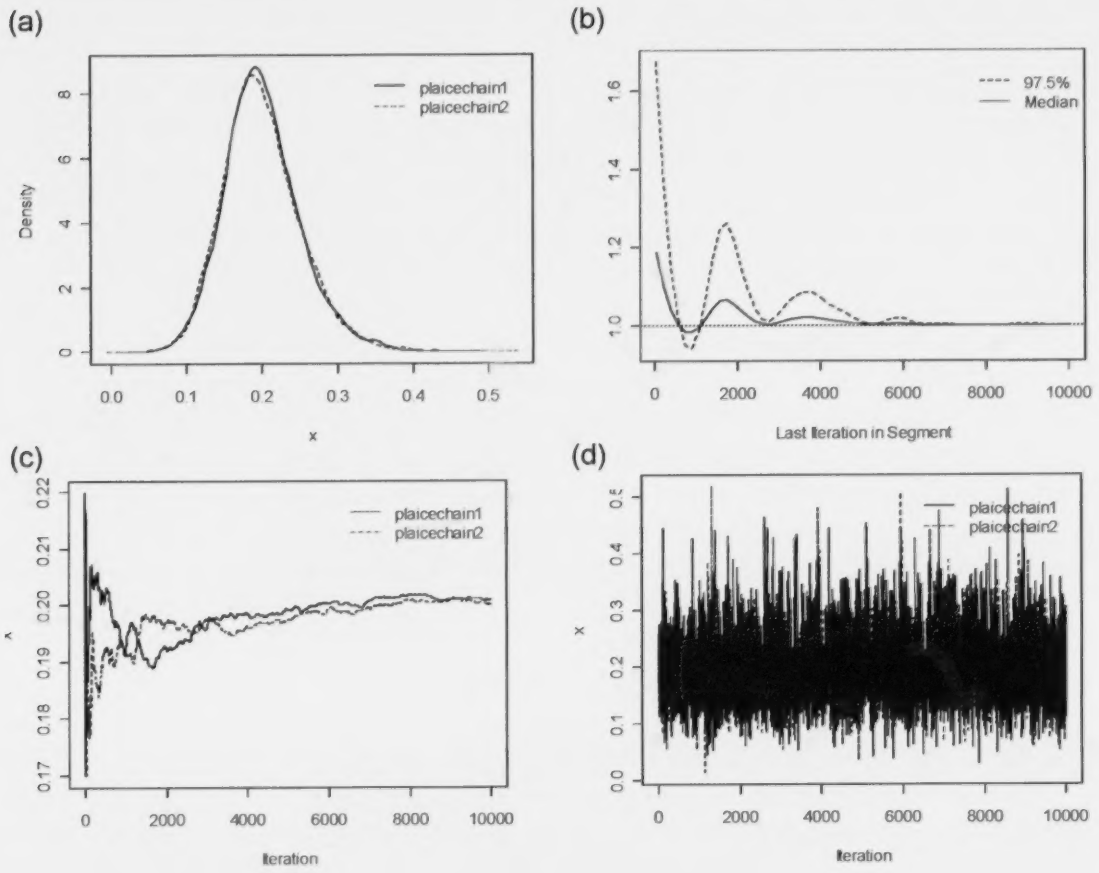

Figure 15: (a) Kernel density estimates of the posterior distribution of r for both chains. (b) Gelman and Rubin shrink factors for r. Gelman & Rubin shrink factors examining the reduction in bias in estimation. The shrink factor approaches 1 when the pooled within-chain variance dominates the between-chain variance. At that point, all chains have escaped the influence of their starting points. (c) Sampler running mean for r. (d) A time series trace of the sampled points for r in both chains.

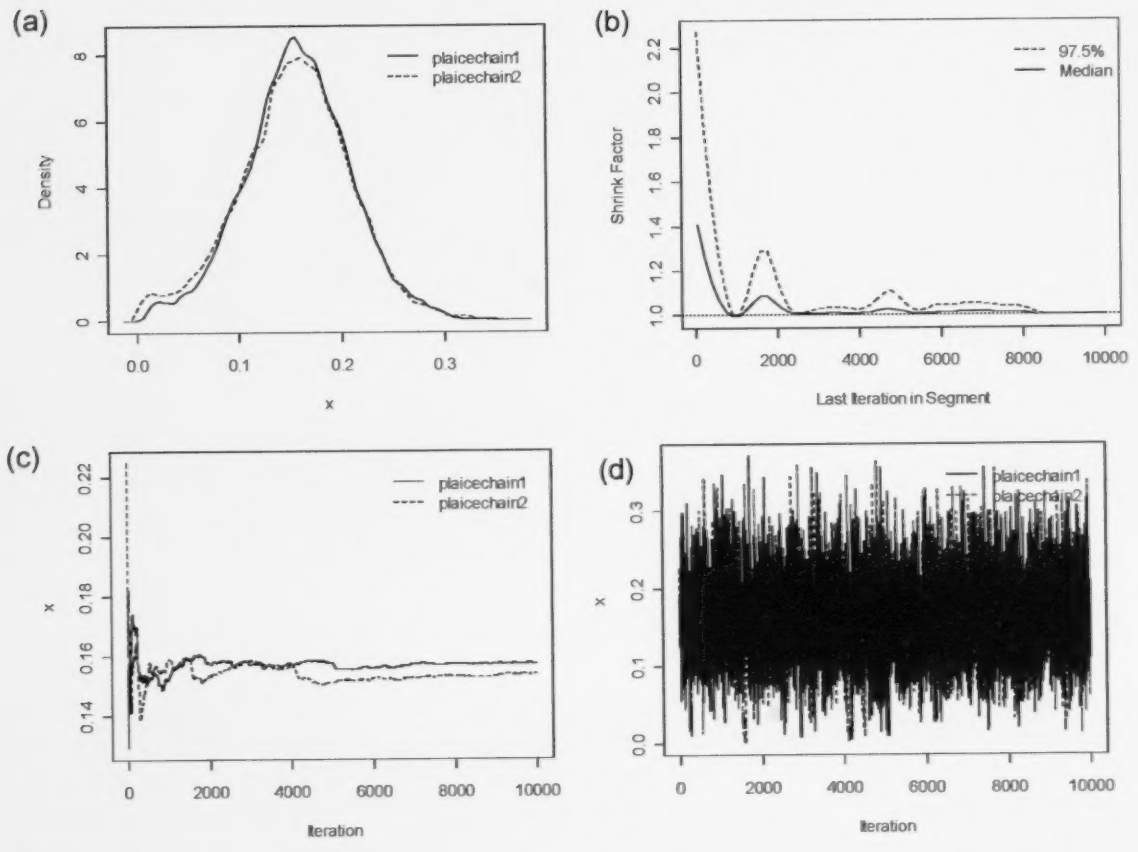

Figure 16: (a) Kernel density estimates of the posterior distribution of sigma for both chains. (b) Gelman and Rubin shrink factors for sigma. Gelman & Rubin shrink factors examining the reduction in bias in estimation. The shrink factor approaches 1 when the pooled within-chain variance dominates the between-chain variance. At that point, all chains have escaped the influence of their starting points. (c) Sampler running mean for sigma. (d) A time series trace of the sampled points for sigma in both chains.

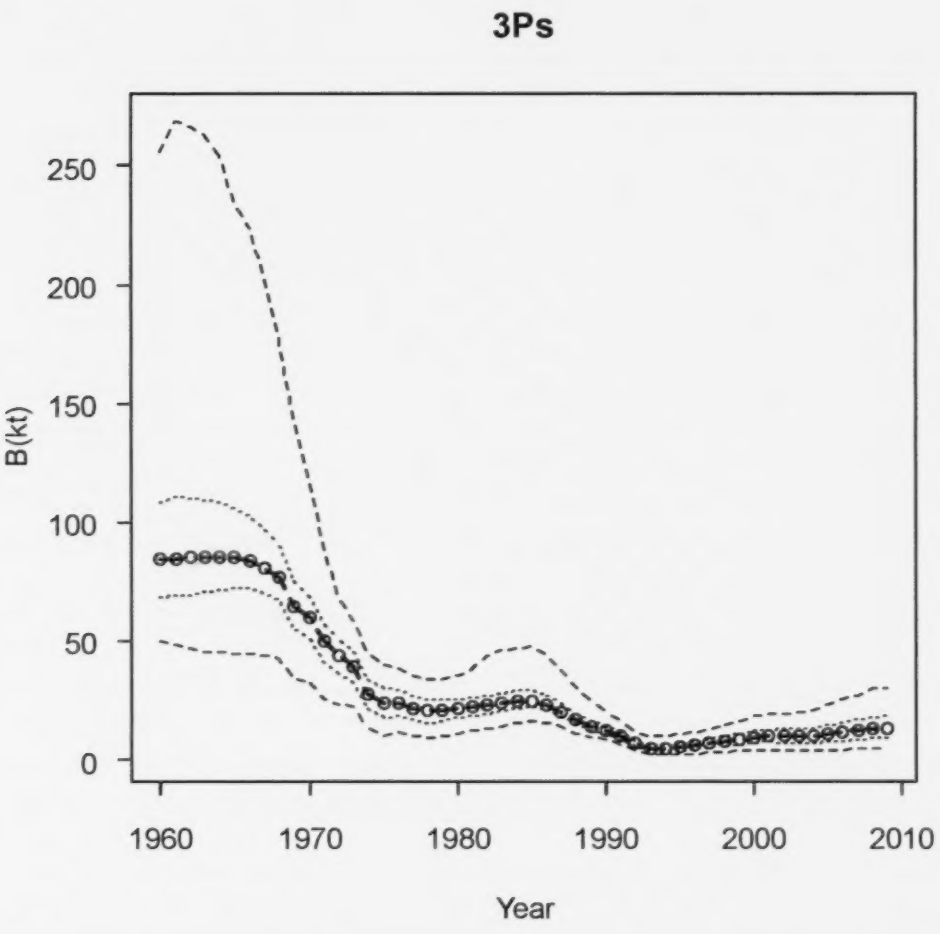

Figure 17: Schaefer surplus production model of biomass ('000t) from 1960-2009 (dashed line) for 3Ps American plaice. Dotted lines represent 50 % and 95 % credible intervals.

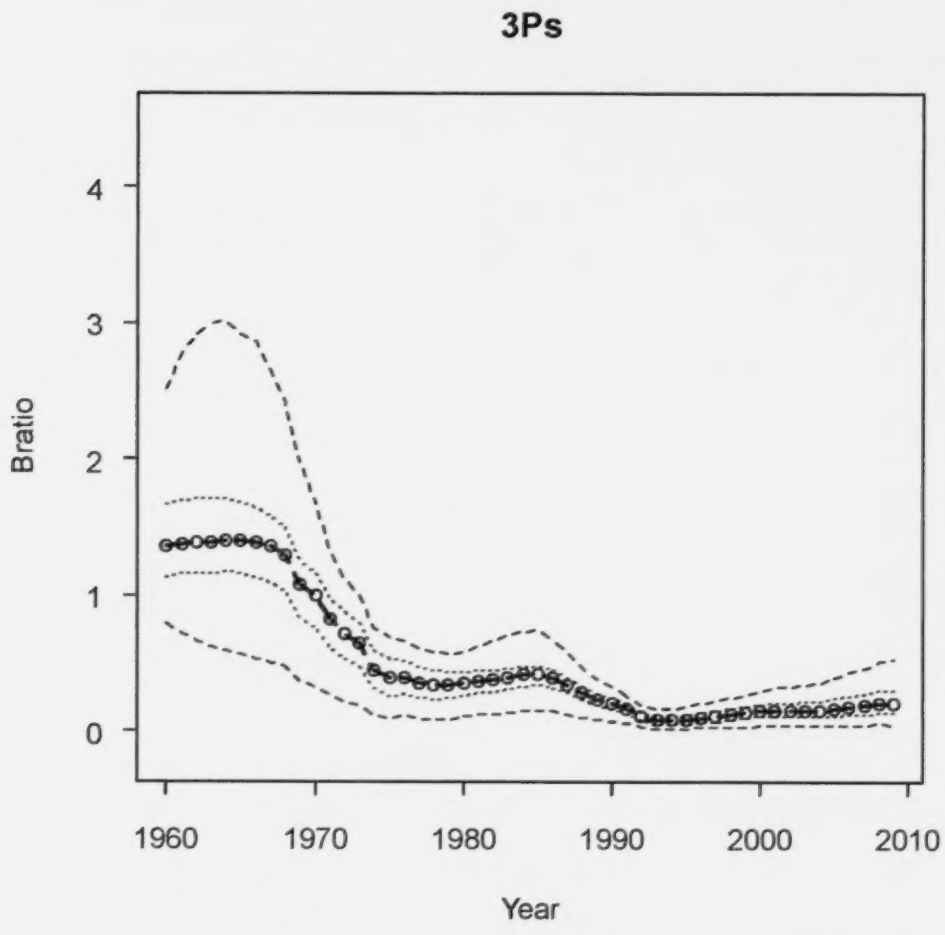

Figure 18: Schaefer surplus production model of B_{ratio} (B/B_{MSY}) from 1960-2009 (dashed line) for 3Ps American plaice. Dotted lines represent 50 % and 95 % credible intervals.

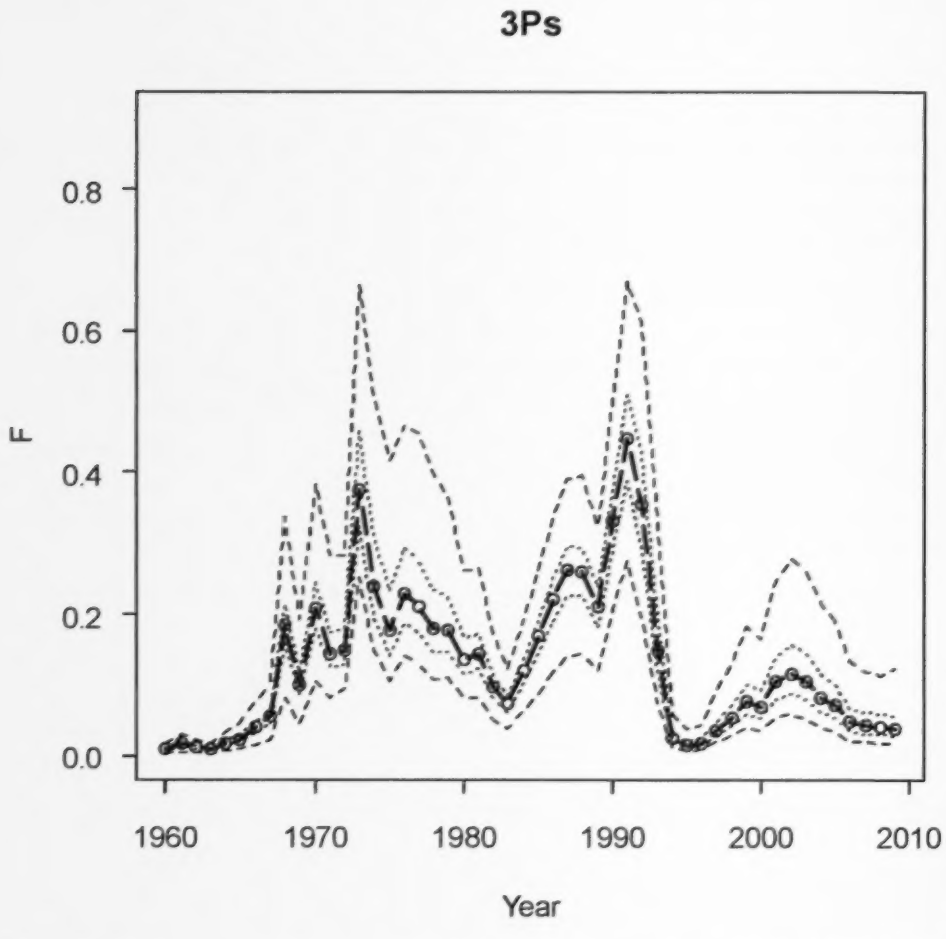

Figure 19: Modeled values for F, fisheries mortality, from 1960-2009 (dashed line) for 3Ps American plaice. Dotted lines represent 50 % and 95 % credible intervals.

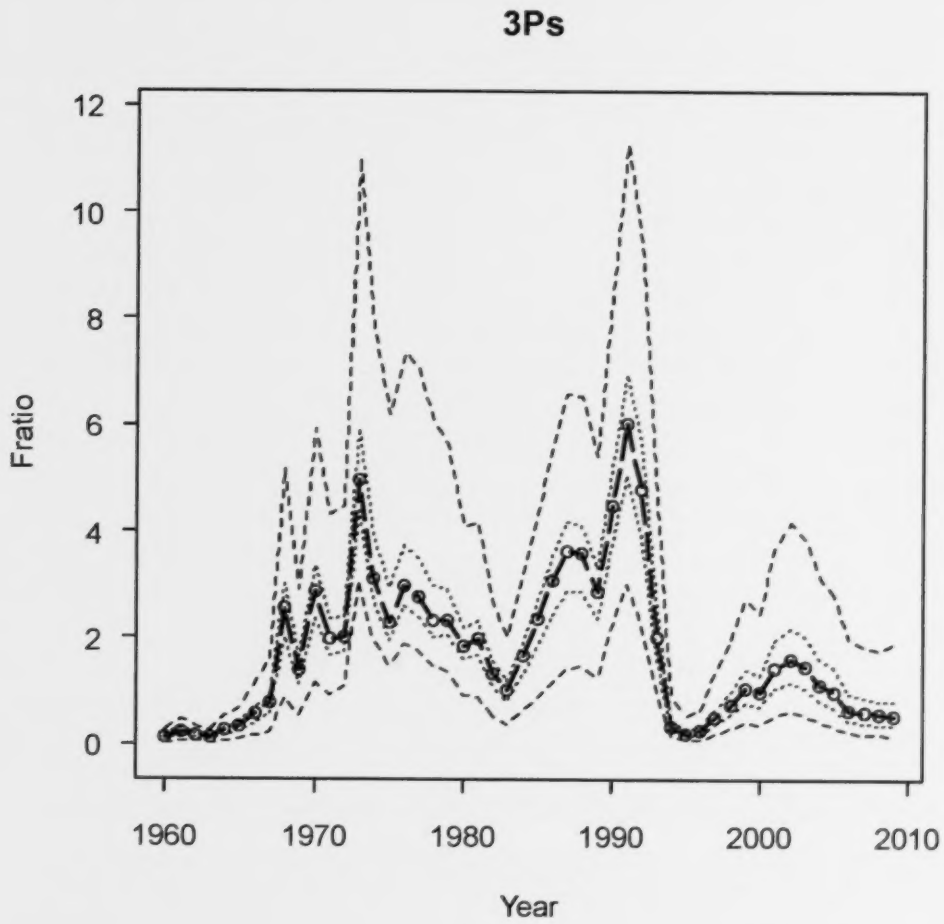

Figure 20: Modeled values for F_{ratio}, the ratio of fishing mortality to that estimated for F_{MSY}, from 1960-2009 (dashed line) for 3Ps American plaice. Dotted lines represent 50 % and 95 % credible intervals.

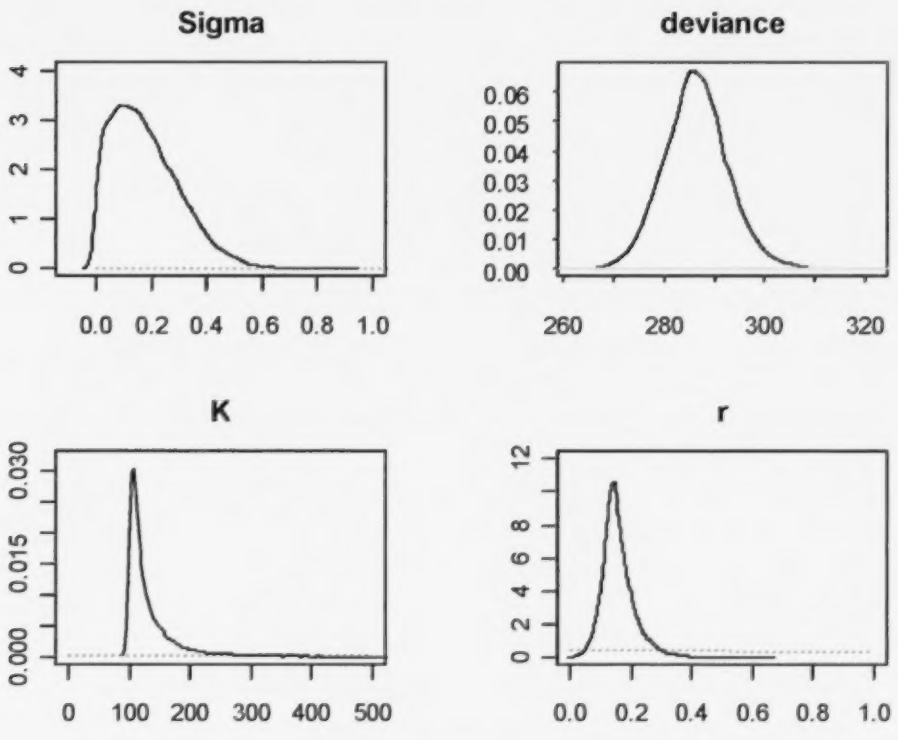

Figure 21: Posterior distributions for process error precision (Sigma), deviance, carrying capacity (K) and the intrinsic rate of population growth (r) for 3Ps American plaice. Vague prior distributions are shown for K, r, and Sigma (red dotted lines).

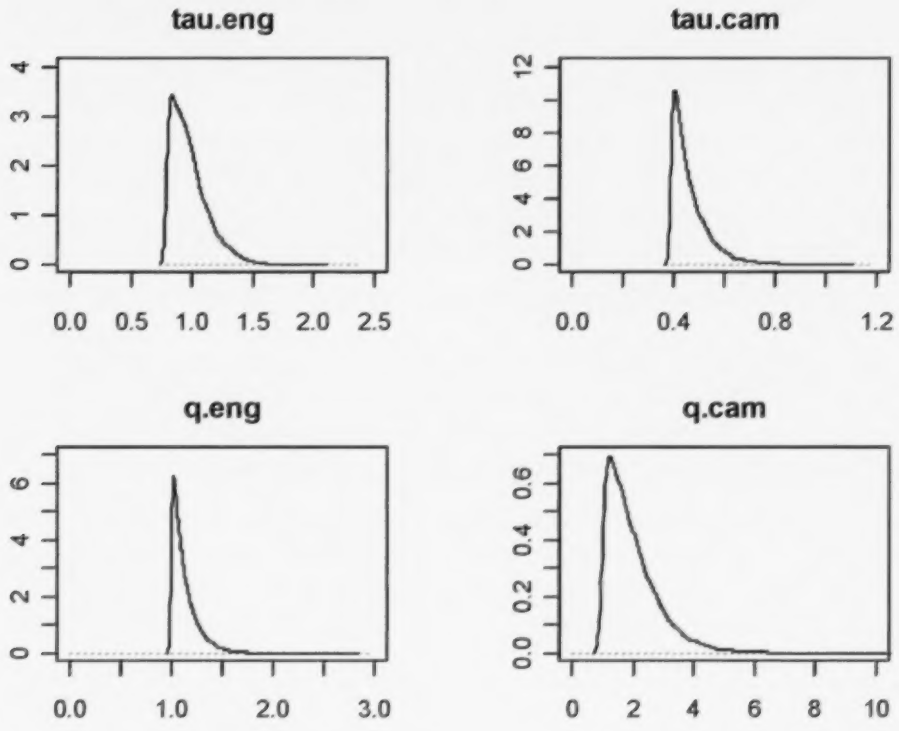

Figure 22: Posterior (solid line) and prior (red dotted lines) distributions for observation error precision (tau) and catchabilities (q) for Engels and Campelen surveys for the 3Ps American plaice BSP model.

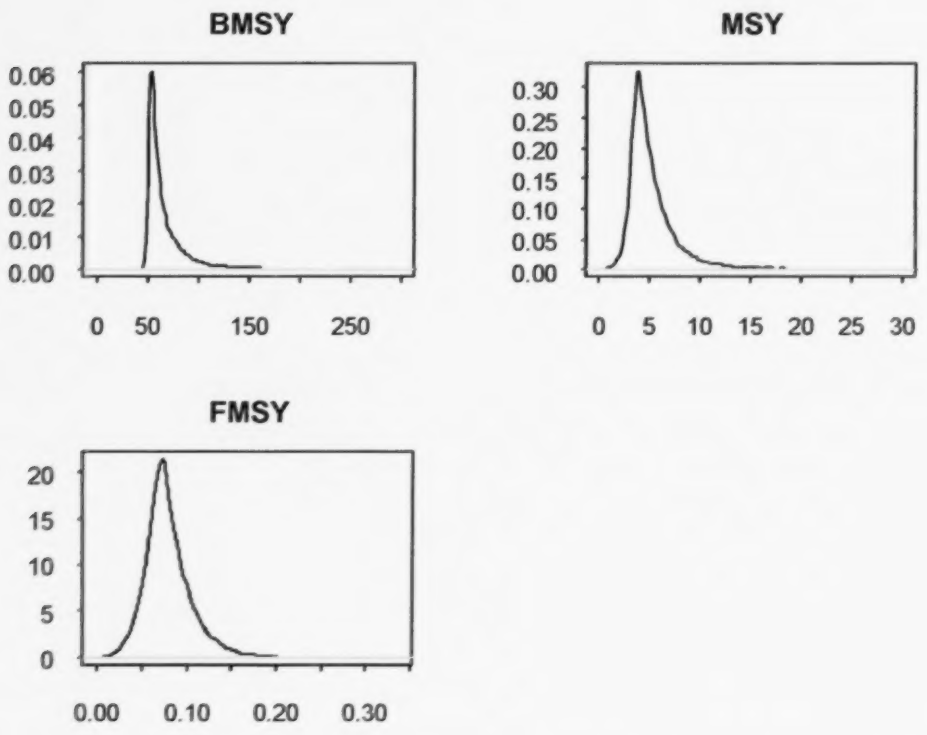

Figure 23: Posterior distributions for Maximum sustainable yield (B_{MSY}), Maximum surplus yield (MSY), and F at maximum sustainable yield (F_{MSY}) for 3Ps American plaice.

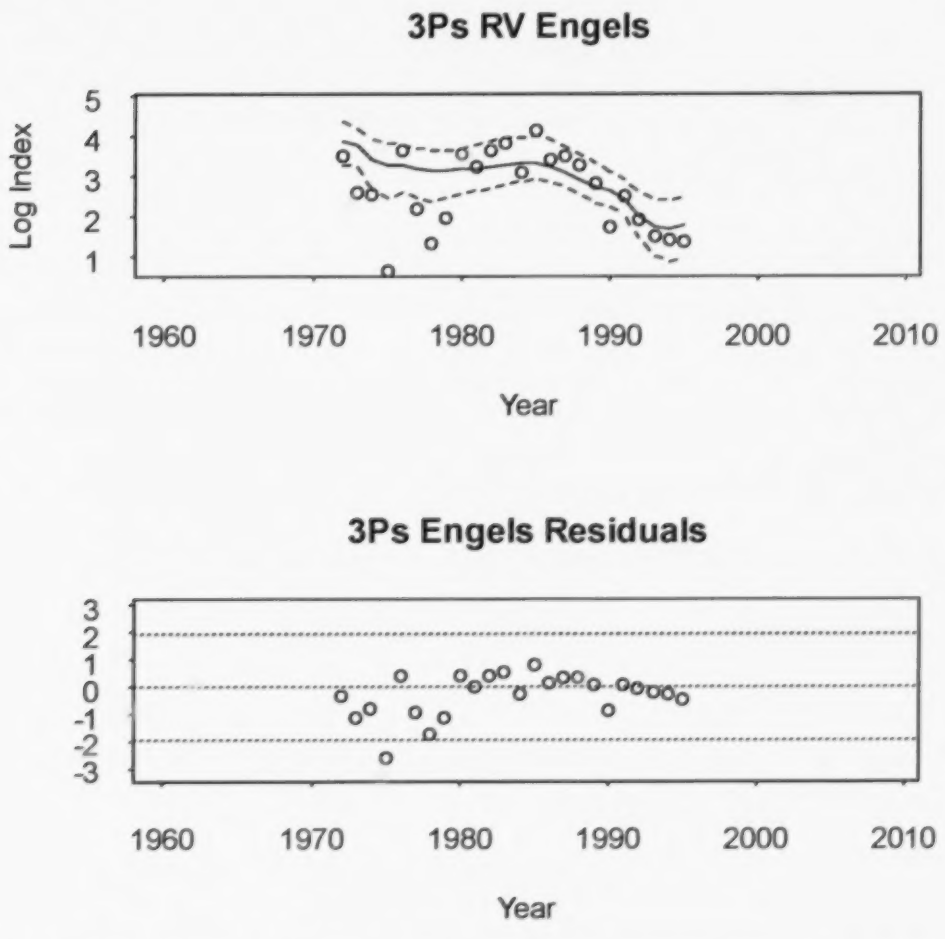

Figure 24: Engels series estimates with 95 % credible intervals (top) and residuals (bottom) for 3ps American plaice.

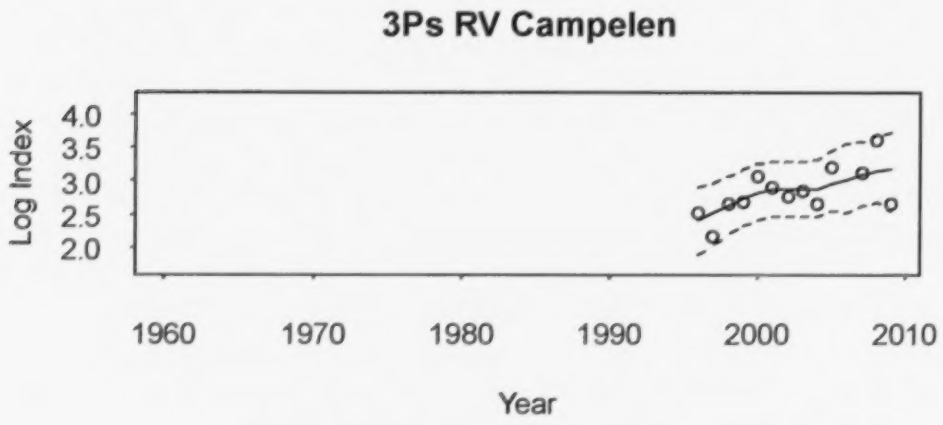

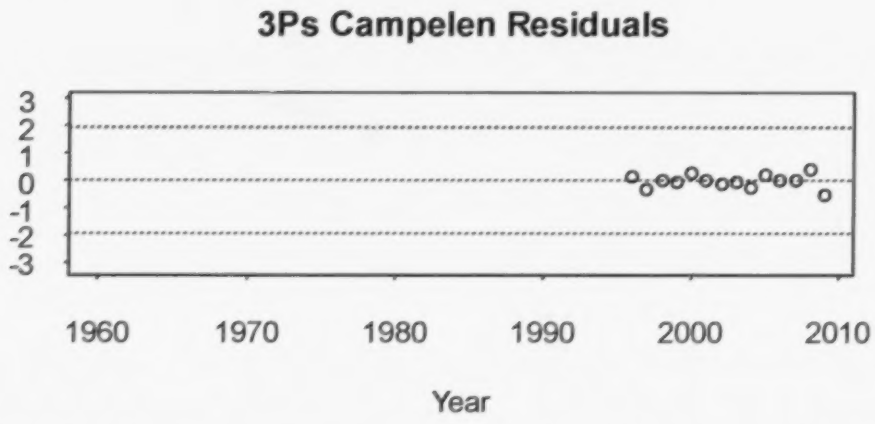

Figure 25: Campelen series estimates with 95 % credible intervals (top) and residuals (bottom) for 3Ps American plaice.

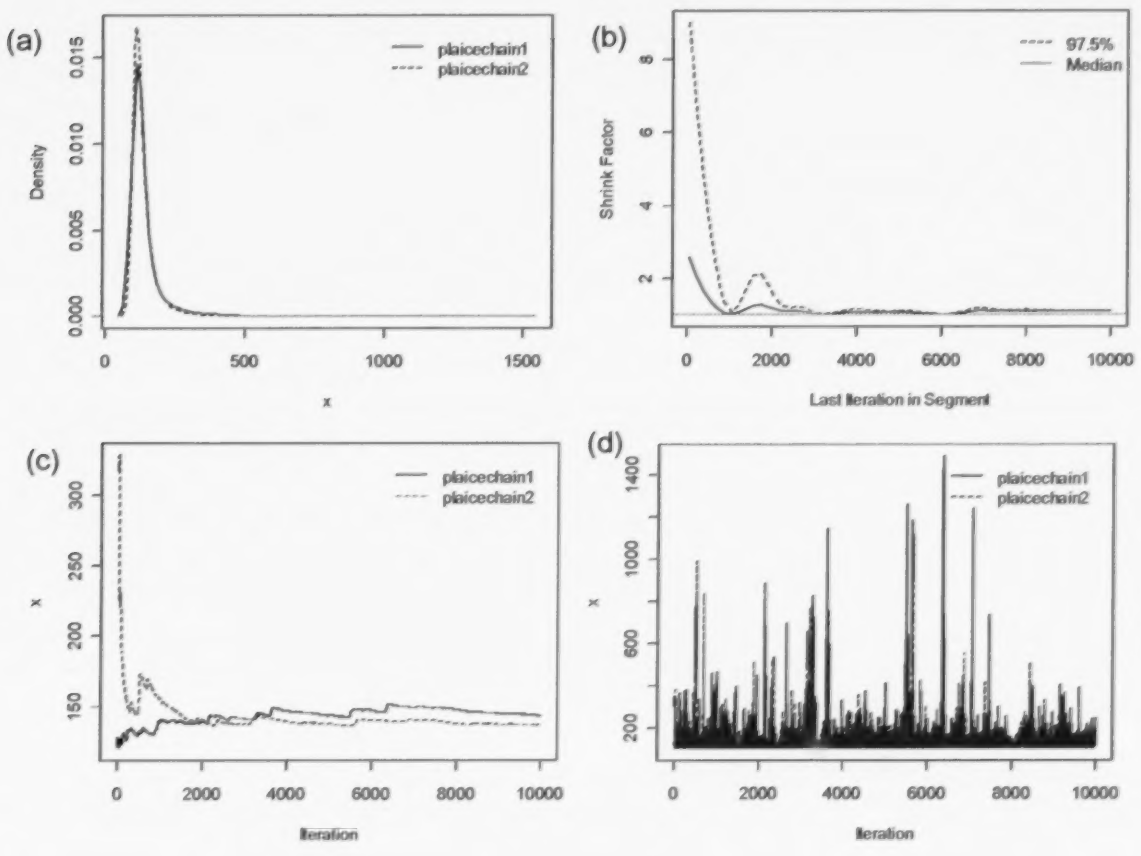

Figure 26: (a) Kernel density estimates of the posterior distribution of K for both chains in the 3Ps BSP model. (b) Gelman and Rubin shrink factors for K. (c) Sampler running mean for K. (d) A time series plot of the sampled points for K in both chains.

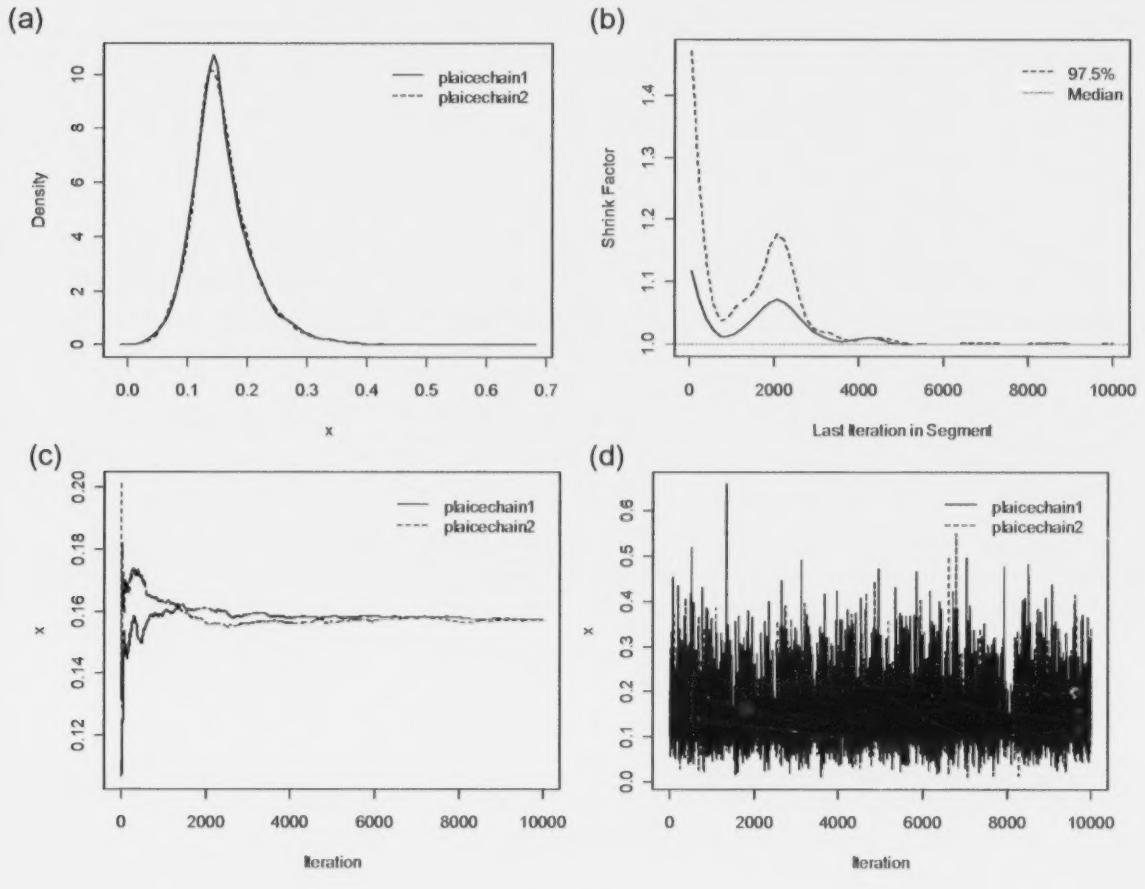

Figure 27: (a) Kernel density estimates of the posterior distribution of r for both chains in the 3Ps BSP model. (b) Gelman and Rubin shrink factors for r. (c) Sampler running mean for r. (d) A time series plot of the sampled points for r in both chains.

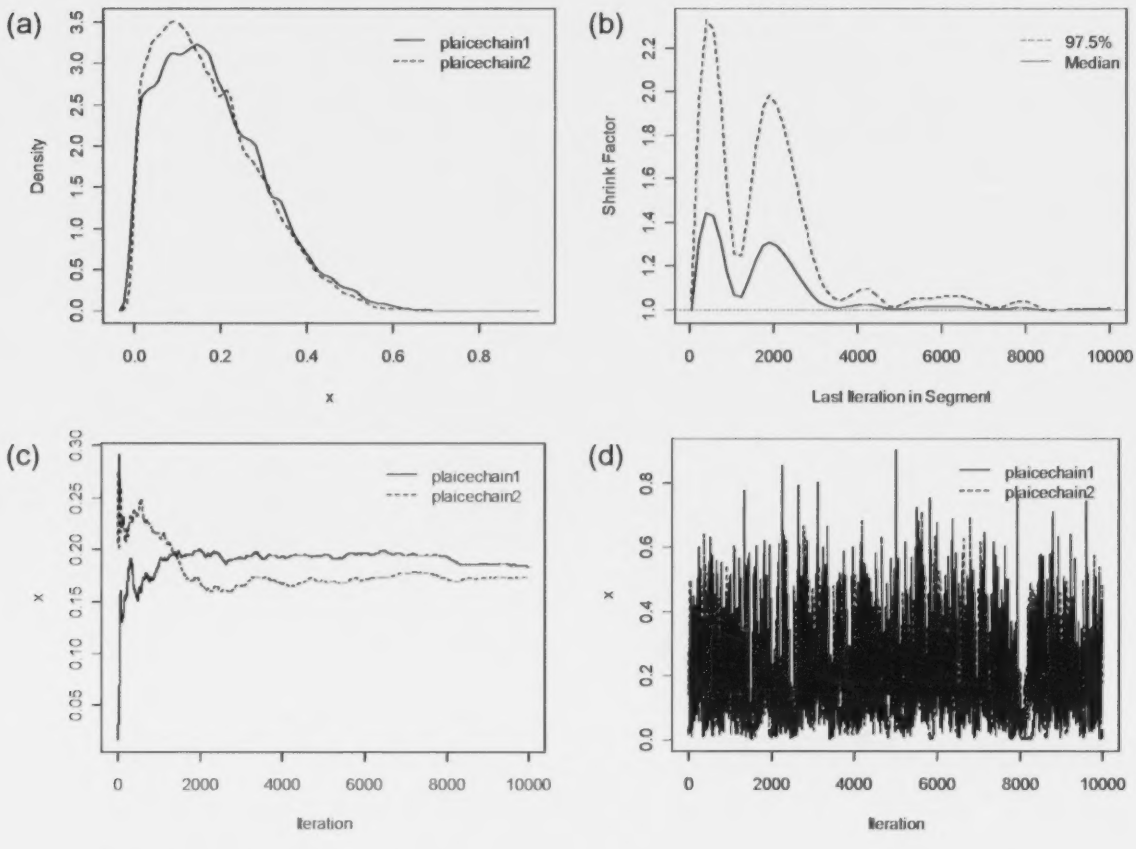

Figure 28: (a) Kernel density estimates of the posterior distribution of sigma for both chains in the 3Ps BSP model. (b) Gelman and Rubin shrink factors for sigma. (c) Sampler running mean for sigma. (d) A time series plot of the sampled points for sigma in both chains.

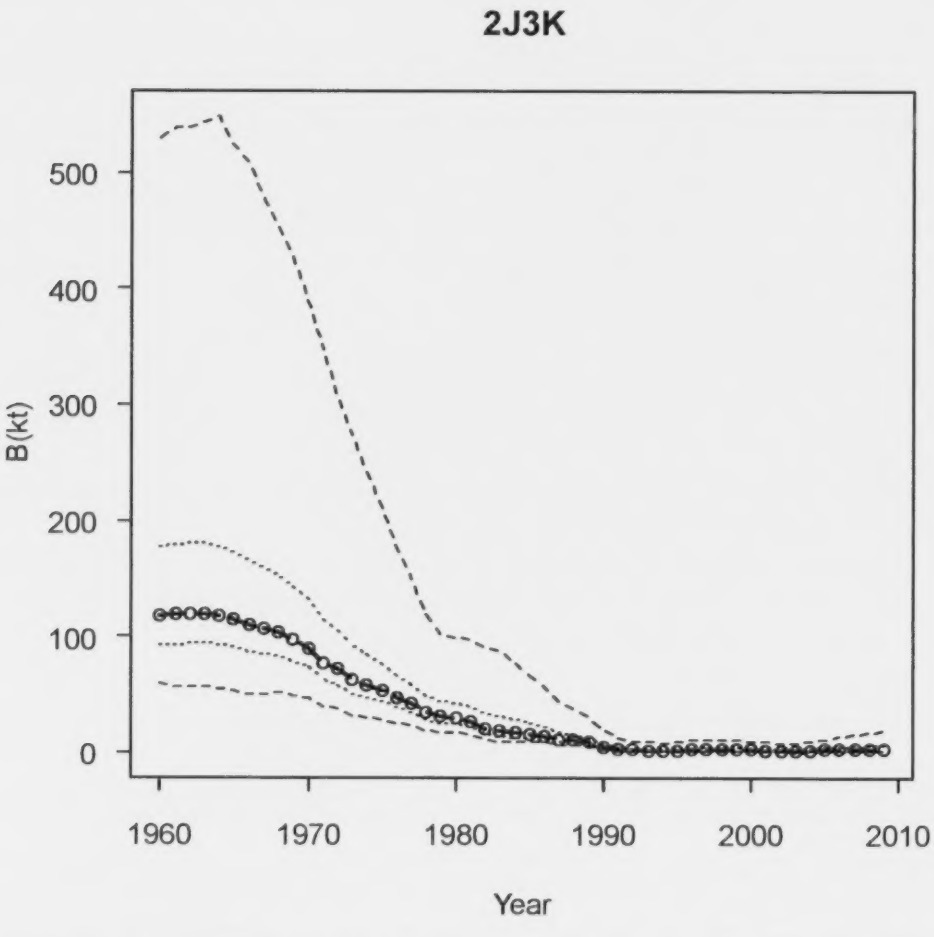

Figure 29: Schaefer surplus production model of biomass ('000t) from 1960-2009 (dashed line) for 2J3K American plaice. Dotted lines represent 50 % and 95 % credible intervals.

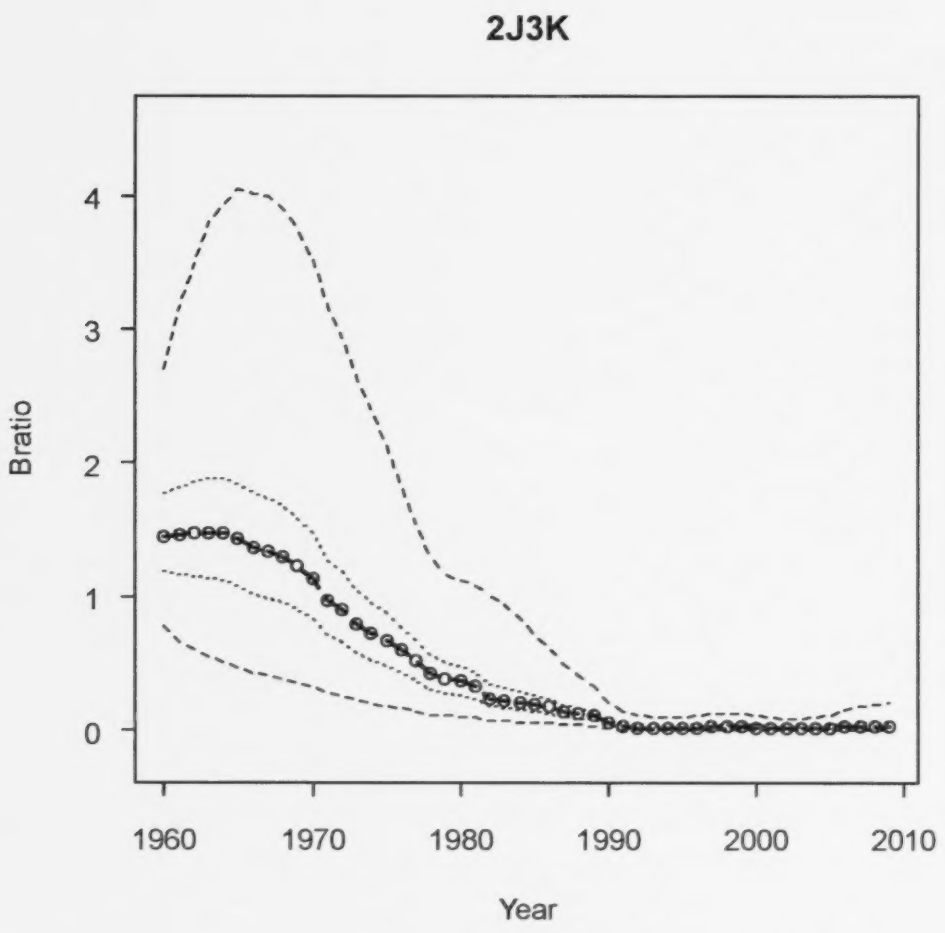

Figure 30: Schaefer surplus production model of B_{ratio} (B/B_{MSY}) from 1960-2009 (dashed line) for 2J3K American plaice. Dotted lines represent 50 % and 95 % credible intervals.

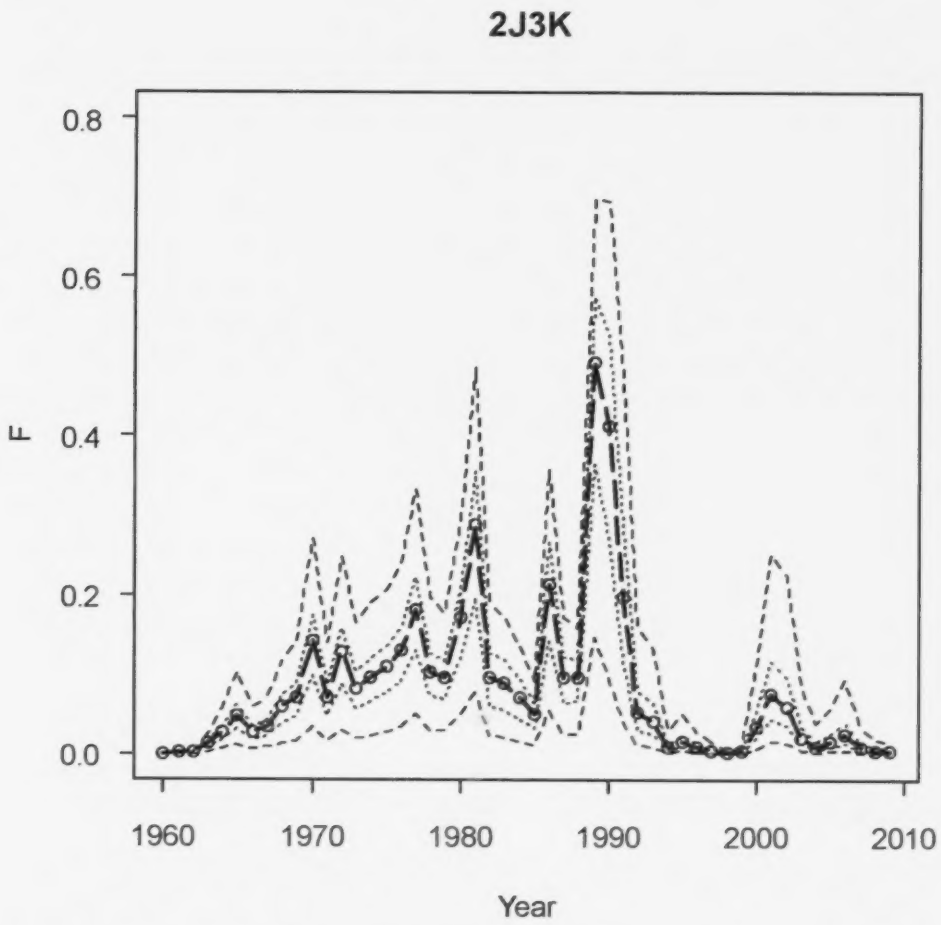

Figure 31: Modeled values for F, fisheries mortality, from 1960-2009 (dashed line) for 2J3K American plaice. Dotted lines represent 50 % and 95 % credible intervals.

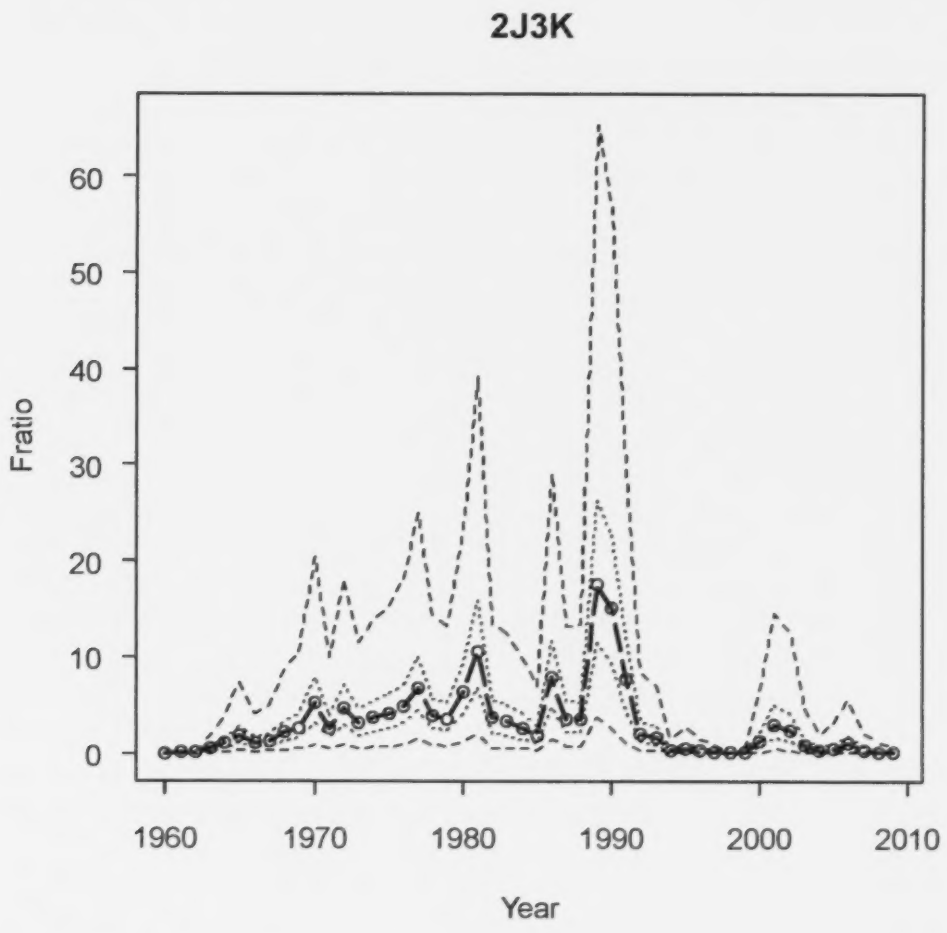

Figure 32: Modeled values for F_{ratio}, the ratio of fishing mortality to that estimated for F_{MSY}, from 1960-2009 (dashed line) for 2J3K American plaice. Dotted lines represent 50 % and 95 % credible intervals.

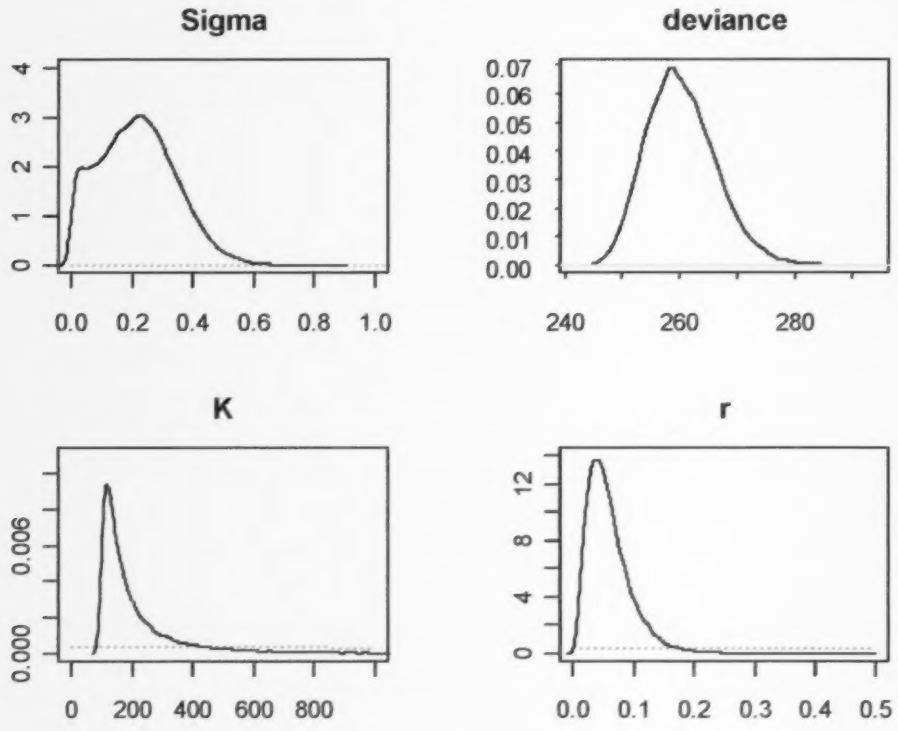

Figure 33: Posterior distributions for process error precision (Sigma), deviance, carrying capacity (K) and the intrinsic rate of population growth (r) for 2J3K American plaice. Vague prior distributions are shown for K, r and Sigma (red dotted lines).

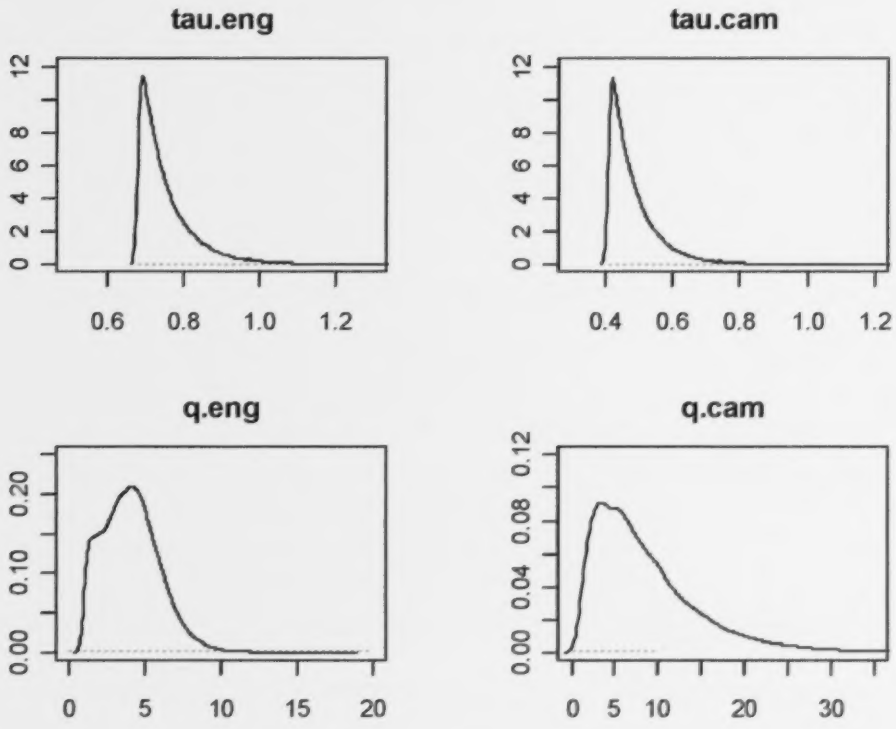

Figure 34: Posterior (solid line) and prior (red dotted line) distributions for observation error precision (tau) and catchabilities (q) for Engels and Campelen surveys for the 2J3K American plaice BSP model.

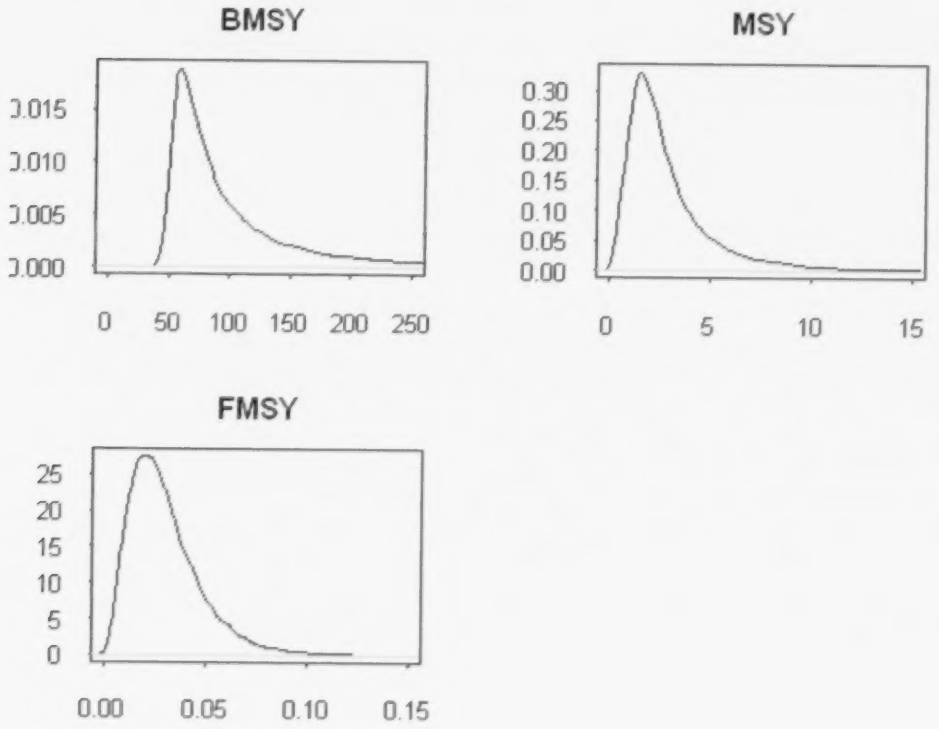

Figure 35: Posterior distributions for Maximum sustainable yield (B_{MSY}), Maximum surplus production (MSY), and F at maximum sustainable yield (F_{MSY}) for 2J3K American plaice.

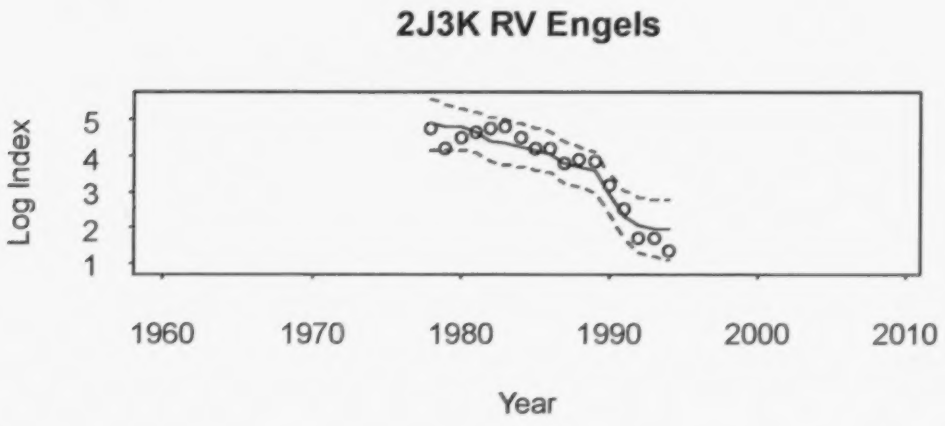

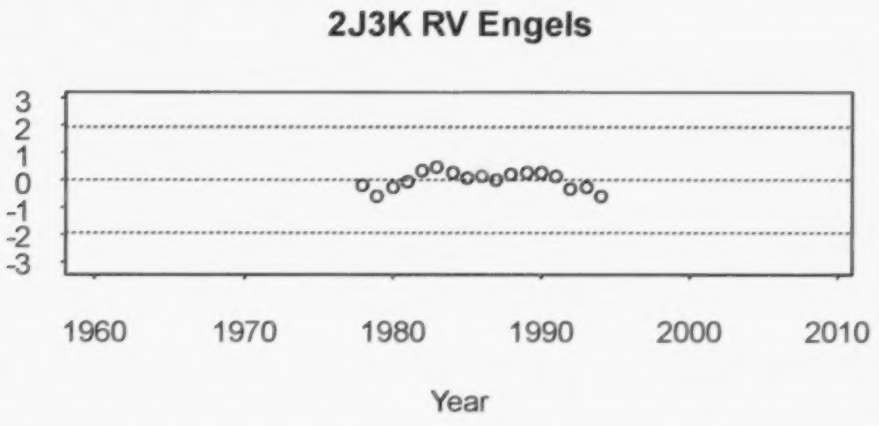

Figure 36: Engels series estimates with 95 % credible intervals (top) and residuals (bottom) for 2J3K American plaice.

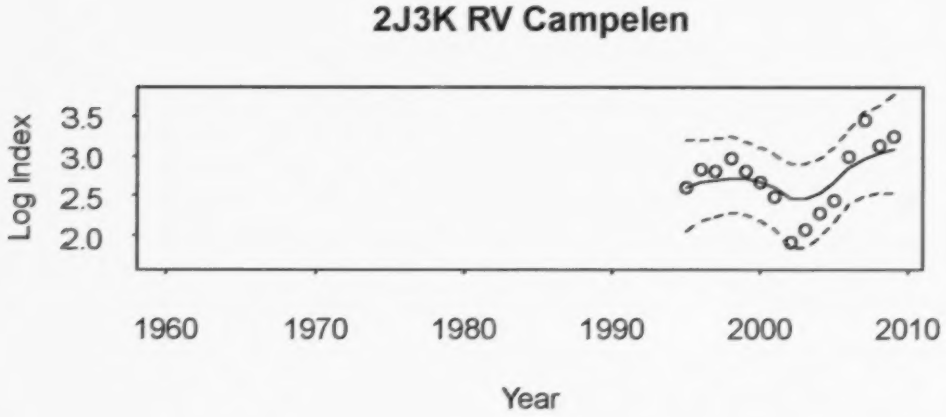

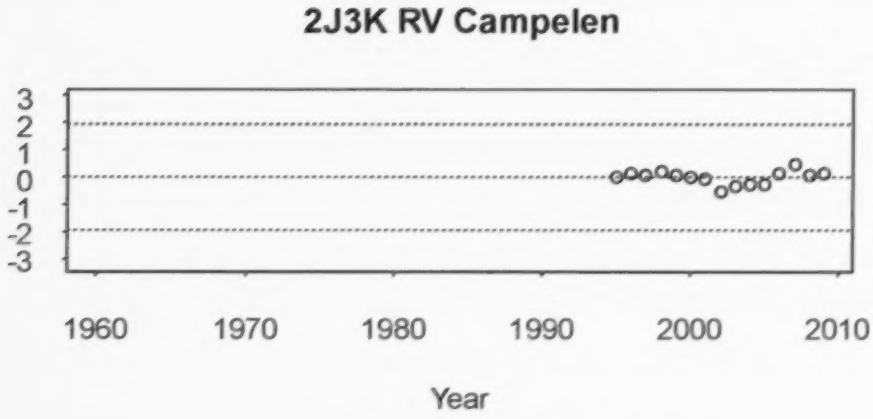

Figure 37: Campelen series estimates with 95 % credible intervals (top) and residuals (bottom) for 2J3K American plaice.

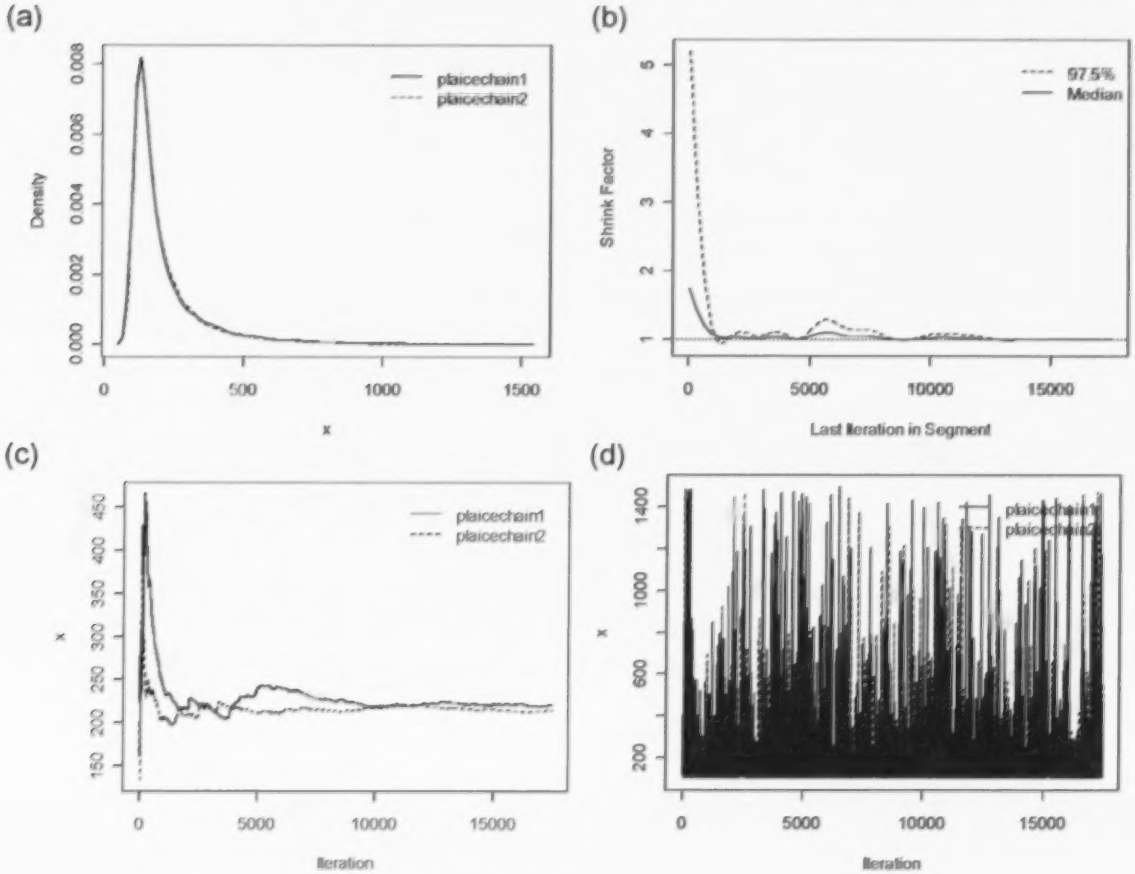

Figure 38: (a) Kernel density estimates of the posterior distribution of K for both chains in the 2J3K BSP model. (b) Gelman and Rubin shrink factors for K. (c) Sampler running mean for K. (d) A time series plot of the sampled points for K in both chains.

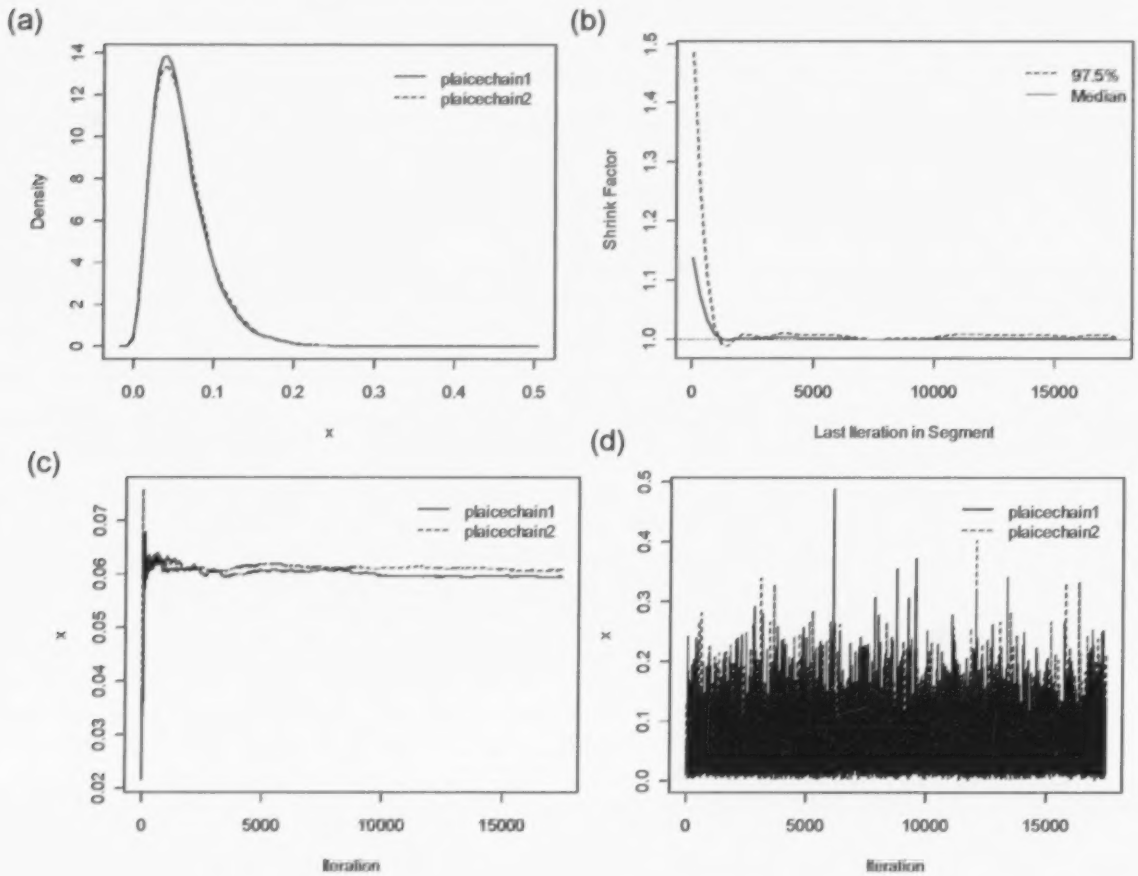

Figure 39: (a) Kernel density estimates of the posterior distribution of r for both chains in the 2J3K BSP model. (b) Gelman and Rubin shrink factors for r. (c) Sampler running mean for r. (d) A time series plot of the sampled points for r in both chains.

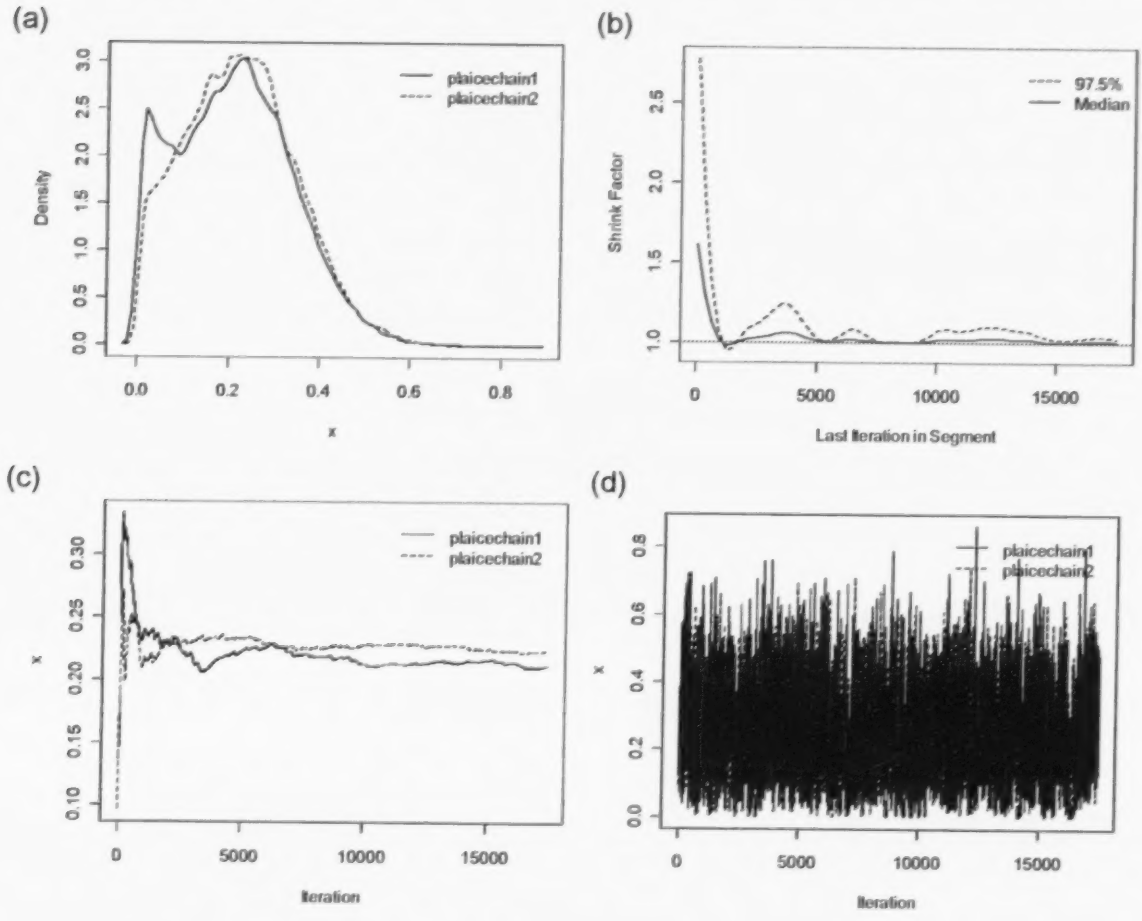

Figure 40: (a) Kernel density estimates of the posterior distribution of sigma for both chains in the 2J3K BSP model. (b) Gelman and Rubin shrink factors for sigma. (c) Sampler running mean for sigma. (d) A time series plot of the sampled points for sigma in both chains.

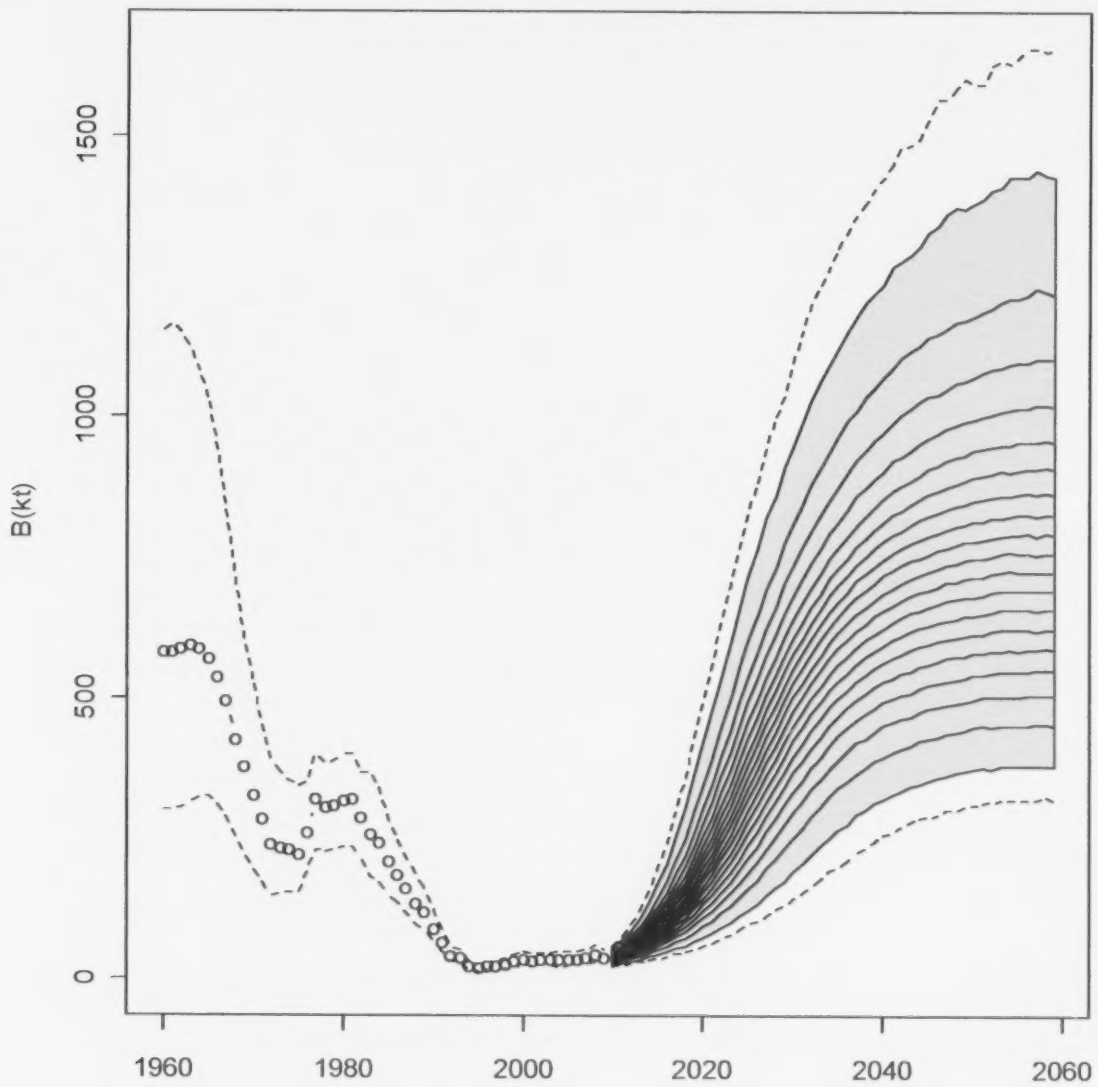

Figure 41: Bayesian surplus-production estimates of historical (1960-2009) and predicted biomass for the next 48 years in area 3LNO. Prediction period shown in red. The prediction is based on a fisheries mortality of F=0.0. Dashed lines encompass the 95 % credible intervals. The lines in the shaded area represent 5 % intervals of the probability distribution for each year and can be read as isolines on a map, with higher line density representing a larger percentage of the distribution.

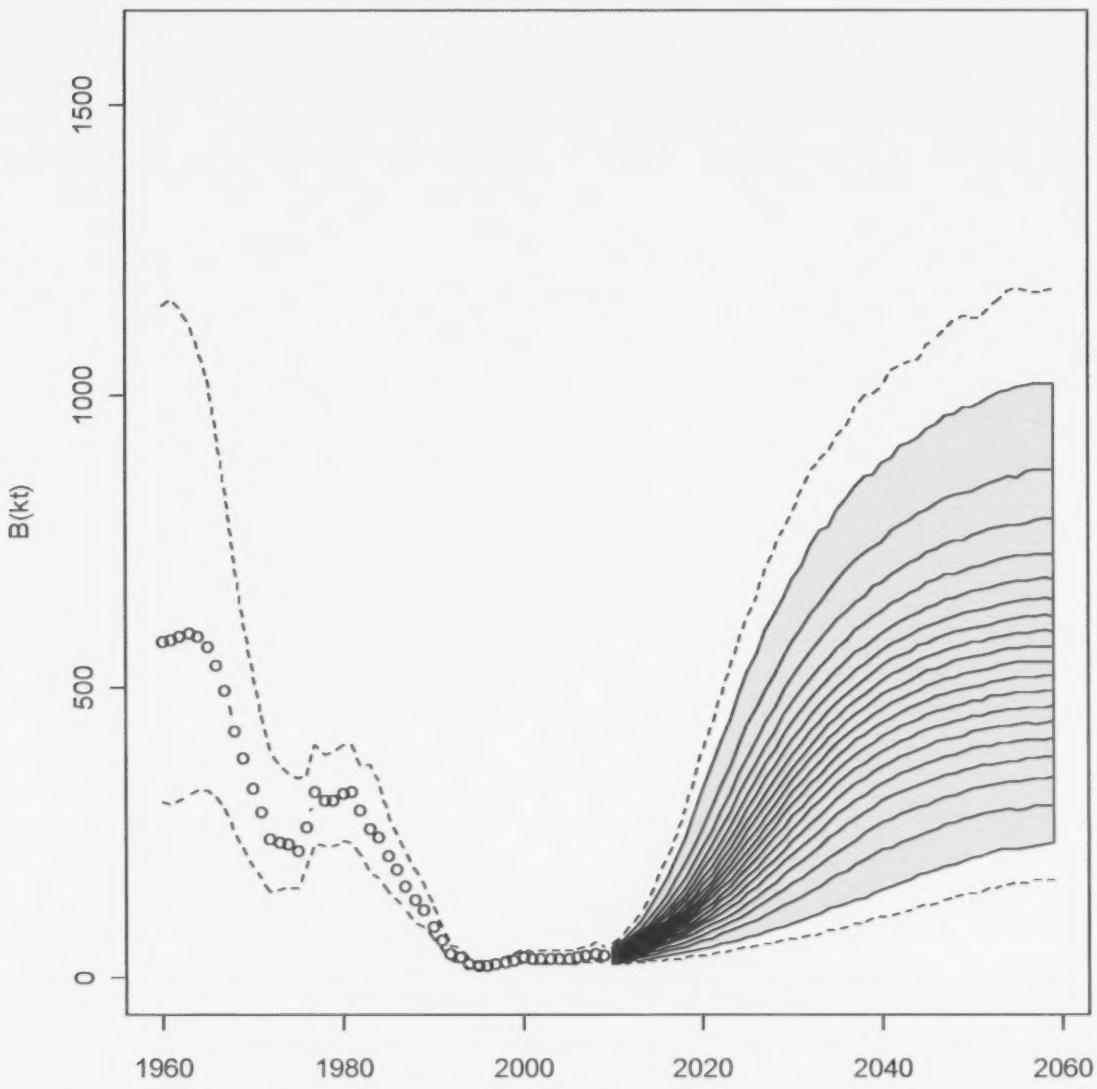

Figure 42: Bayesian surplus-production estimates of historical (1960-2009) and predicted biomass for the next 48 years in area 3LNO. Prediction period shown in red. The prediction is based on a fisheries mortality of Fcurrent=0.048. Dashed lines encompass the 95 % credible intervals. The lines in the shaded area represent 5 % intervals of the probability distribution for each year and can be read as isolines on a map, with higher line density representing a larger percentage of the distribution.

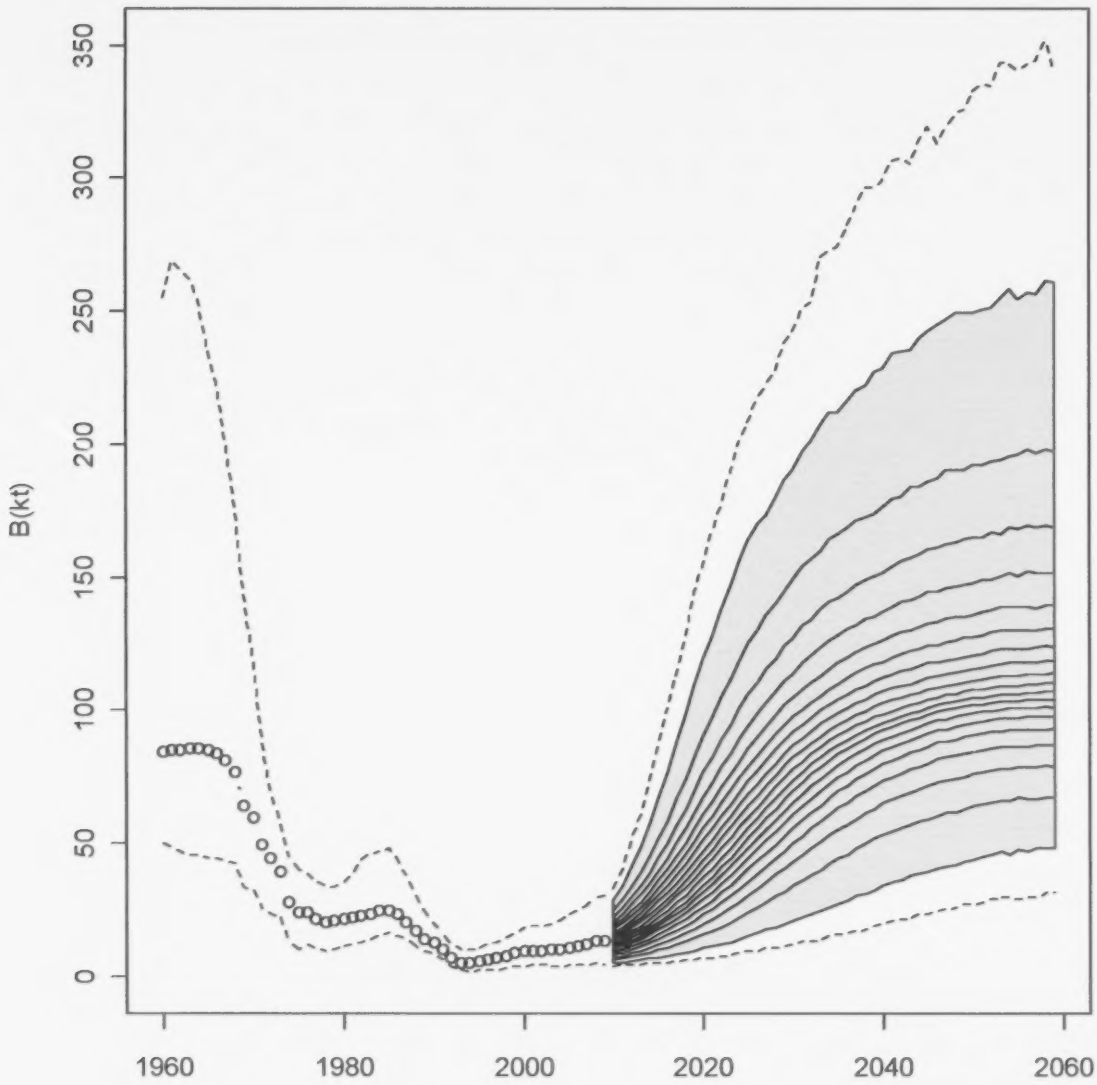

Figure 43: Bayesian surplus-production estimates of historical (1960-2009) and predicted biomass for the next 48 years in area 3Ps. The prediction is based on a fisheries mortality of F=0.0. Dashed lines encompass the 95 % credible intervals. The lines in the shaded area represent 5 % intervals of the probability distribution for each year and can be read as isolines on a map, with higher line density representing a larger percentage of the distribution.

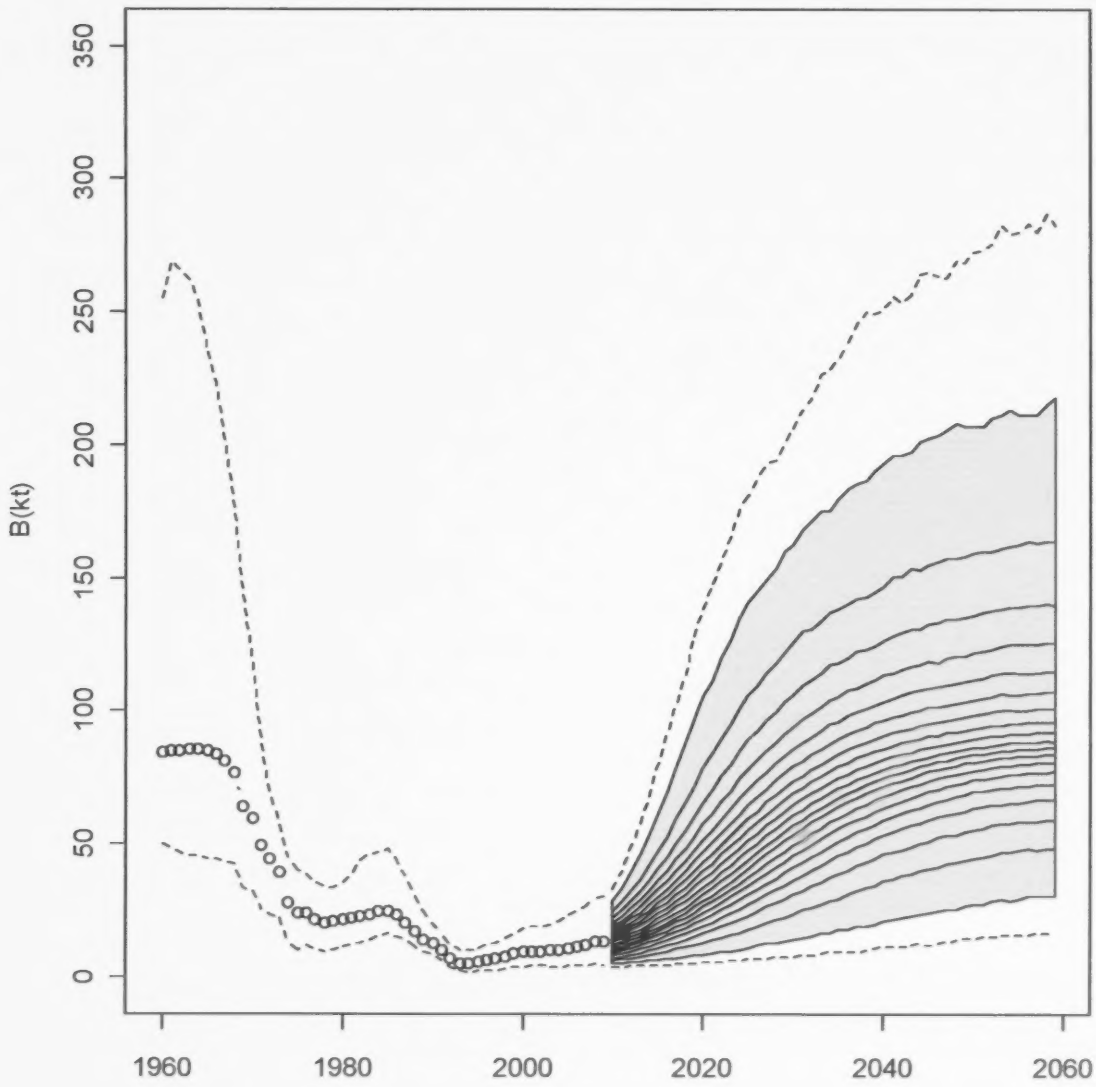

Figure 44: Bayesian surplus-production estimates of historical (1960-2009) and predicted biomass 5 for the next 48 years in area 3Ps. . The prediction is based on a fisheries mortality of Fcurrent=0.0247. Dashed lines encompass the 95 % credible intervals. The lines in the shaded area represent 5 % intervals of the probability distribution for each year and can be read as isolines on a map, with higher line density representing a larger percentage of the distribution.

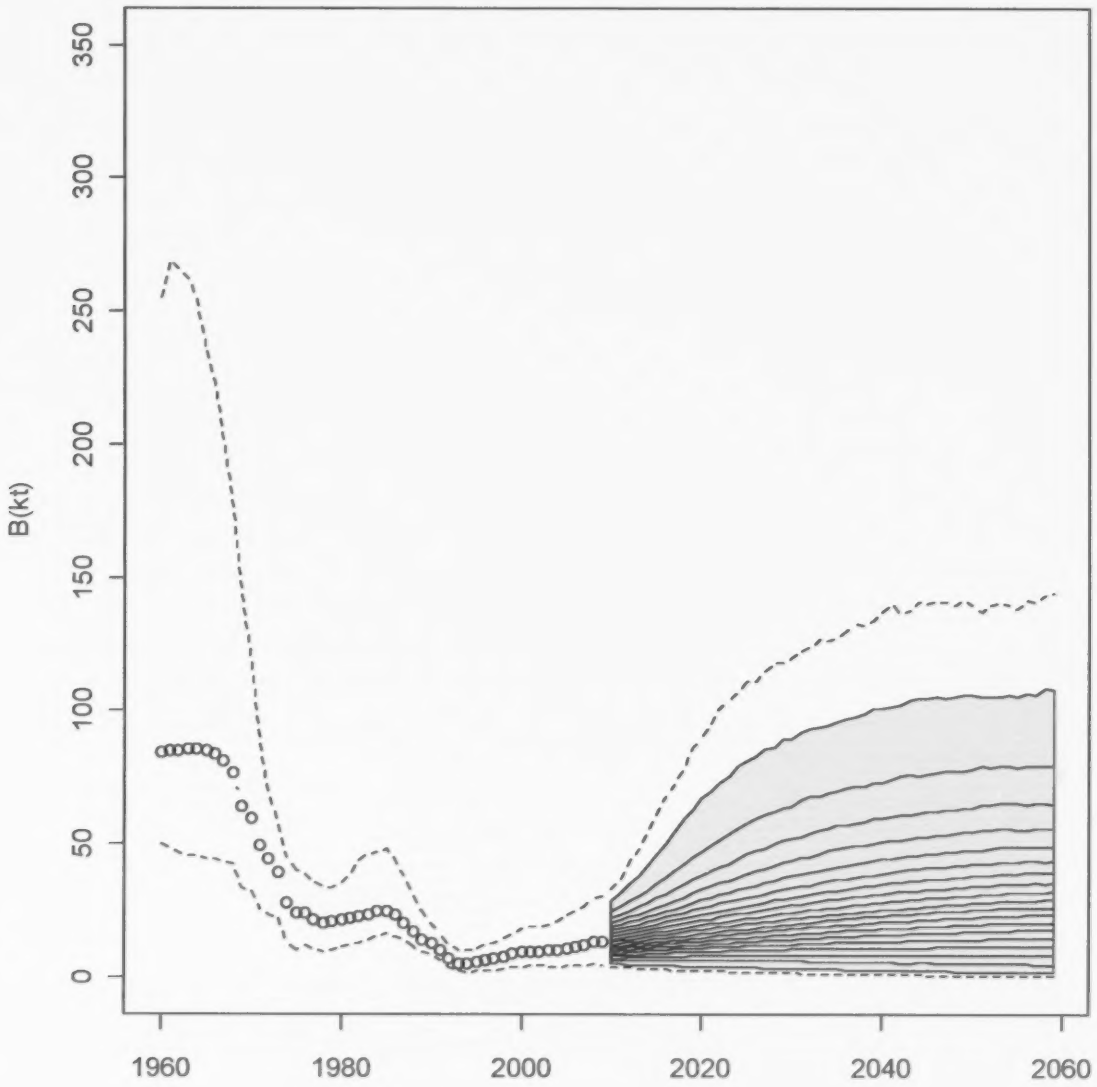

Figure 45: Bayesian surplus-production estimates of historical (1960-2009) and predicted biomass for the next 48 years in area 3Ps The prediction is based on a fisheries mortality of F=0.1. Dashed lines encompass the 95 % credible intervals. The lines in the shaded area represent 5 % intervals of the probability distribution for each year and can be read as isolines on a map, with higher line density representing a larger percentage of the distribution.

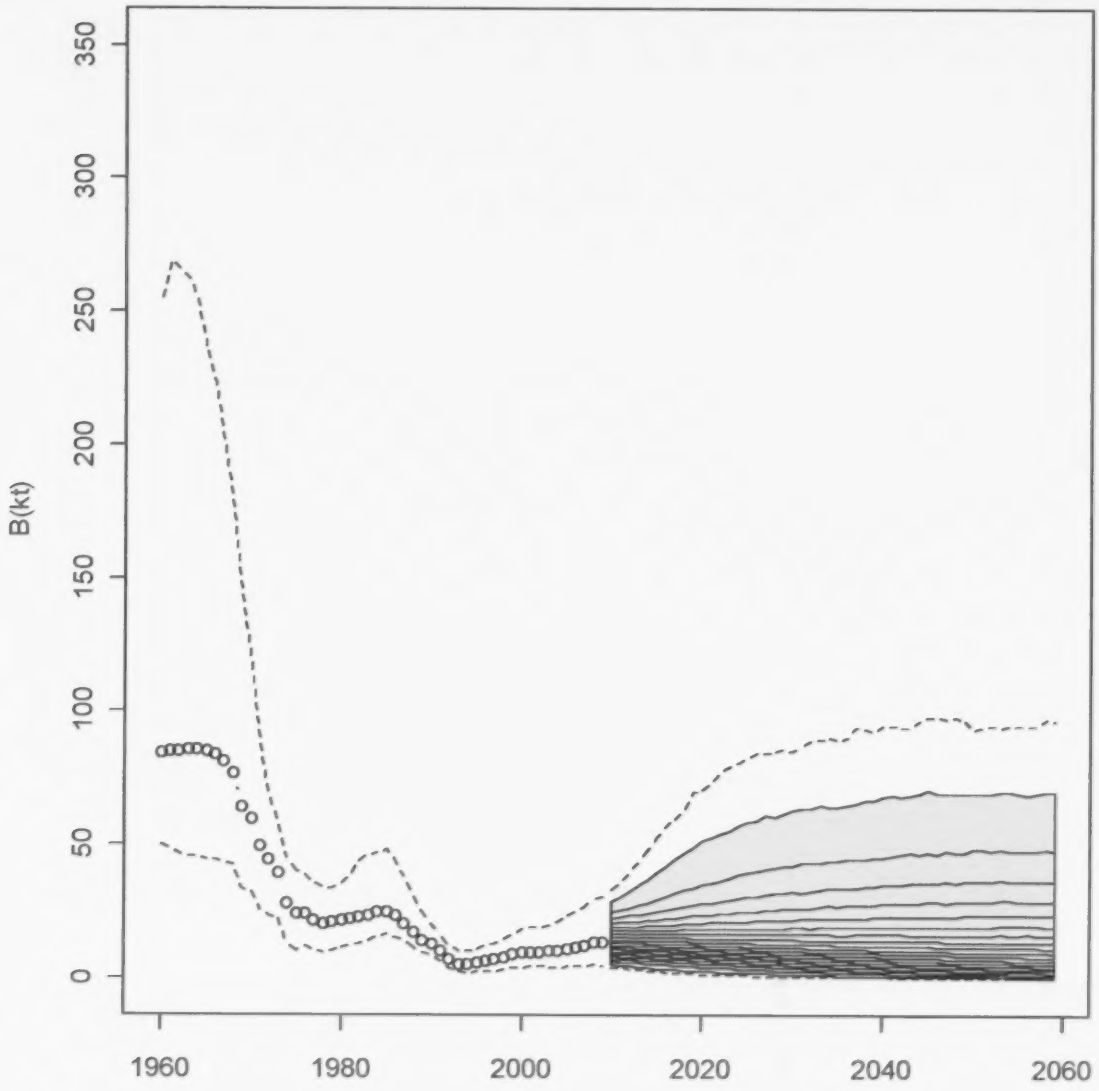

Figure 46: Bayesian surplus-production estimates of historical (1960-2009) and predicted biomass for the next 48 years in area 3Ps. Prediction period shown in red. The prediction is based on a fisheries mortality of F=0.137 (30 % decrease in stock biomass - allowable harm). Dashed lines encompass the 95 % credible intervals. The lines in the shaded area represent 5 % intervals of the probability distribution for each year and can be read as isolines on a map, with higher line density representing a larger percentage of the distribution.

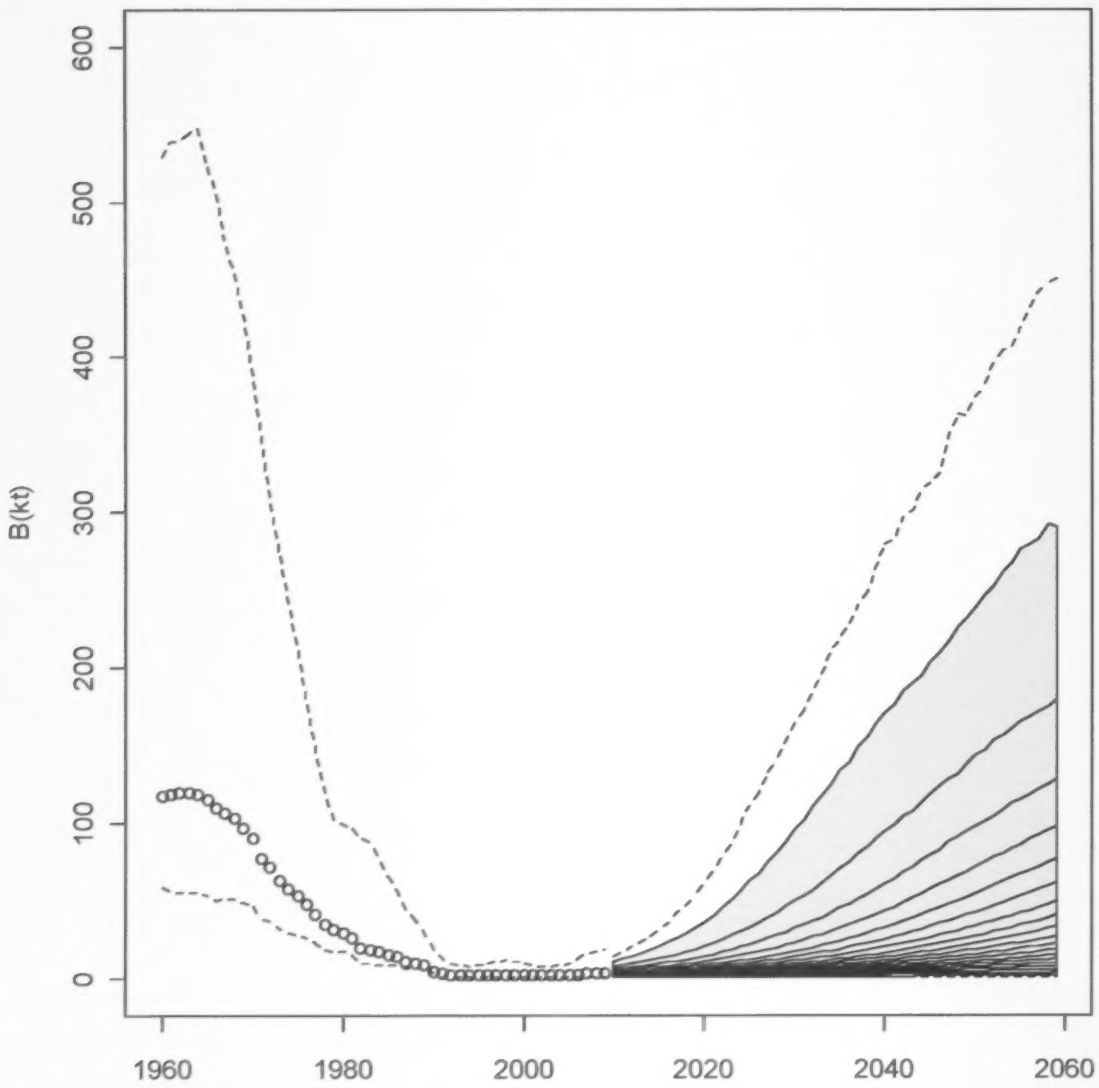

Figure 47: Bayesian surplus-production estimates of historical (1960-2009) and predicted biomass for the next 48 years in area 2J3K. Prediction period shown in red. The prediction is based on a fisheries mortality of F=0.0. Dashed lines encompass the 95 % credible intervals. The lines in the shaded area represent 5 % intervals of the probability distribution for each year and can be read as isolines on a map, with higher line density representing a larger percentage of the distribution.

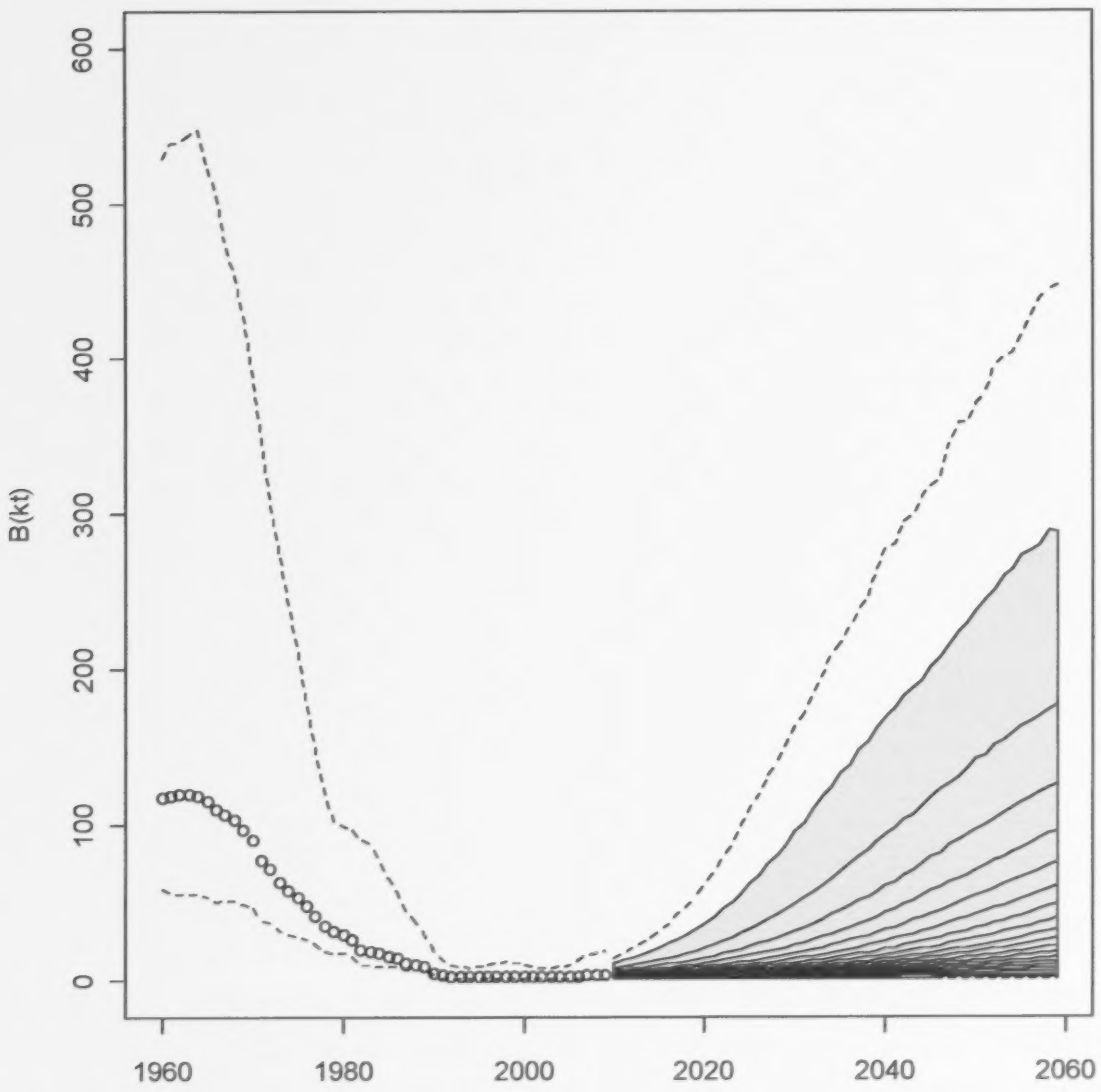

Figure 48: Bayesian surplus-production estimates of historical (1960-2009) and predicted biomass for the next 48 years in area 2J3K. Prediction period shown in red. The prediction is based on a fisheries mortality of Fcurrent=0.00055. Dashed lines encompass the 95 % credible intervals. The lines in the shaded area represent 5 % intervals of the probability distribution for each year and can be read as isolines on a map, with higher line density representing a larger percentage of the distribution.

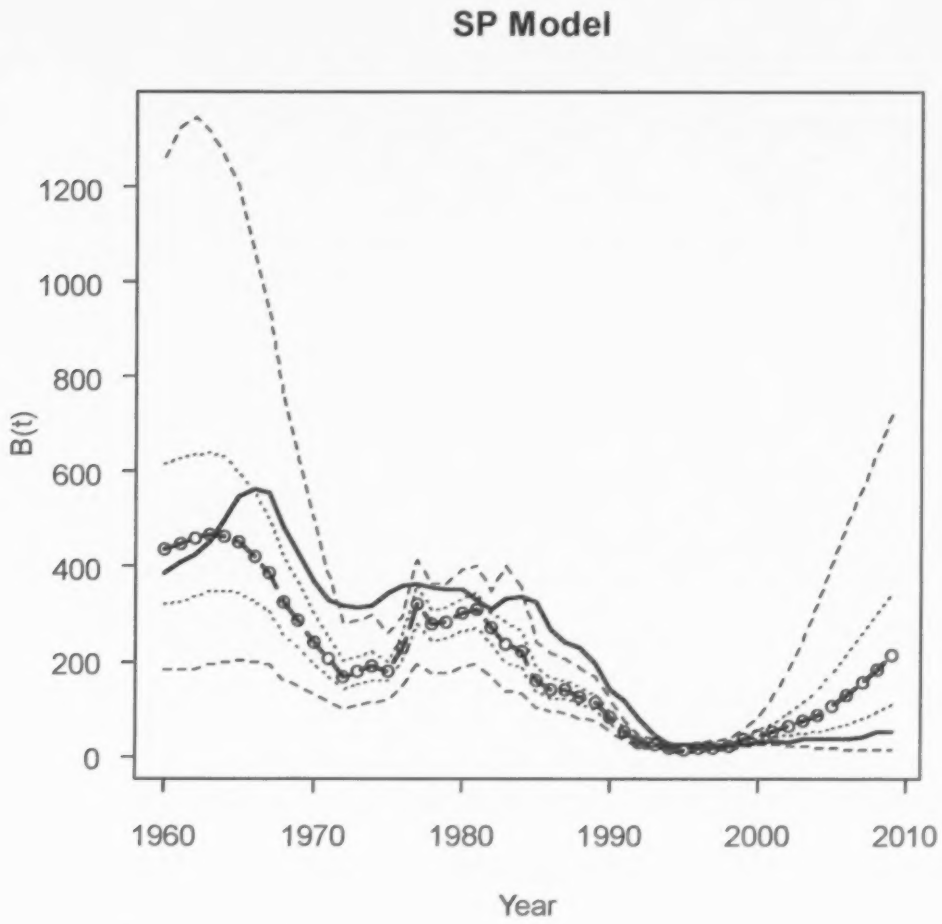

Figure 49: Schaefer surplus production model of biomass ('000t) from 1960-2009 (dashed line) for 3LNO American plaice. Dotted lines represent 50 % and 95 % credible intervals while the solid line is an age-based virtual population analysis (VPA) displayed here for comparison. The last 10 years of survey data have been removed to allow the model to predict the period between 2000-2009.

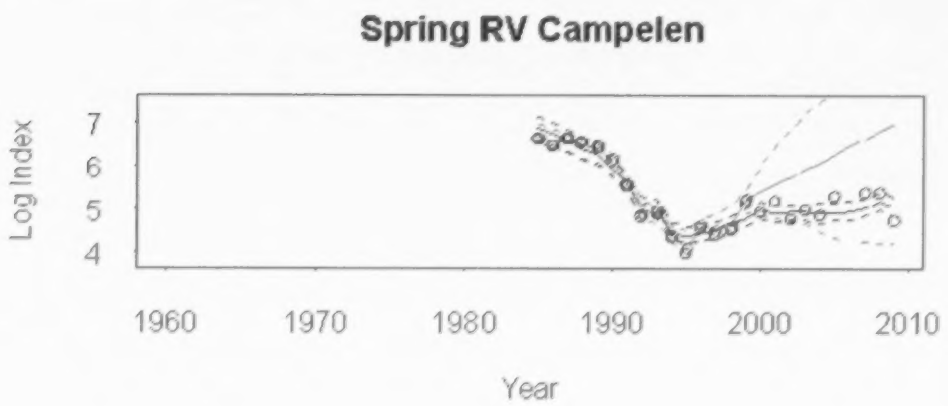

Figure 50: The "original" 3LNO Campelen Spring index model fit compared to that predicted by the SP model if the last 10 years of data are removed (shown in blue).

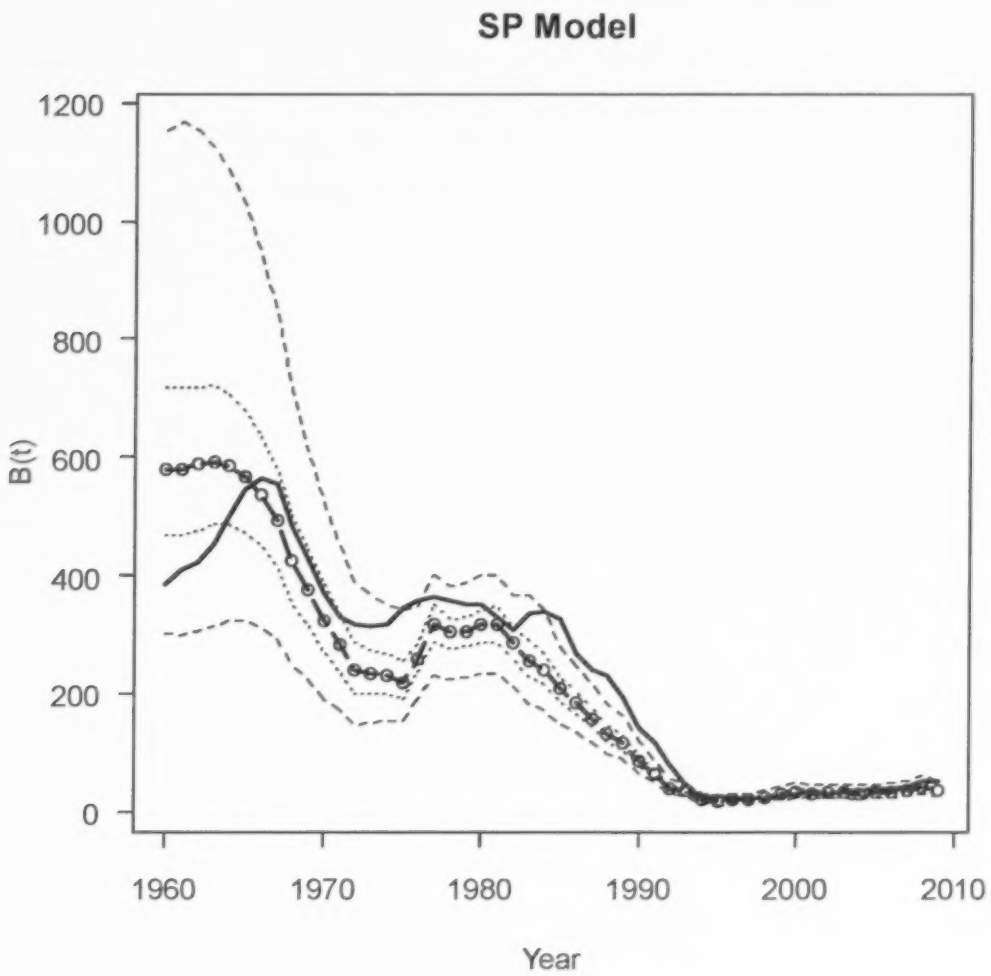

Figure 51a: Schaefer surplus production model 1 of biomass ('000t) from 1960-2009 (dashed line with circles) for 3LNO American plaice. Dotted lines represent 50 % and 95 % credible intervals while the solid line is an age-based virtual population analysis (VPA) displayed here for comparison.

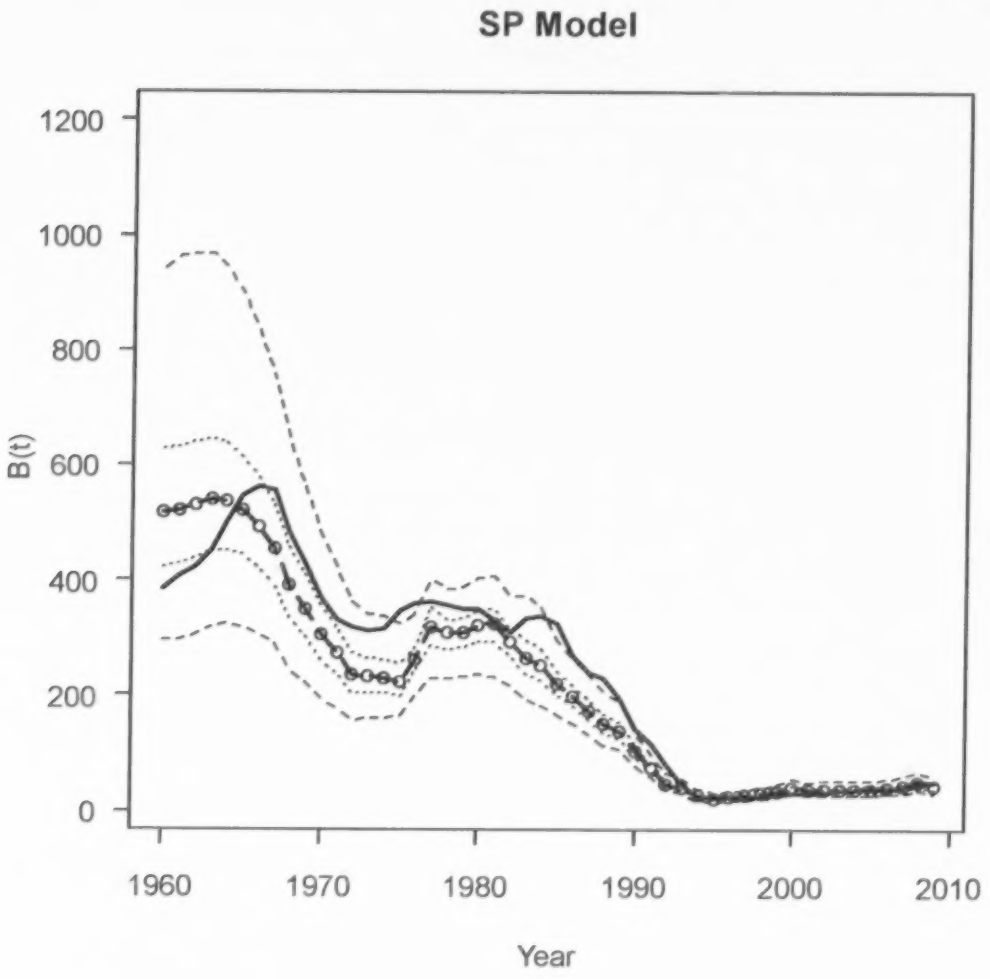

Figure 51b: Schaefer surplus production model 2 of biomass ('000t) from 1960-2009 (dashed line with circles) for 3LNO American plaice. The model divides the series into two periods (1960-1988 and 1989-2009) to estimate two levels of population productivity (r1 & r2 respectively). Dotted lines represent 50 % and 95 % credible intervals while the solid line is an age-based virtual population analysis (VPA) Displayed here for comparison.

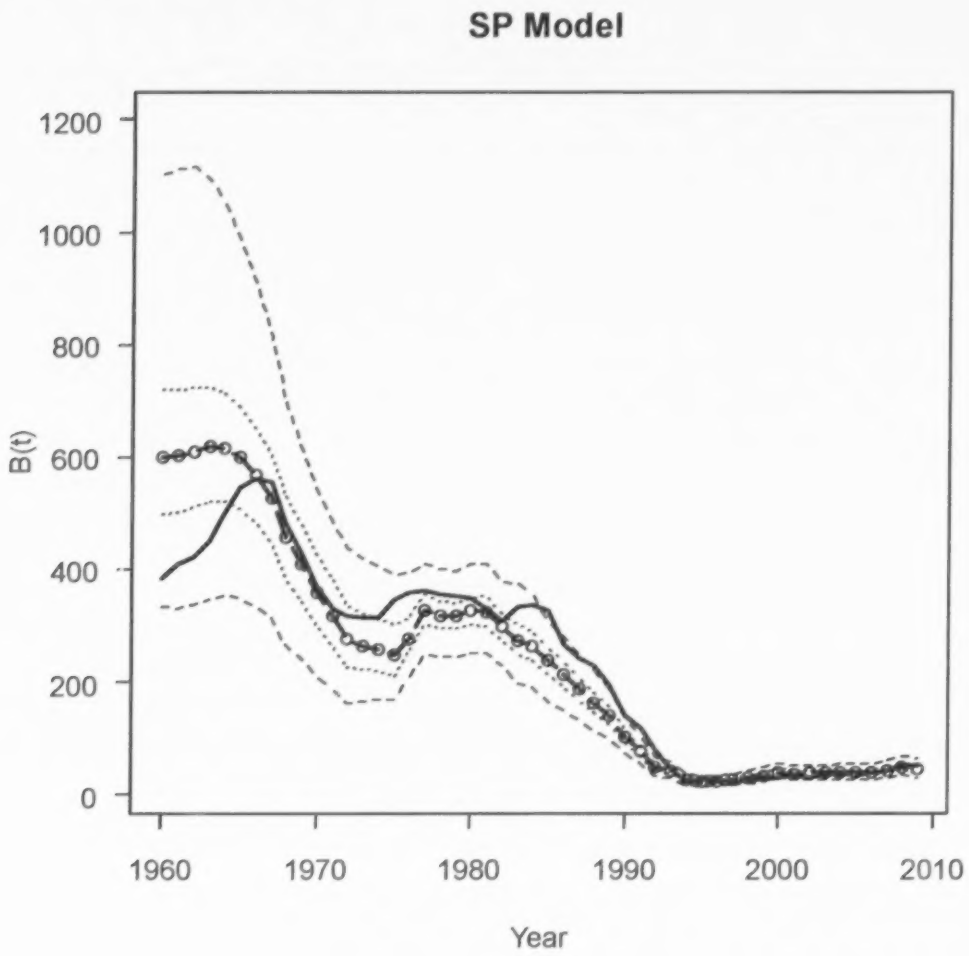

Figure 51c: Schaefer surplus production model 3 of biomass ('000t) from 1960-2009 (dashed line with circles) for 3LNO American plaice. The model divides the series into three periods (1960-1988, 1989-1996, & 1997-2009) to estimate two levels of population productivity, r1 & r2, where r1 represents 1960-1988 & 1997-2009; r2 is estimated using 1989-1996 data. Dotted lines represent 50 % and 95 % credible intervals while the solid line is an age-based virtual population analysis (VPA) displayed here for comparison.

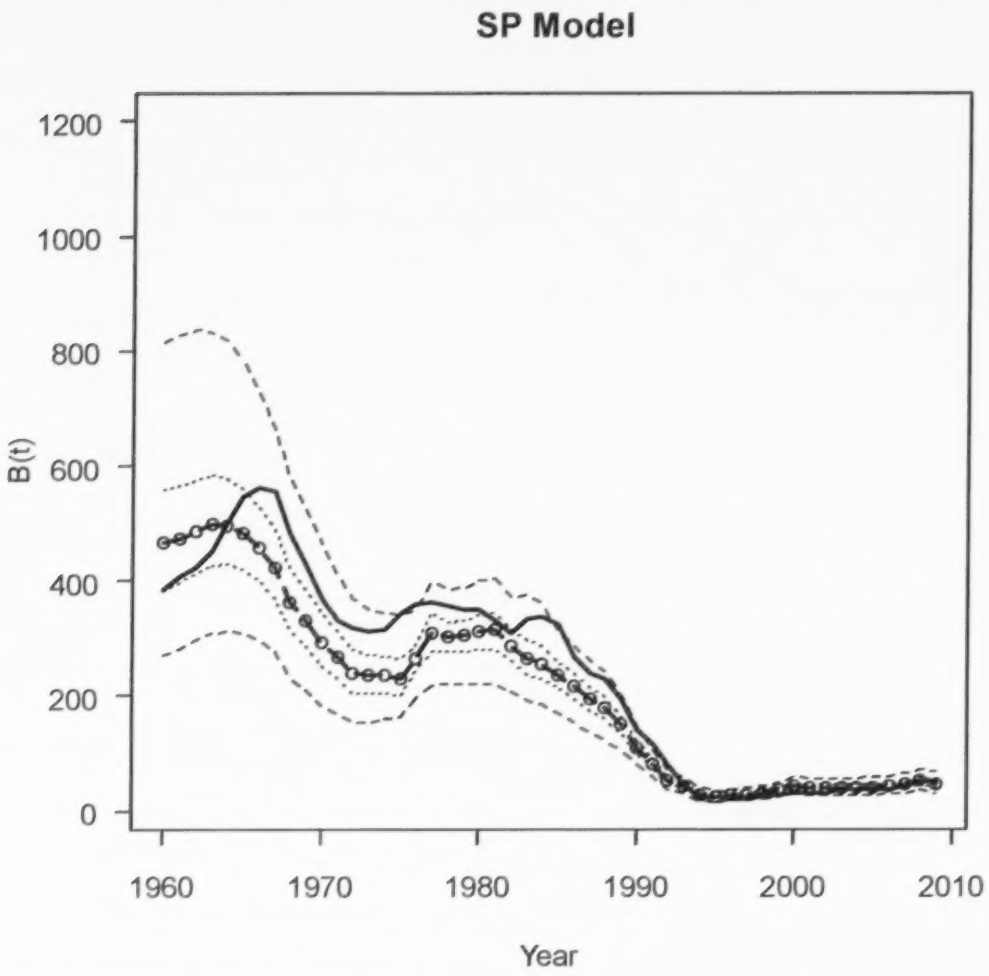

Figure 51d: Schaefer surplus production model 4 of biomass ('000t) from 1960-2009 (dashed line with circles) for 3LNO American plaice. The model divides the series into three periods (1960-1988, 1989-1996, & 1997-2009) to estimate three levels of population productivity (r1, r2, & r3 respectively). Dotted lines represent 50 % and 95 % credible intervals while the solid line is an age-based virtual population analysis (VPA) displayed here for comparison.

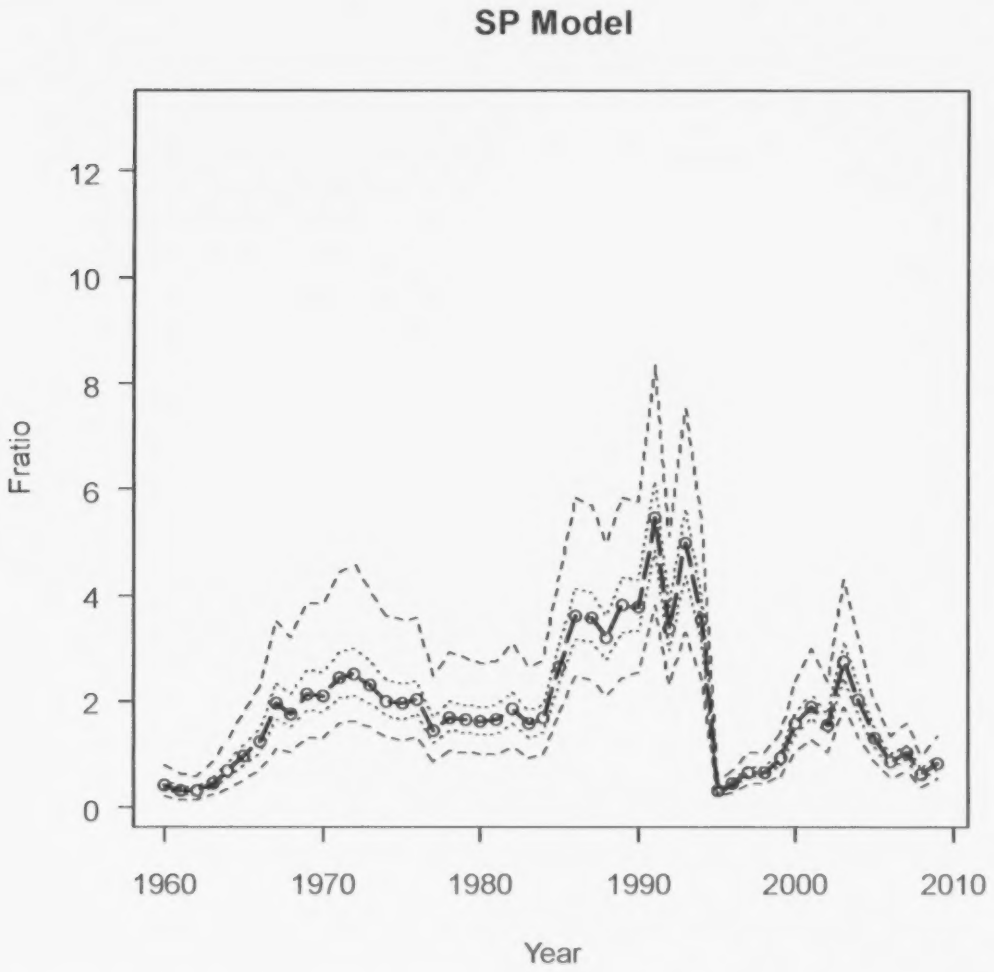

Figure 52a: Model 1 estimates of the F_{ratio}, the ratio of fishing mortality to that estimated for F_{MSY}, from 1960-2009 (dashed line with circles) for 3LNO American plaice. Dotted lines represent 50 % and 95 % credible intervals.

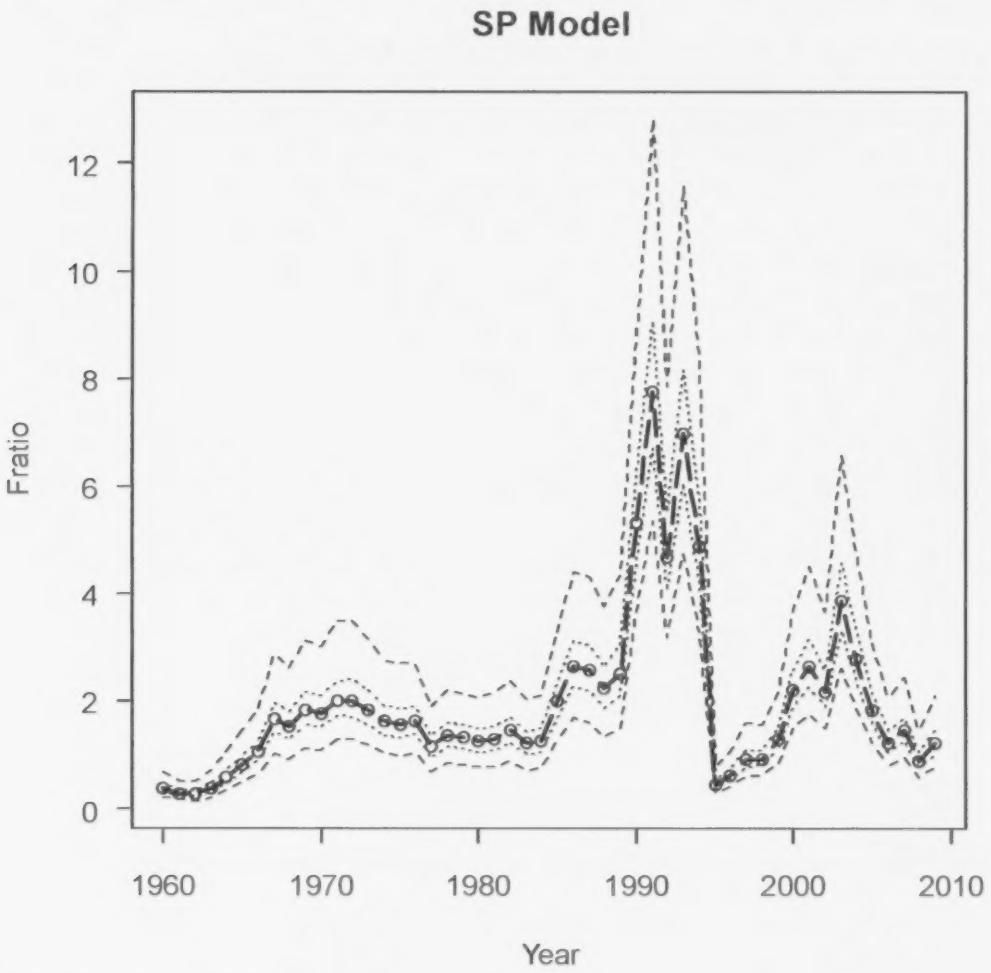

Figure 52b: Model 2 estimates of the F_{ratio}, the ratio of fishing mortality to that estimated for F_{MSY}, from 1960-2009 (dashed line with circles) for 3LNO American plaice. Dotted lines represent 50 % and 95 % credible intervals.

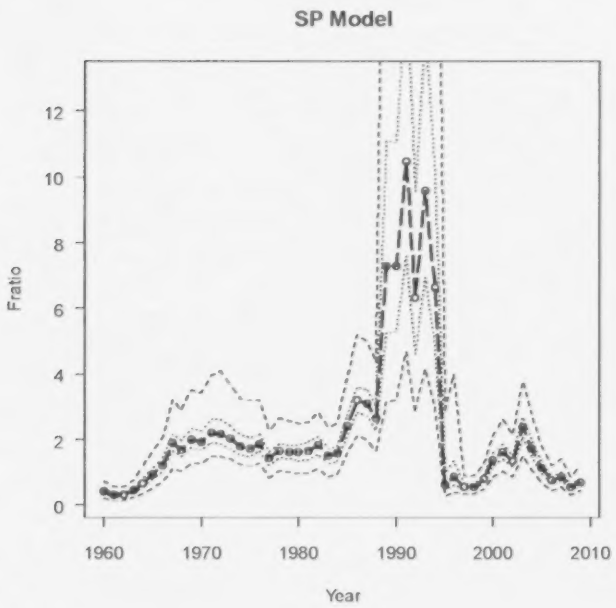

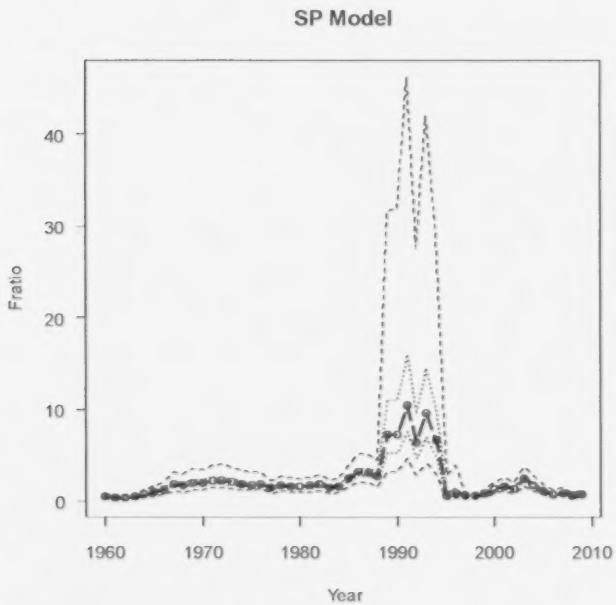

Figure 52c: Model 3 estimates of the F_{ratio}, the ratio of fishing mortality to that estimated for F_{MSY}, from 1960-2009 (dashed line with circles) for 3LNO American plaice. Dotted lines represent 50 % and 95 % credible intervals. Both panels show the same data with the above panel on the same scale as figures 2a-b for comparison.

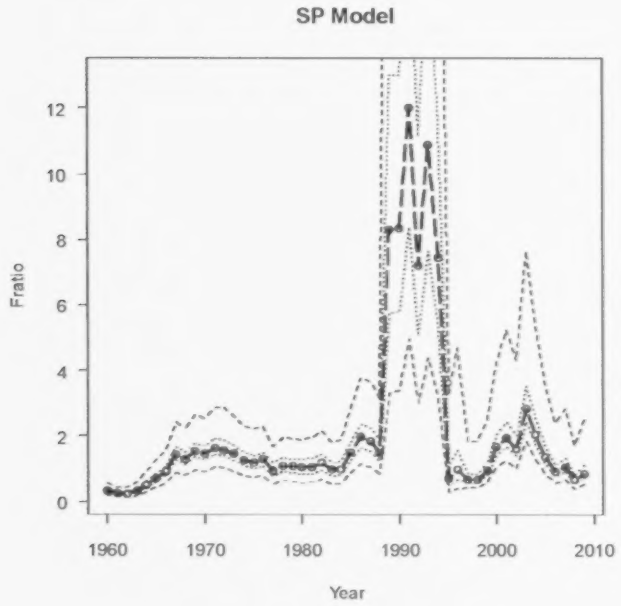

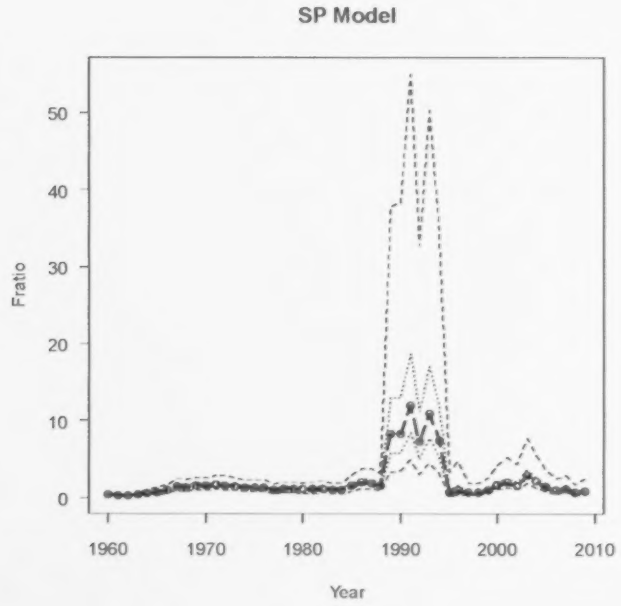

Figure 52d: Model 4 estimates of the F_{ratio}, the ratio of fishing mortality to that estimated for F_{MSY}, from 1960-2009 (dashed line with circles) for 3LNO American plaice. Dotted lines represent 50 % and 95 % credible intervals. Both panels show the same data with the above panel on the same scale as figures 2a-b for comparison.

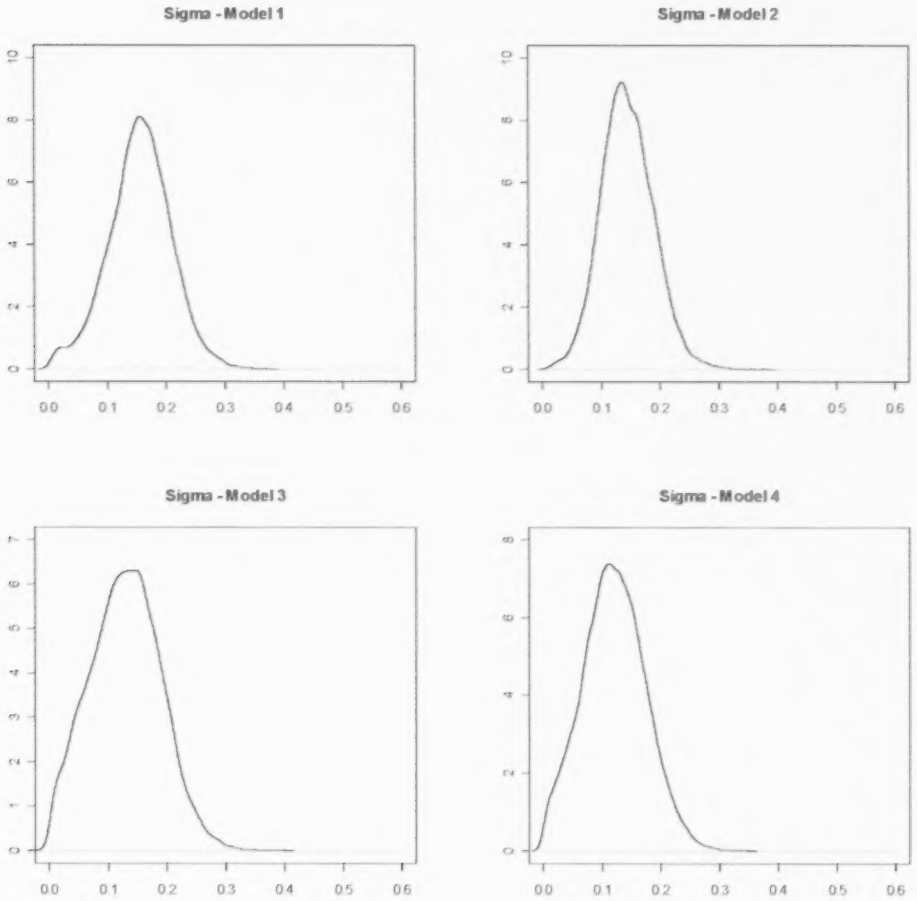

Figure 53: Posterior distributions for process error precision (Sigma) for models 1-4 in 3LNO American plaice. Prior distributions are illustrated using red dotted lines.

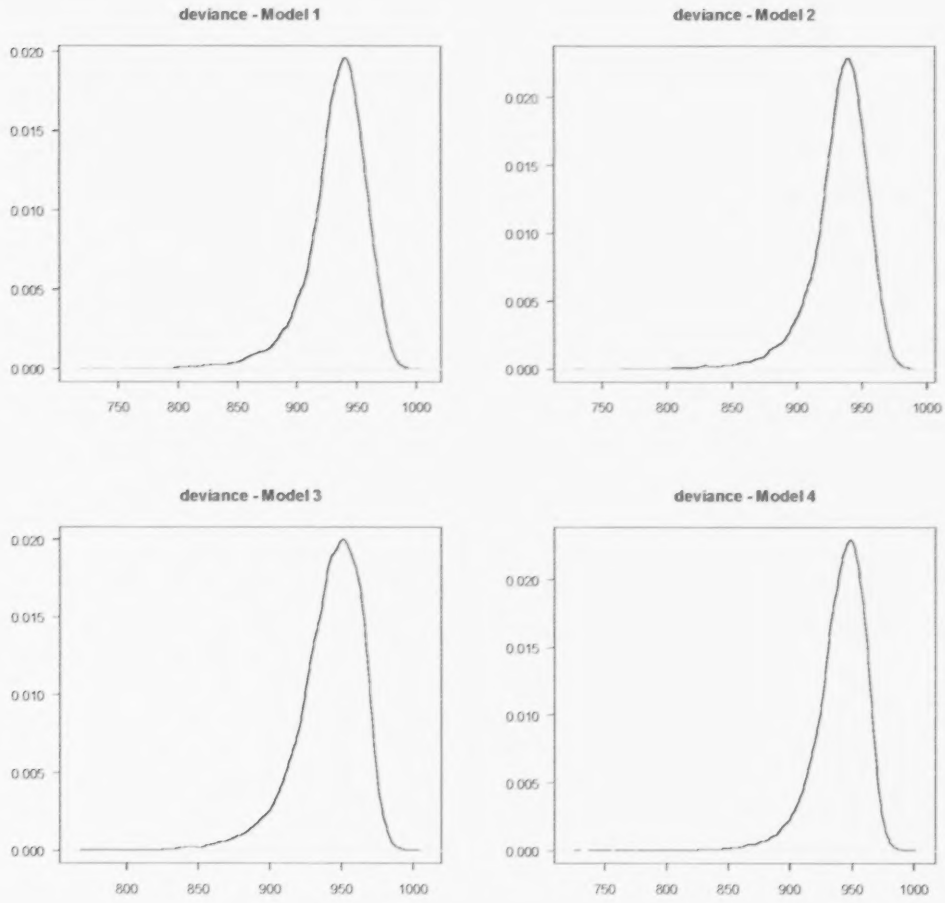

Figure 54: Posterior distributions for deviance in models 1-4 for 3LNO American plaice.

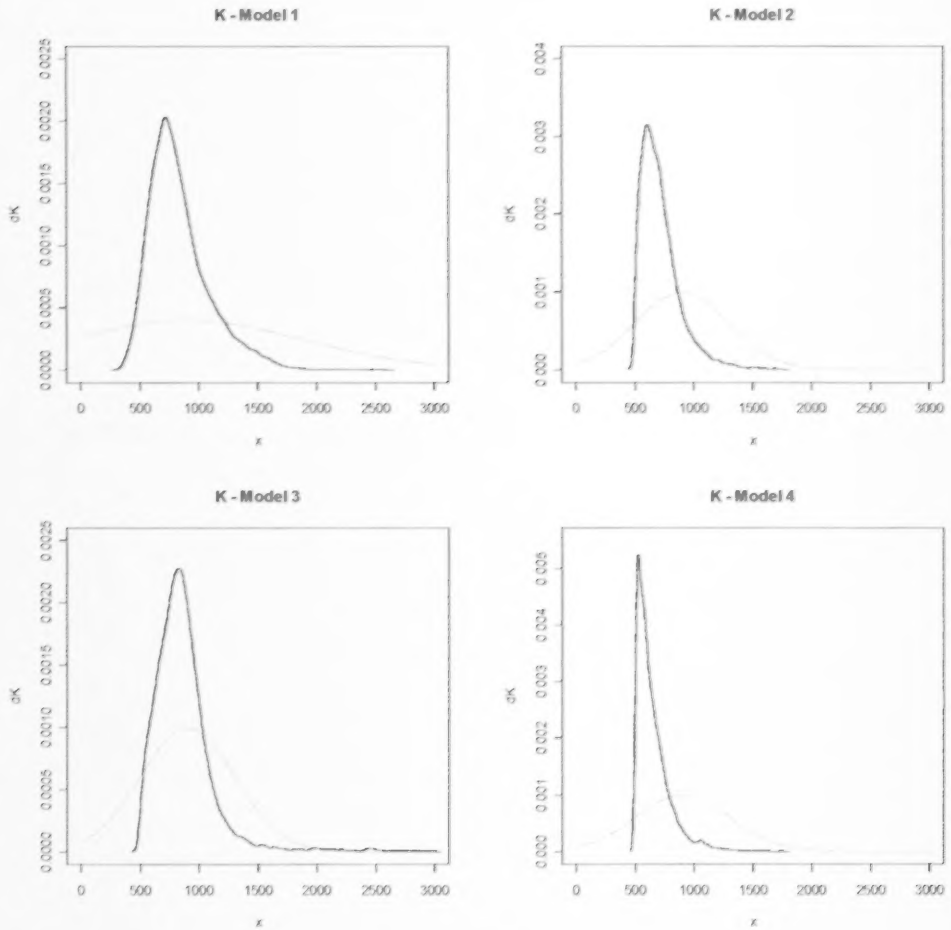

Figure 55: Posterior distributions for K, carrying capacity, for models 1-4 in 3LNO American plaice. Prior distributions are illustrated using red dotted lines.

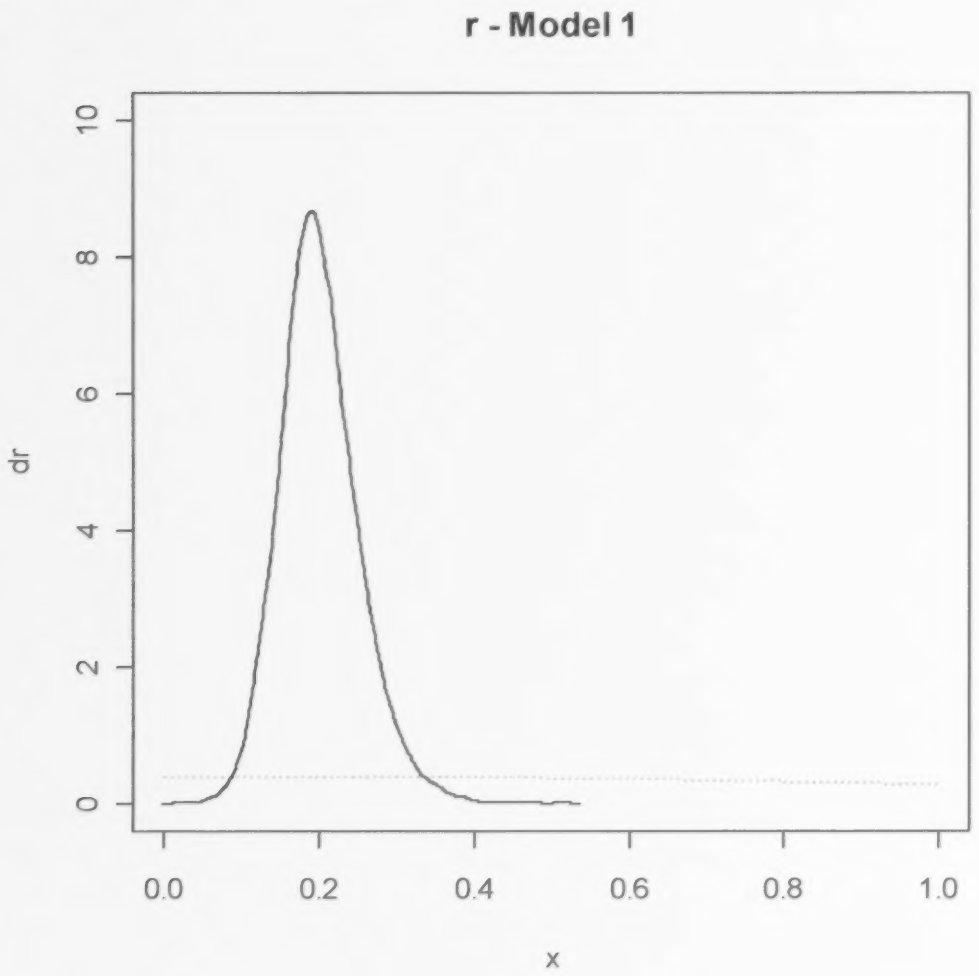

Figure 56: Posterior distribution of r, the intrinsic rate of population growth, for model 1 in 3LNO American plaice. The prior distribution is illustrated using a red dotted line.

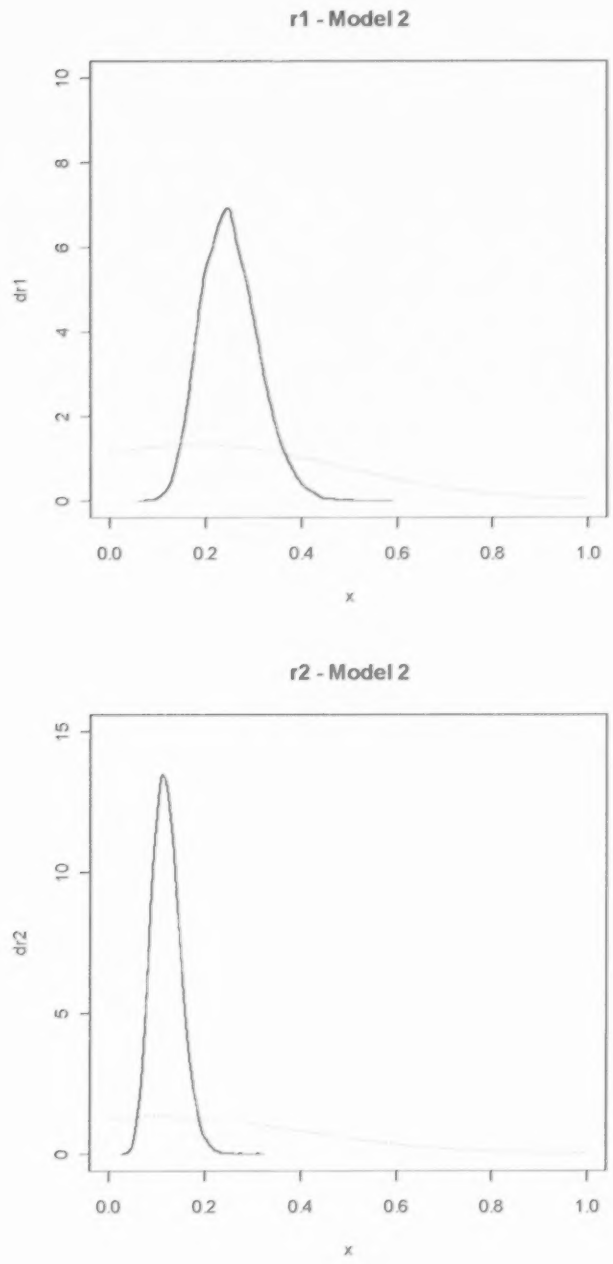

Figure 57: Posterior distributions of r, the intrinsic rate of population growth, for model 2 in 3LNO American plaice. In this model, the series is divided into two periods (1960-1988 & 1989-2009) represented by r1 and r2 respectively. Prior distributions are illustrated using red dotted lines.

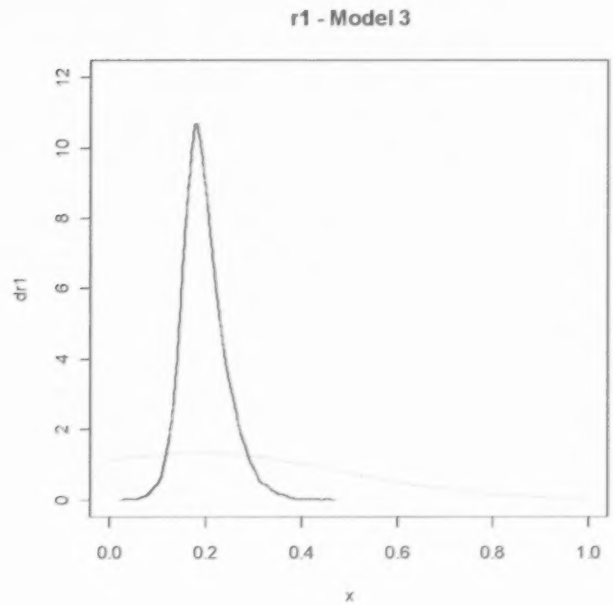

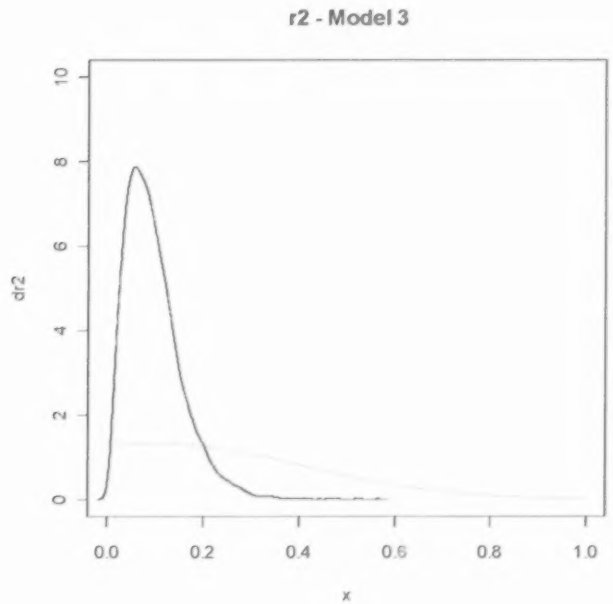

Figure 58: Posterior distributions of r, the intrinsic rate of population growth, for model 3 in 3LNO American plaice. The model divides the series into three periods (1960-1988, 1989-1996, & 1997-2009) to estimate two levels of population productivity, r1 & r2, where r1 represents 1960-1988 & 1997-2009; r2 is estimated using data from 1989-1996. Prior distributions are illustrated using red dotted lines.

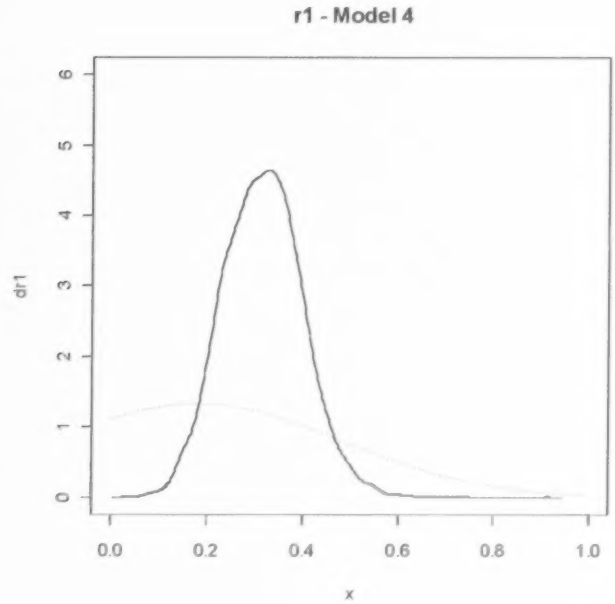

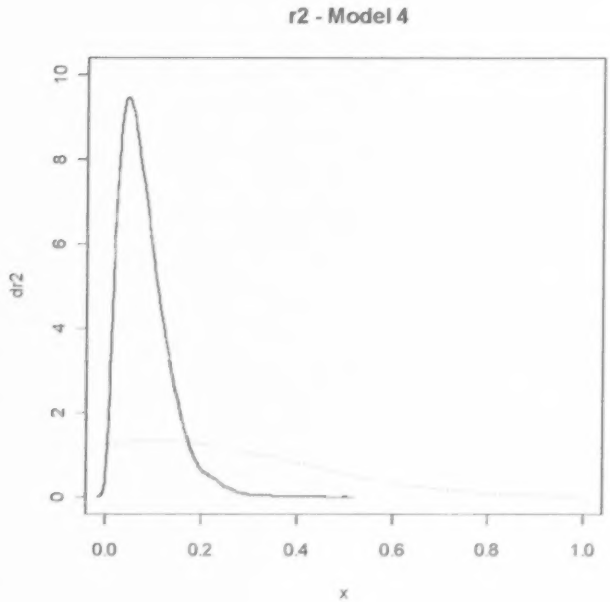

Figure 59a-b: Posterior distributions of r, the intrinsic rate of population growth, for model 4 in 3LNO American plaice. The model divides the series into three periods (1960-1988, 1989-1996, & 1997-2009) to estimate three levels of population productivity (r1, r2, & r3 respectively).. Prior distributions are illustrated using red dotted lines.

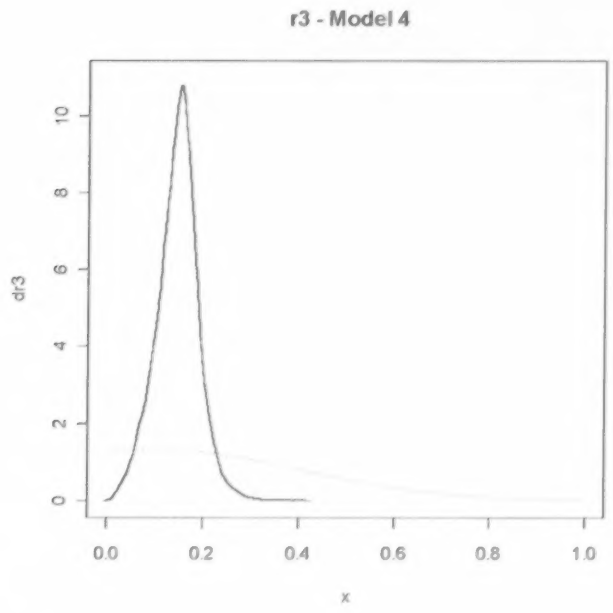

Figure 59c: Posterior distributions of r, the intrinsic rate of population growth, for model 4 in 3LNO American plaice. The model divides the series into three periods (1960-1988, 1989-1996, & 1997-2009) to estimate three levels of population productivity (r1, r2, & r3 respectively). Prior distributions are illustrated using red dotted lines.

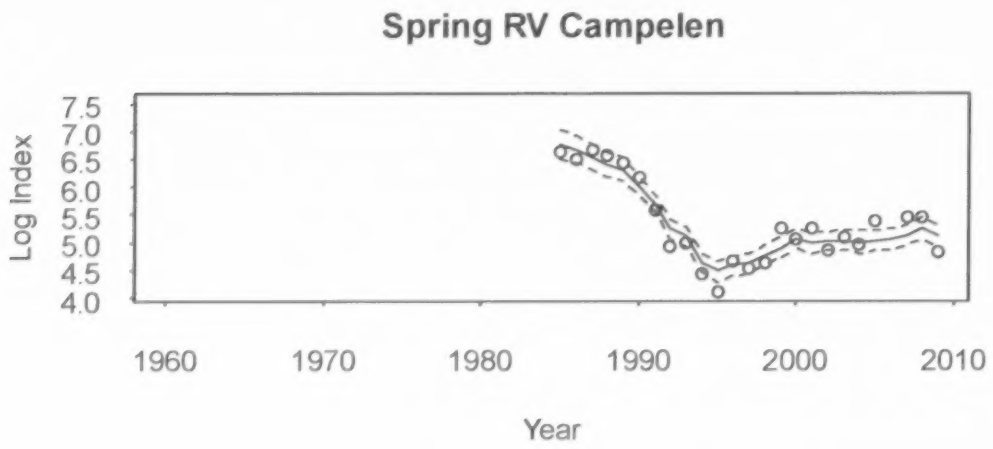

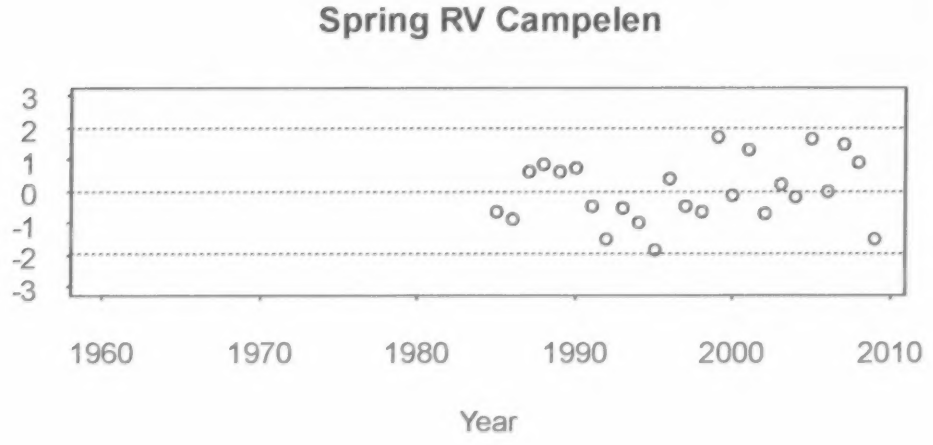

Figure 60a: Converted Spring Campelen series estimates with 95 % credible intervals (top) and standardized residuals (bottom) for 3LNO American plaice. Figures illustrate fit from model 2.

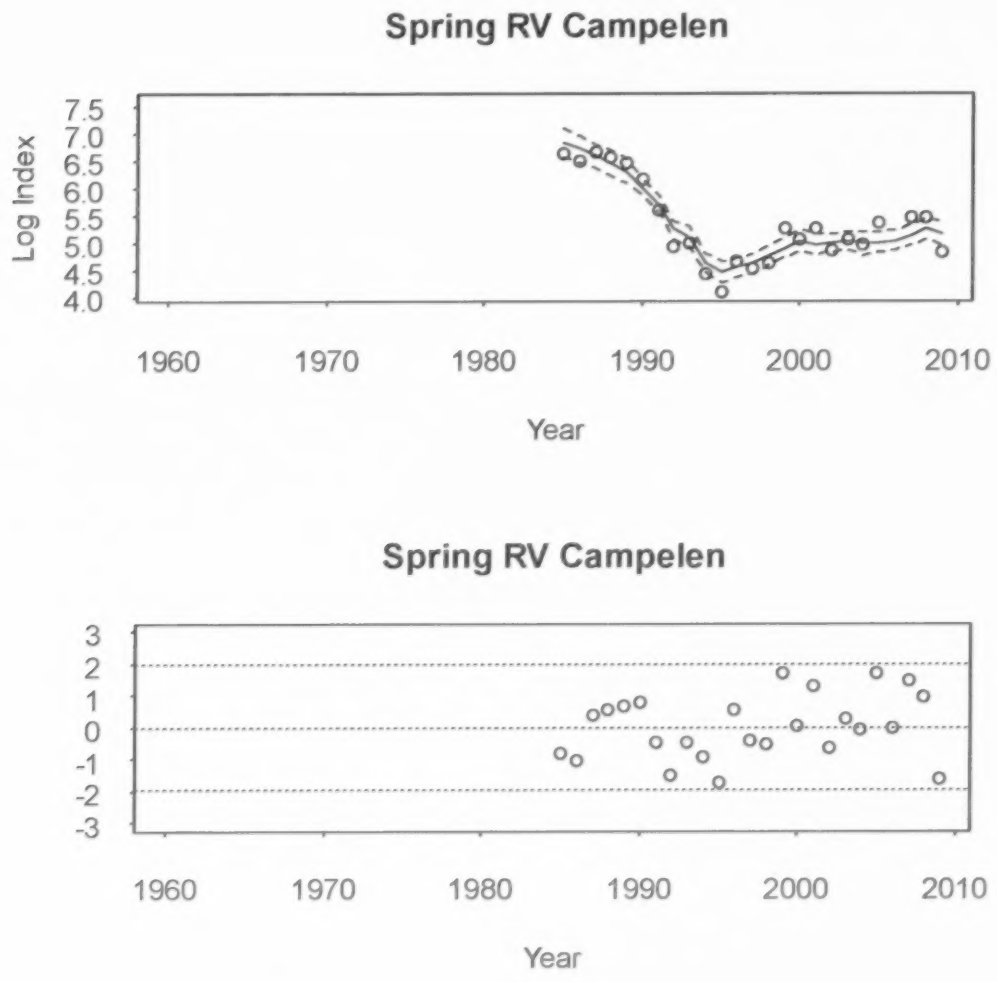

Figure 60b: Converted Spring Campelen series estimates with 95 % credible intervals (top) and standardized residuals (bottom) for 3LNO American plaice. Figures illustrate fit from model 3.

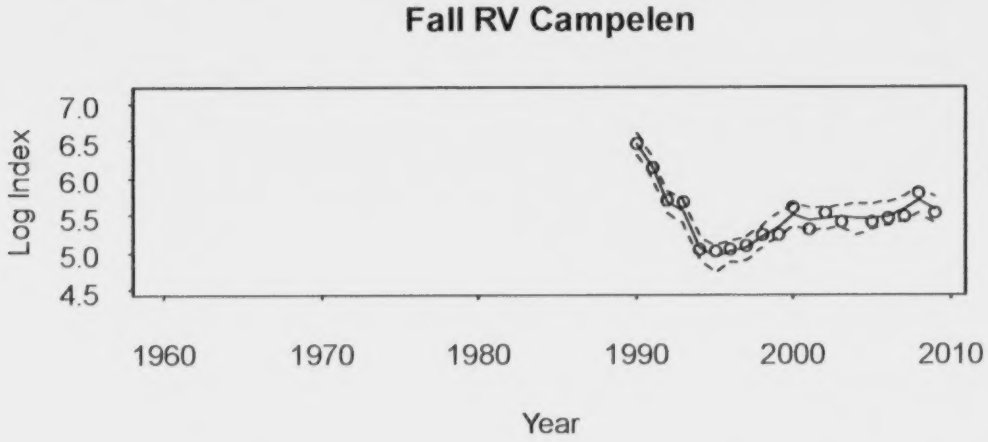

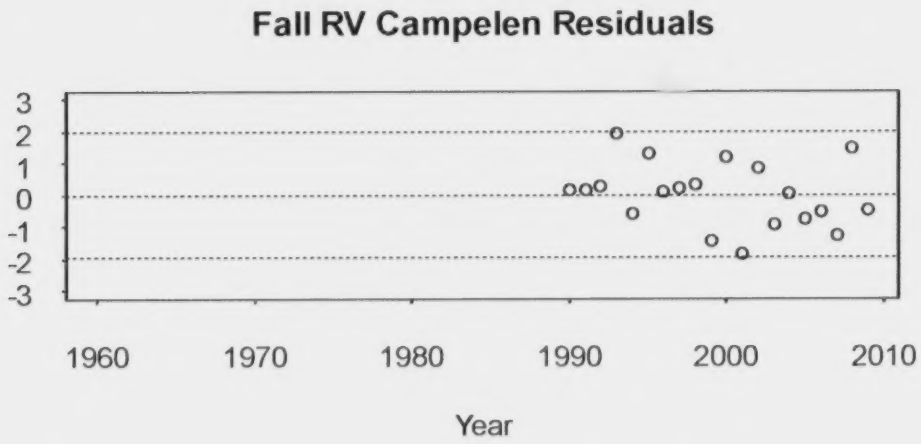

Figure 61a: Converted Fall Campelen series estimates with 95 % credible intervals (top) and standardized residuals (bottom) for 3LNO American plaice. Figures illustrate fit from model 2.

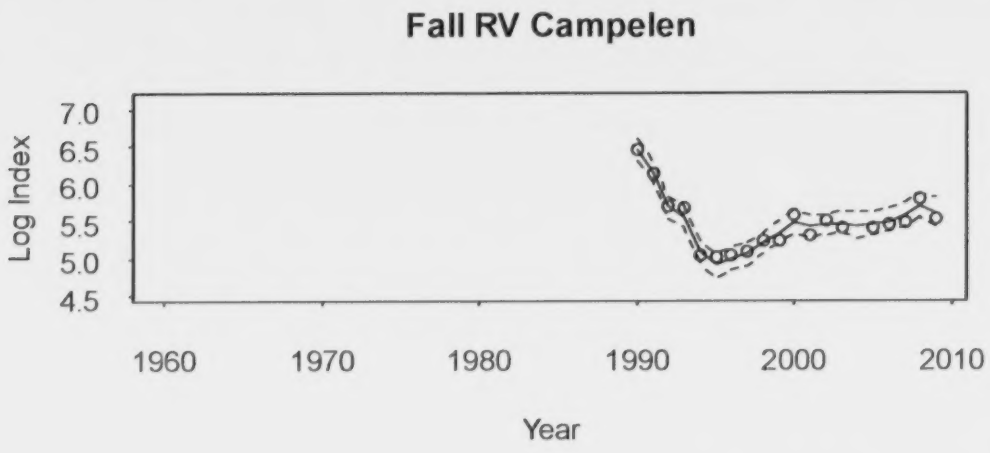

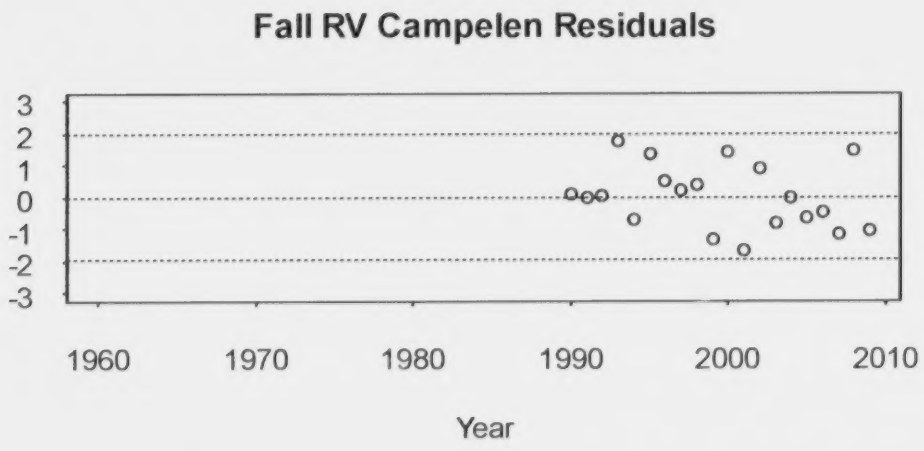

Figure 61b: Converted Fall Campelen series estimates with 95 % credible intervals (top) and standardized residuals (bottom) for 3LNO American plaice. Figures illustrate fit from model 3.

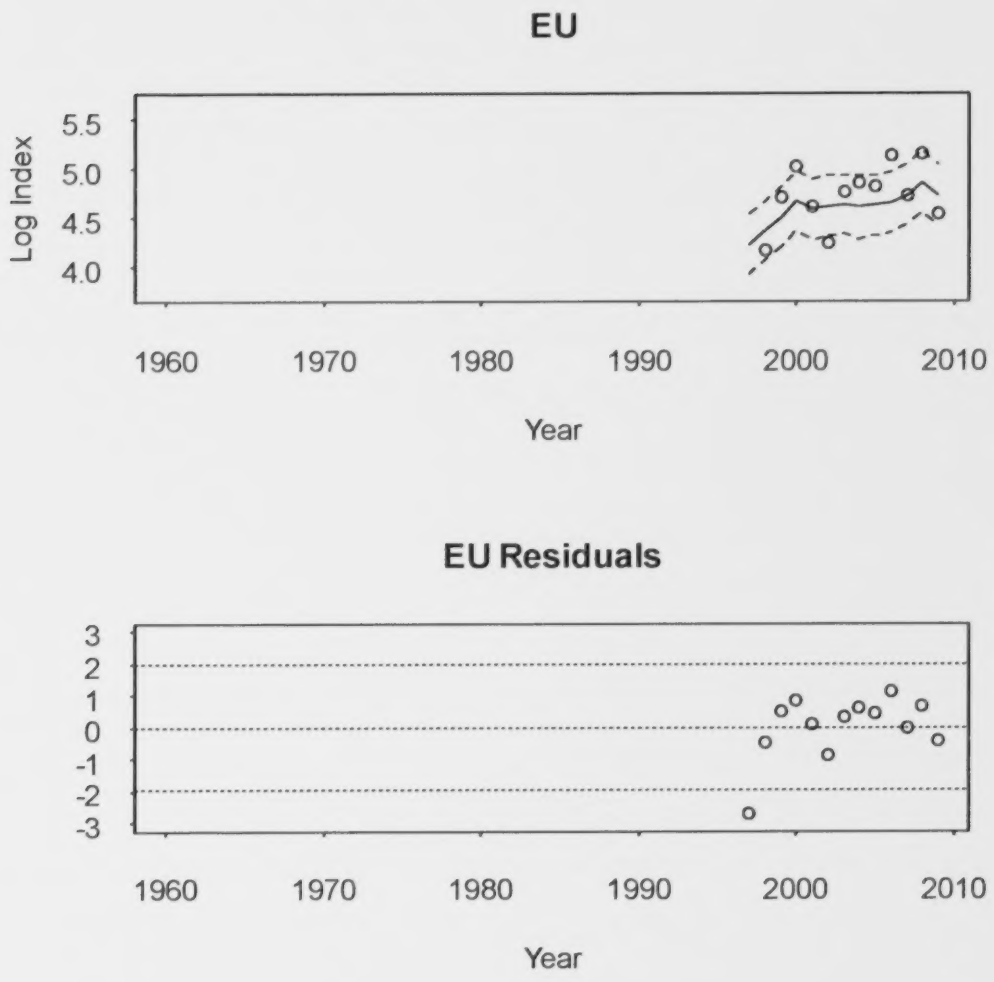

Figure 62a: European Union series estimates with 95 % credible intervals (top) and standardized residuals (bottom) for 3LNO American plaice. Figures illustrate fit from model 2.

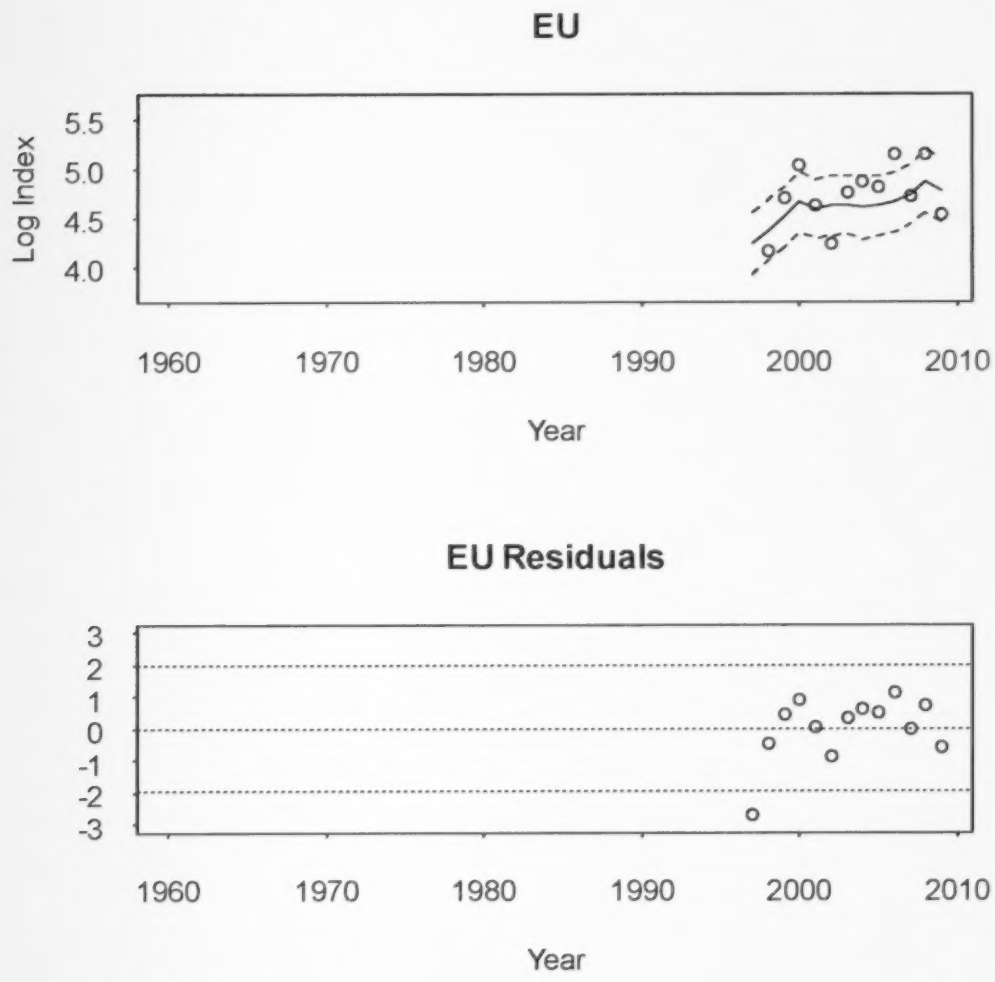

Figure 62b: European Union series estimates with 95 % credible intervals (top) and standardized residuals (bottom) for 3LNO American plaice. Figures illustrate fit from model 3.

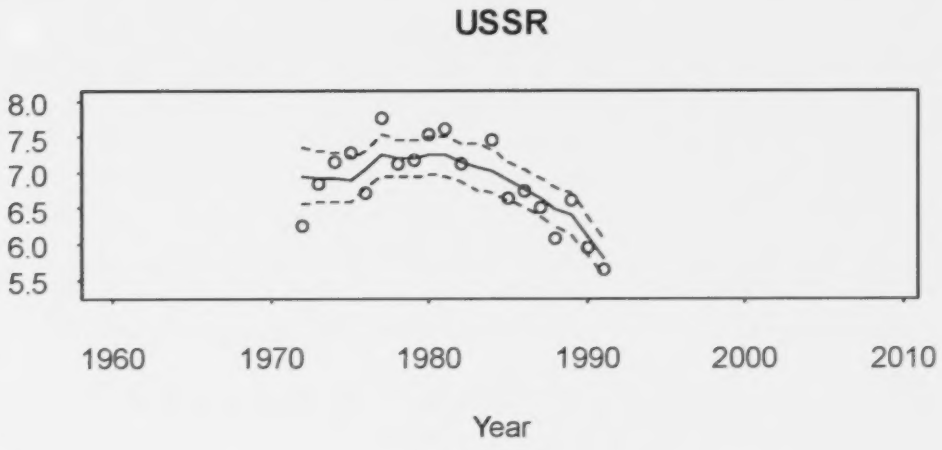

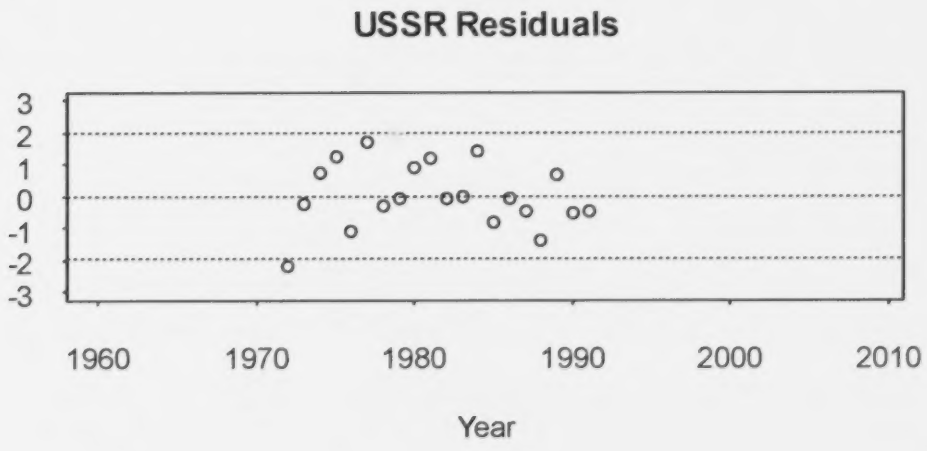

Figure 63a: USSR series estimates with 95 % credible intervals (top) and standardized residuals (bottom) for 3LNO American plaice. Figures illustrate fit from model 2.

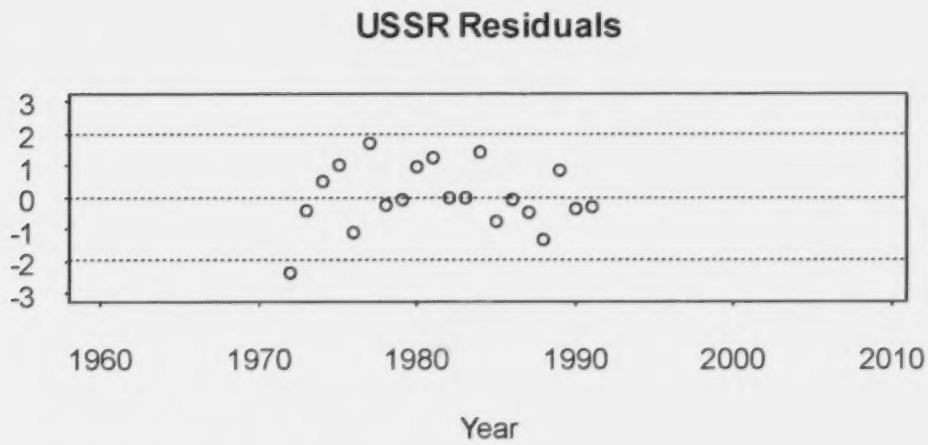

Figure 63b: USSR series estimates with 95 % credible intervals (top) and standardized residuals (bottom) for 3LNO American plaice. Figures illustrate fit from model 3.

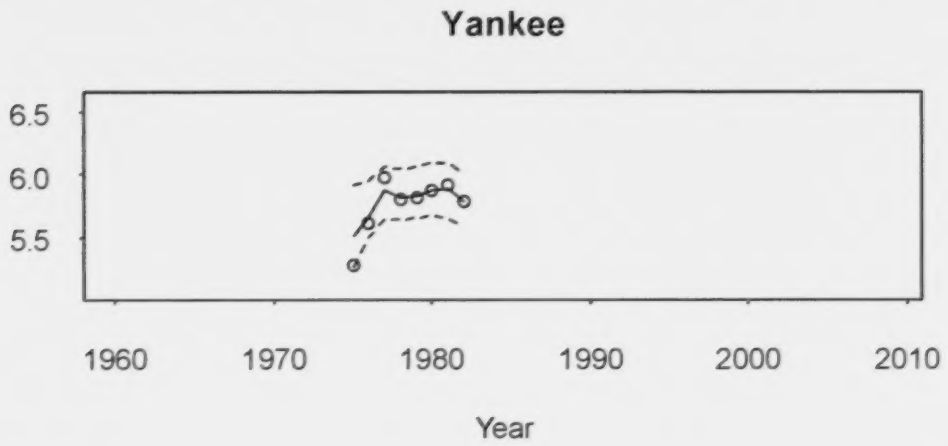

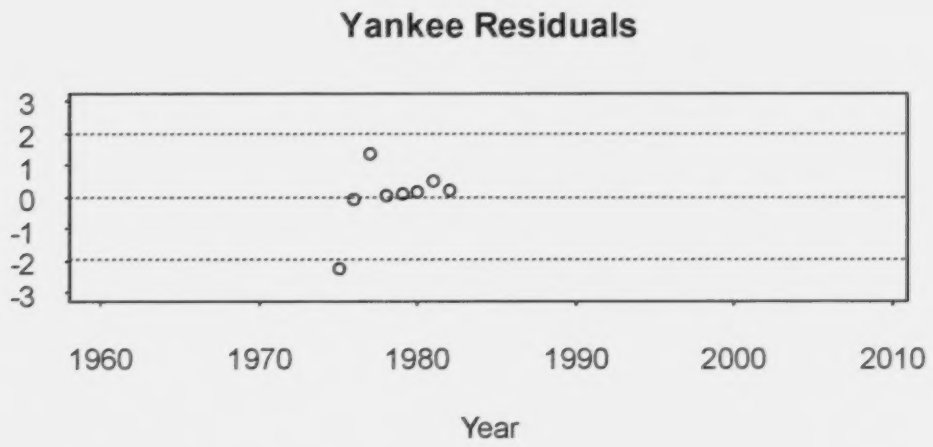

Figure 64a: Yankee trawl series estimates with 95 % credible intervals (top) and standardized residuals (bottom) for 3LNO American plaice. Figures illustrate fit from model 2.

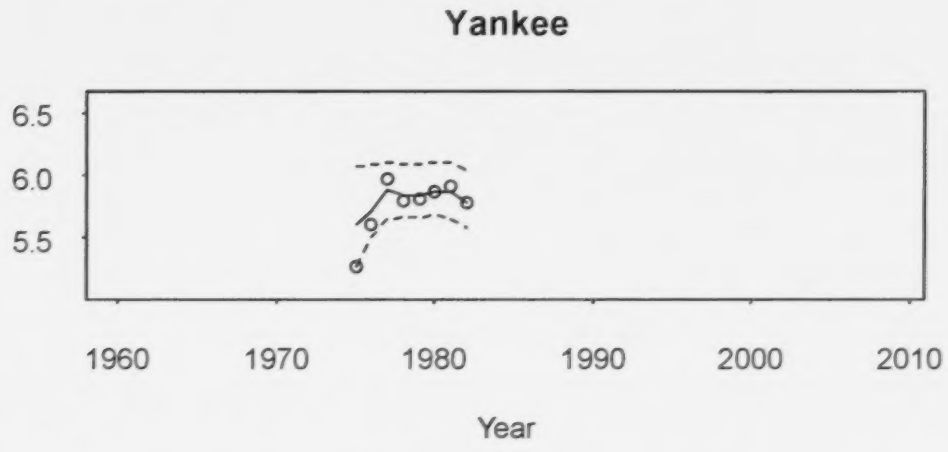

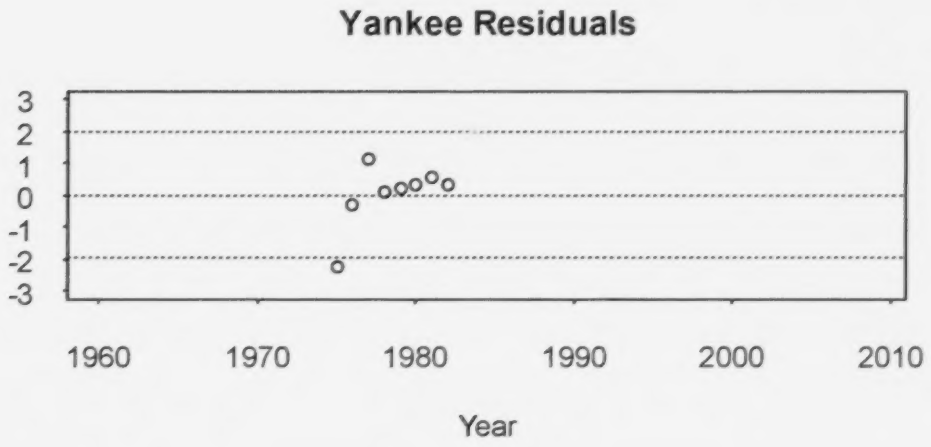

Figure 64b: Yankee trawl series estimates with 95 % credible intervals (top) and standardized residuals (bottom) for 3LNO American plaice. Figures illustrate fit from model 3.

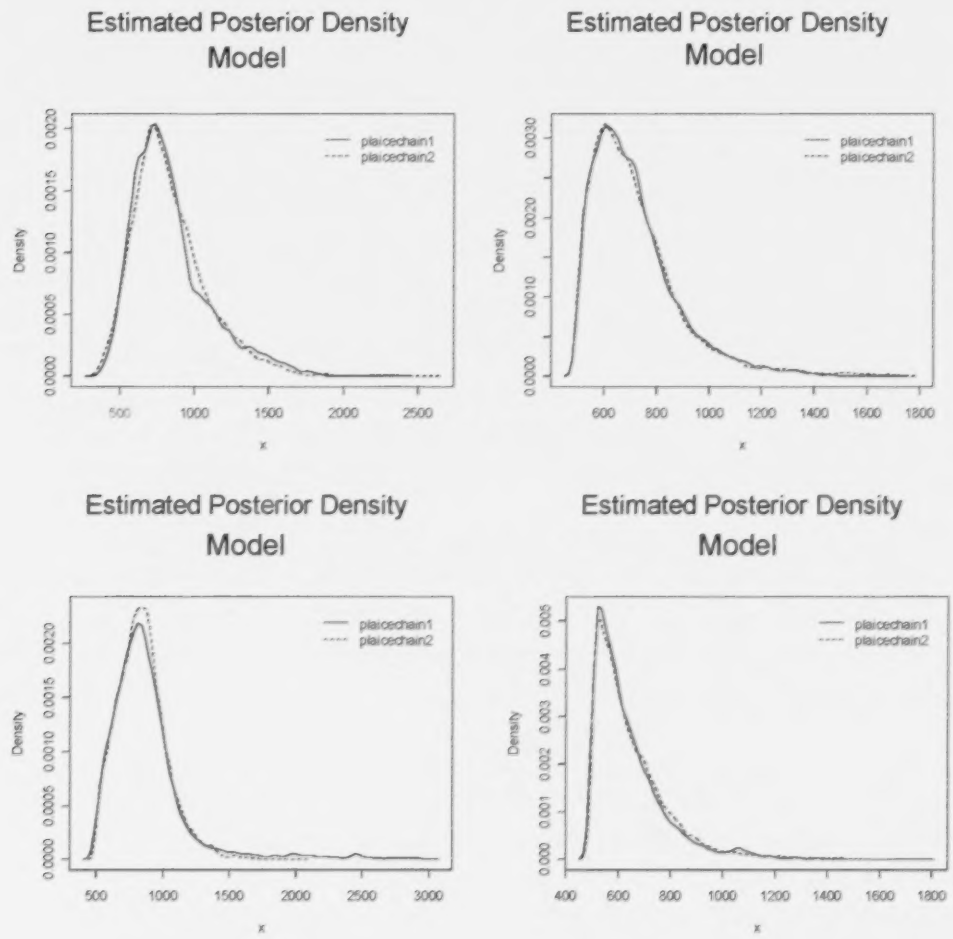

Figure 65: Kernel density estimates of the posterior distribution of K for both chains in models 1-4 for 3LNO American plaice.

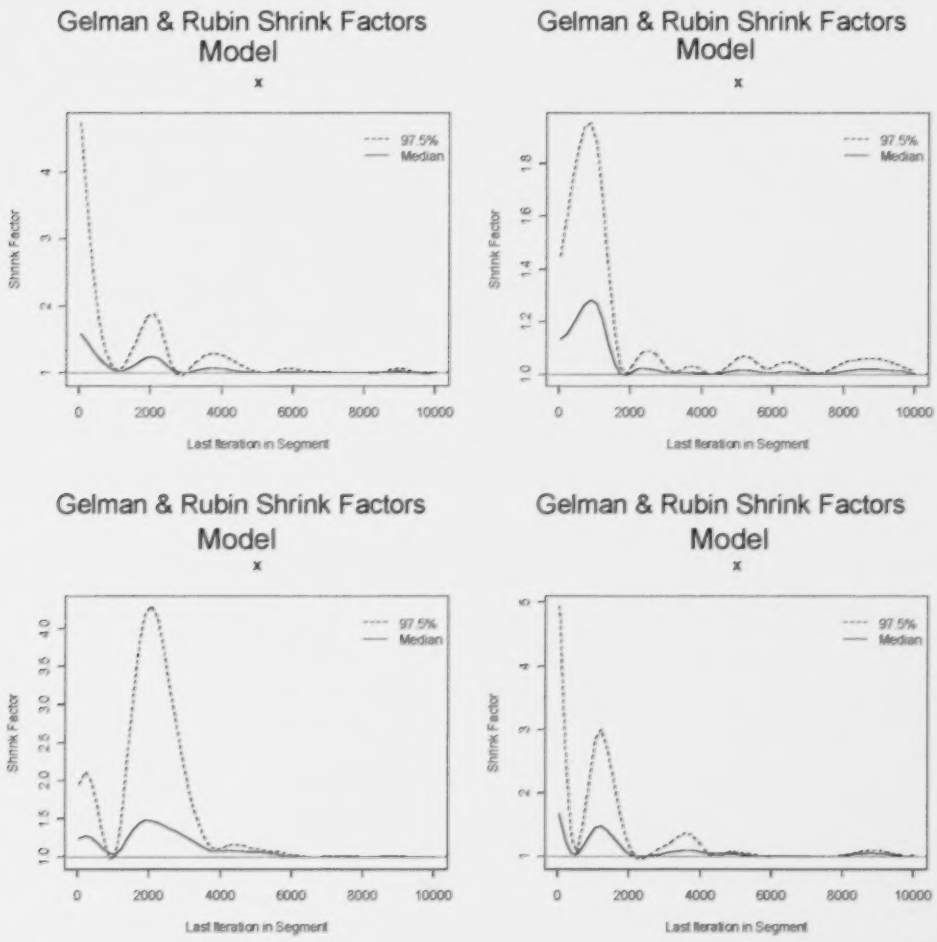

Figure 66: Gelman & Rubin shrink factors for K in models 1-4 for 3LNO American plaice. Gelman & Rubin shrink factors examine the reduction in bias in estimation. The shrink factor approaches 1 when the pooled within-chain variance dominates the between-chain variance. At that point, all chains have escaped the influence of their starting points.

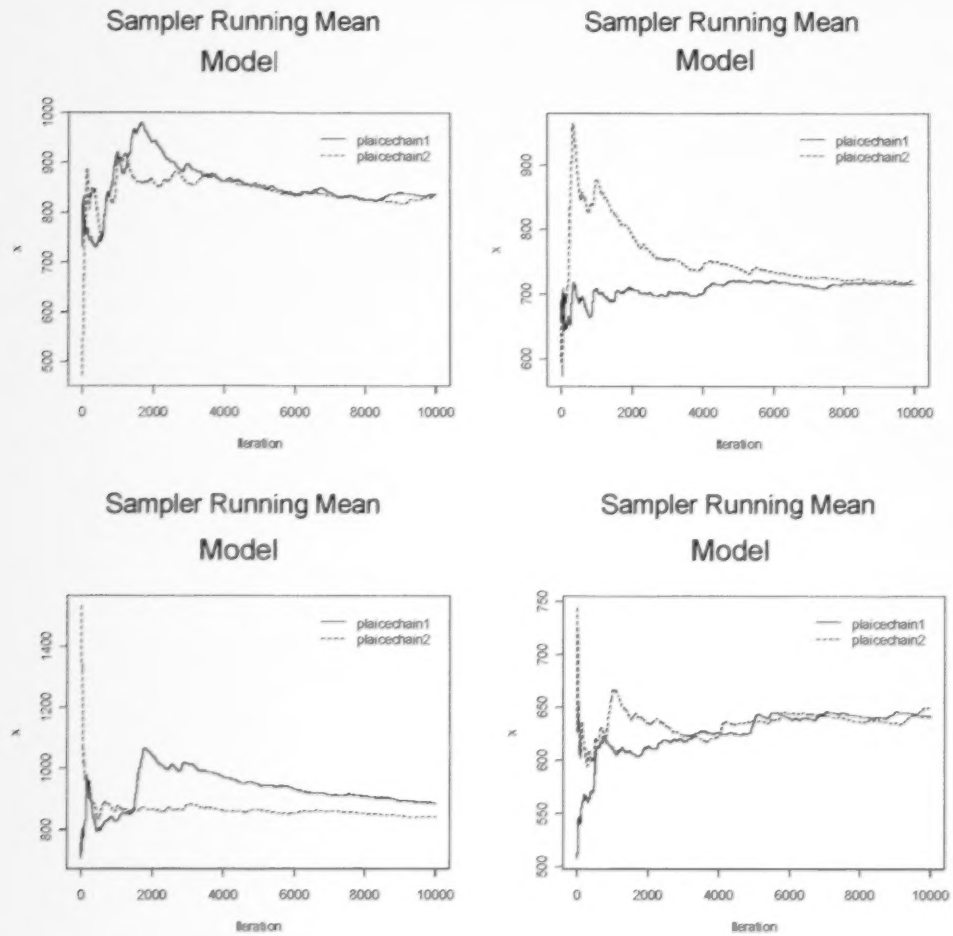

Figure 67: Sampler running mean for both chains of K, carrying capacity, in models 1-4 for 3LNO American plaice. Chains are considered to have converged when they overlap.

3Ps

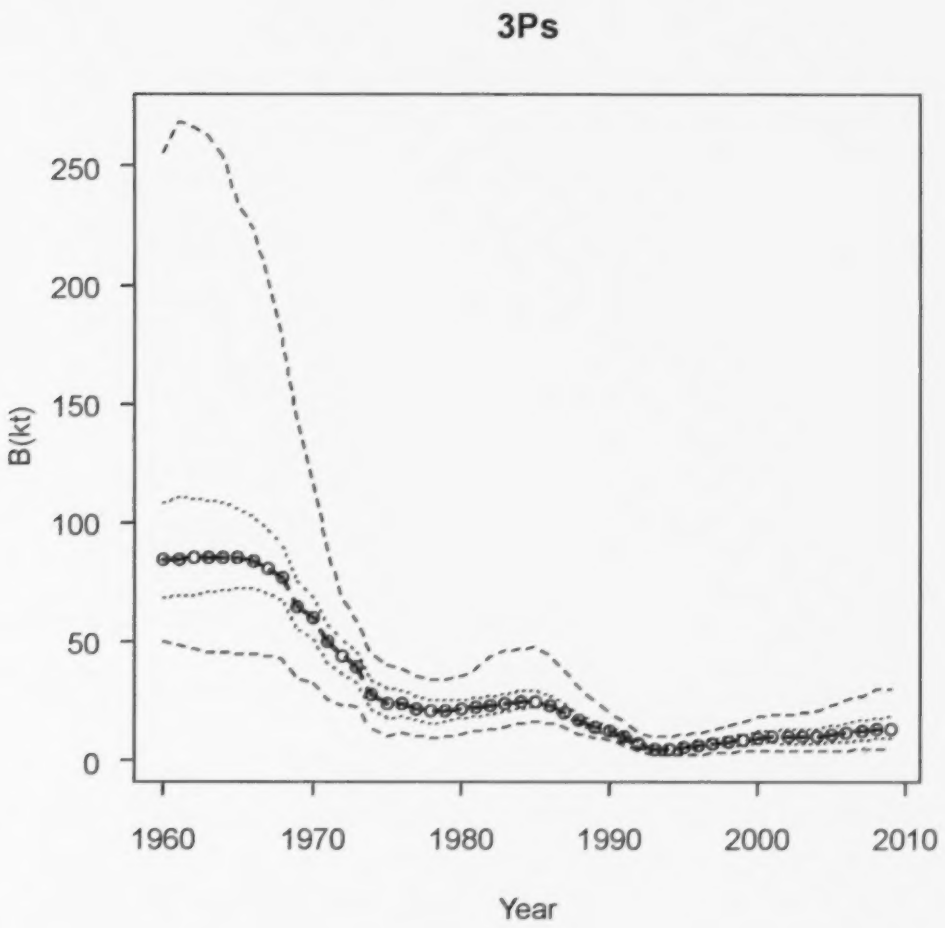

Figure 68a: Schaefer surplus production model 1 of biomass ('000t) from 1960-2009 (dashed line with circles) for 3Ps American plaice. Dotted lines represent 50 % and 95 % credible intervals.

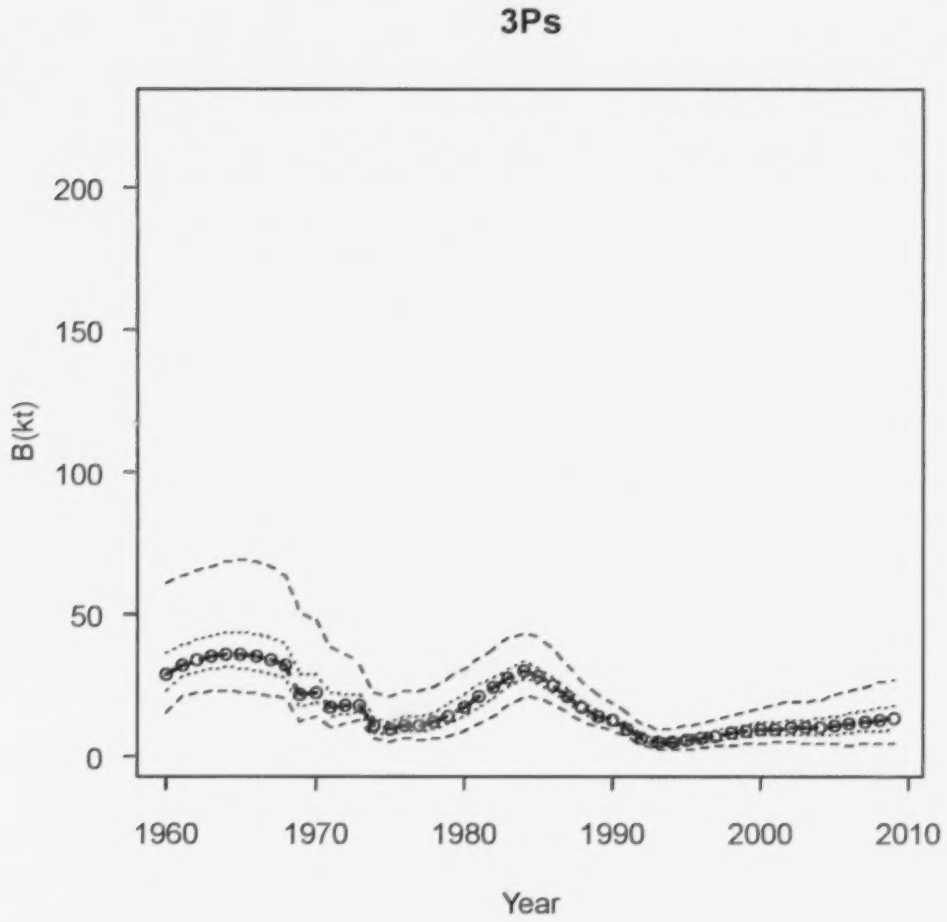

Figure 68b: Schaefer surplus production model 2 of biomass ('000t) from 1960-2009 (dashed line with circles) for 3Ps American plaice. The model divides the series into two periods (1960-1984 & 1985-2009) to estimate two levels of population productivity (r1 & r2 respectively). Dotted lines represent 50 % and 95 % credible intervals.

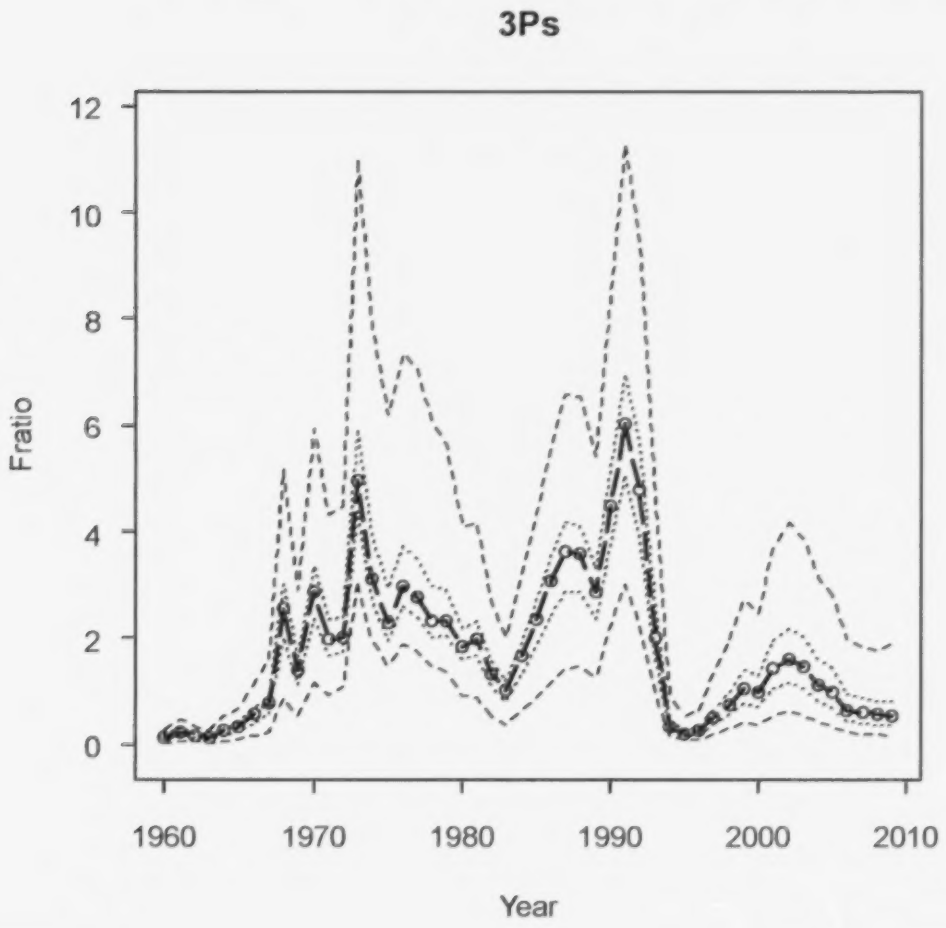

Figure 69a: Model 1 estimates of the F_{ratio}, the ratio of fishing mortality to that estimated for F_{MSY}, from 1960-2009 (dashed line with circles) for 3Ps American plaice. Dotted lines represent 50 % and 95 % credible intervals.

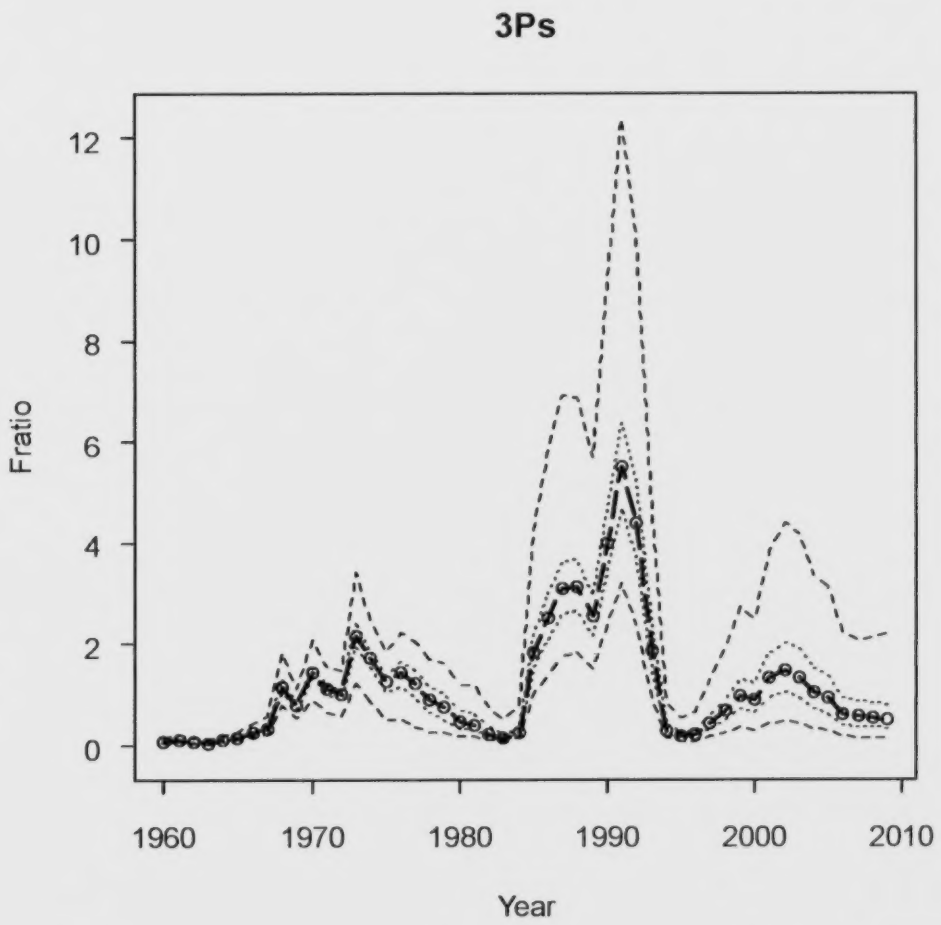

Figure 69b: Model 2 estimates of the F_{ratio}, the ratio of fishing mortality to that estimated for F_{MSY}, from 1960-2009 (dashed line with circles) for 3Ps American plaice. Dotted lines represent 50 % and 95 % credible intervals

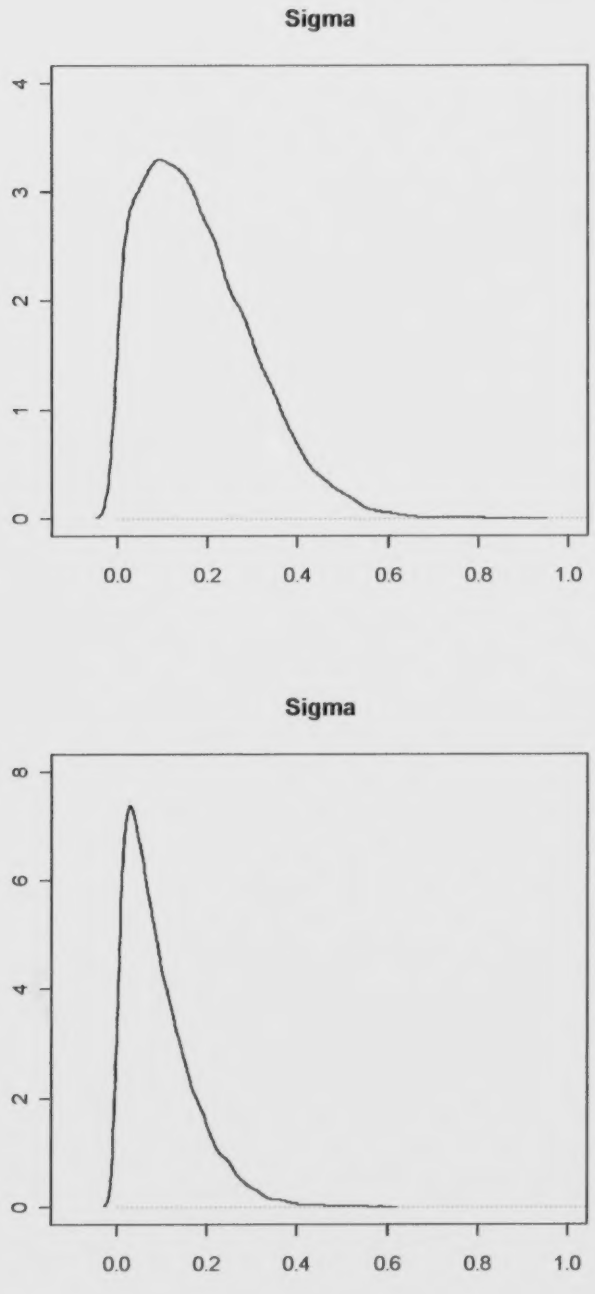

Figure 70: Posterior distributions for process error precision (Sigma) for models 1 & 2 in 3Ps American plaice. Prior distributions are illustrated using red dotted lines.

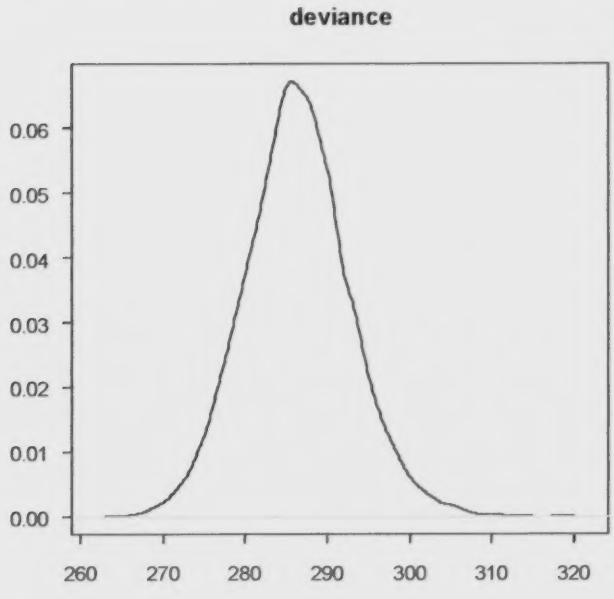

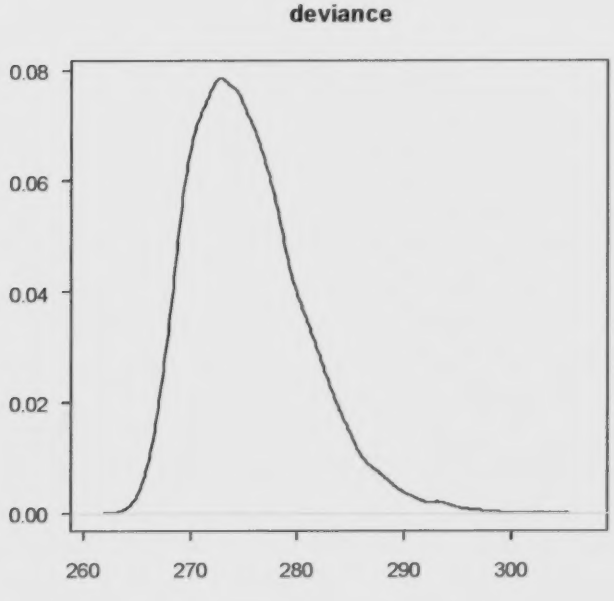

Figure 71: Posterior distributions for deviance in models 1 & 2 for 3Ps American plaice.

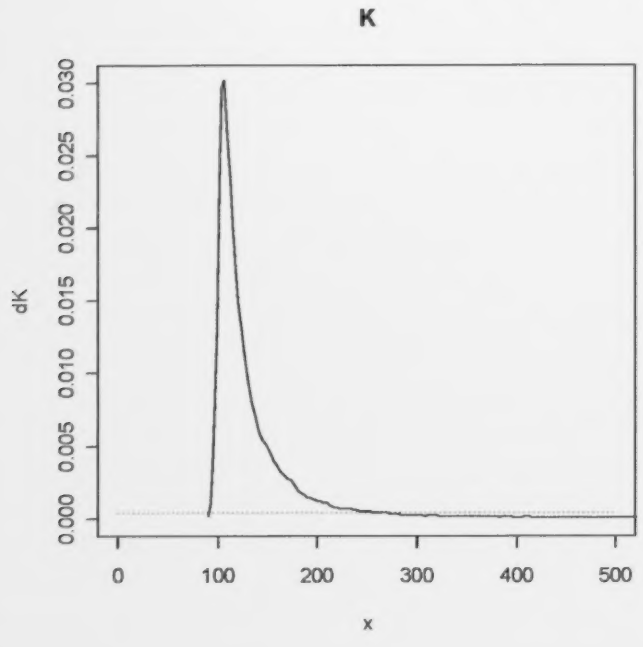

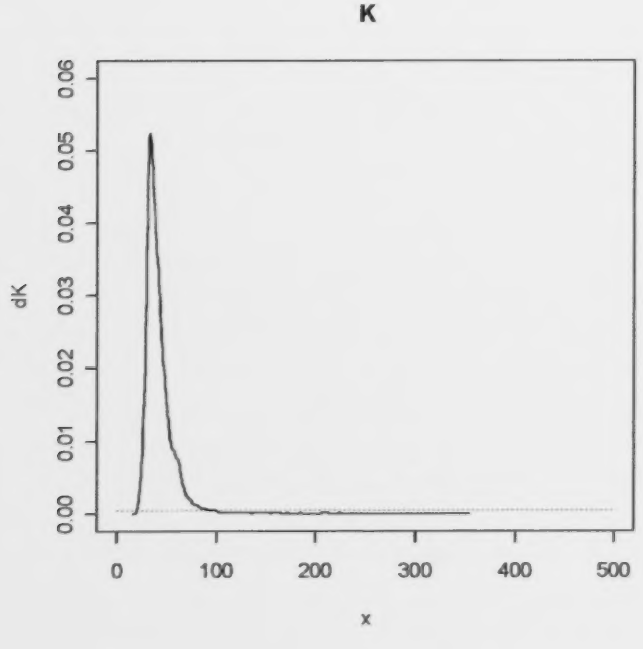

Figure 72: Posterior distributions for K, carrying capacity, for models 1 & 2 in 3Ps American plaice. Prior distributions are illustrated using red dotted lines.

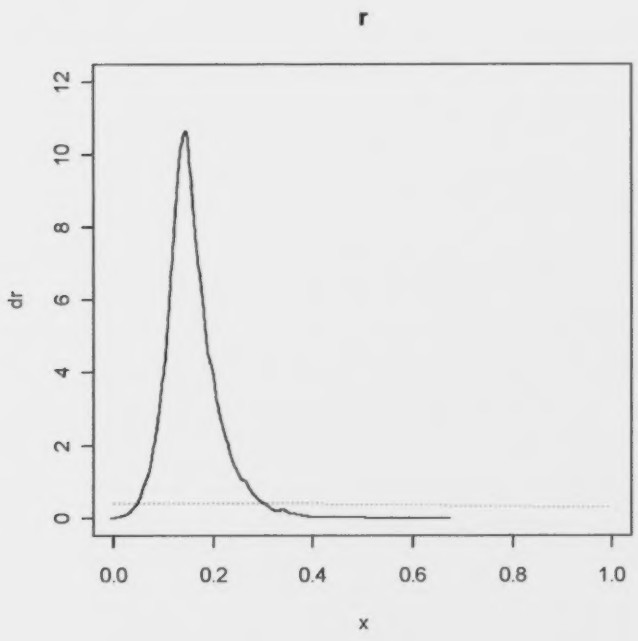

Figure 73: Posterior distribution of r, the intrinsic rate of population growth, for model 1 in 3Ps American plaice. The prior distribution is illustrated using a red dotted line.

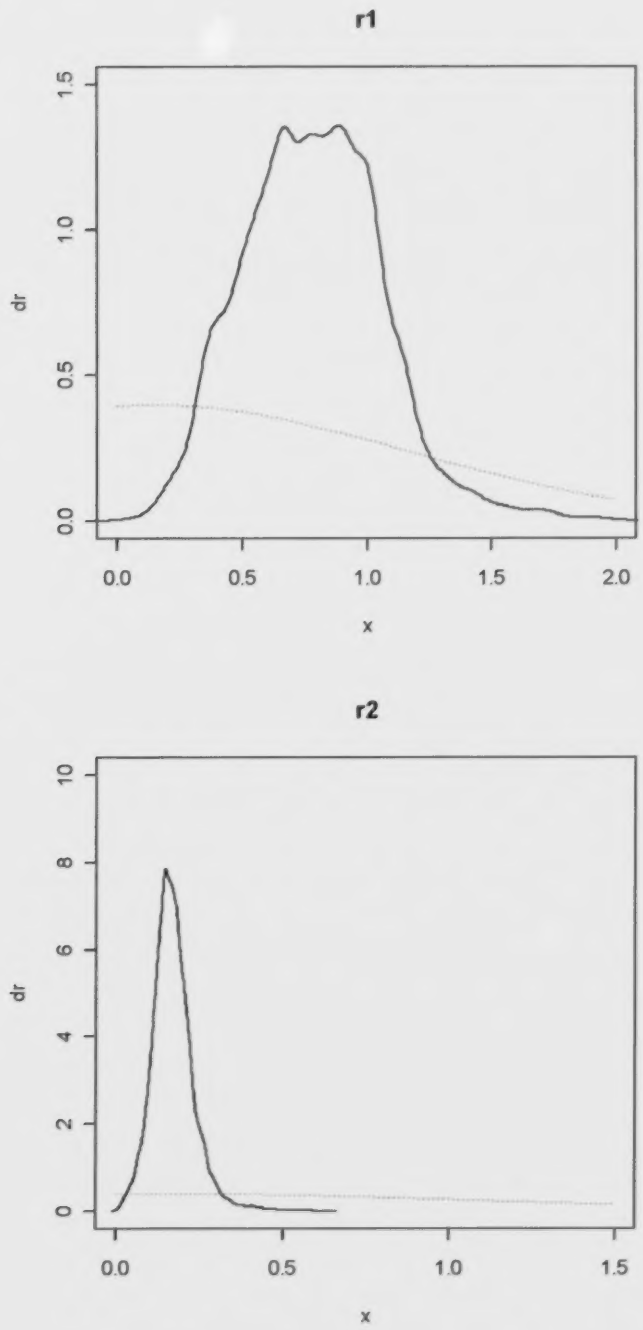

Figure 74: Posterior distributions of r, the intrinsic rate of population growth, for model 2 in 3Ps American plaice. In this model, the series is divided into two periods (1960-1984 & 1985-2009) represented by r1 and r2 respectively. Prior distributions are illustrated using red dotted lines.

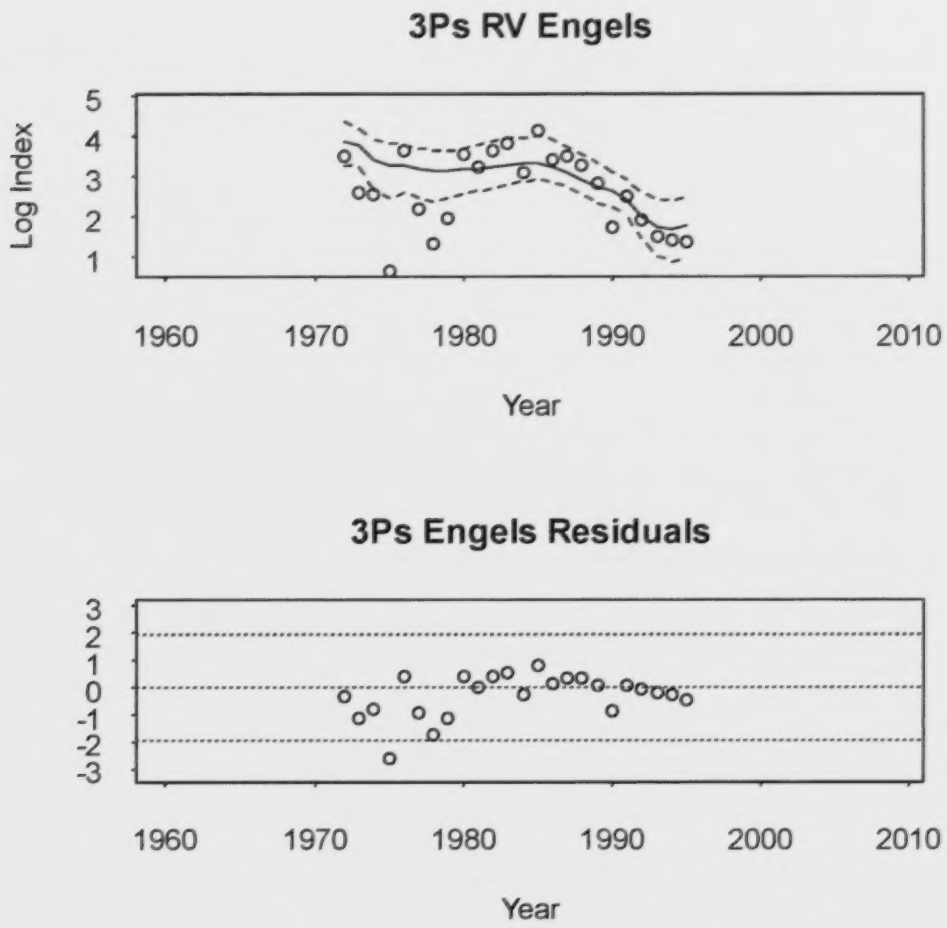

Figure 75a: Canadian Engels trawl series estimates with 95 % credible intervals (top) and standardized residuals (bottom) for 3Ps American plaice. Figures illustrate fit from model 1.

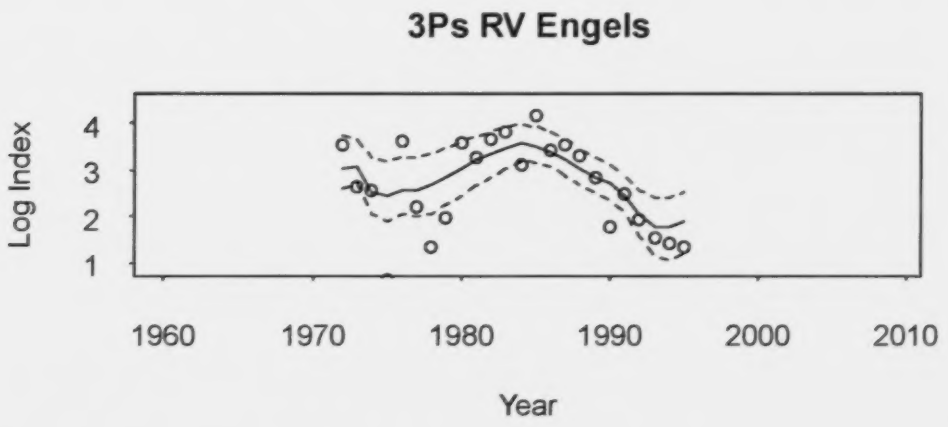

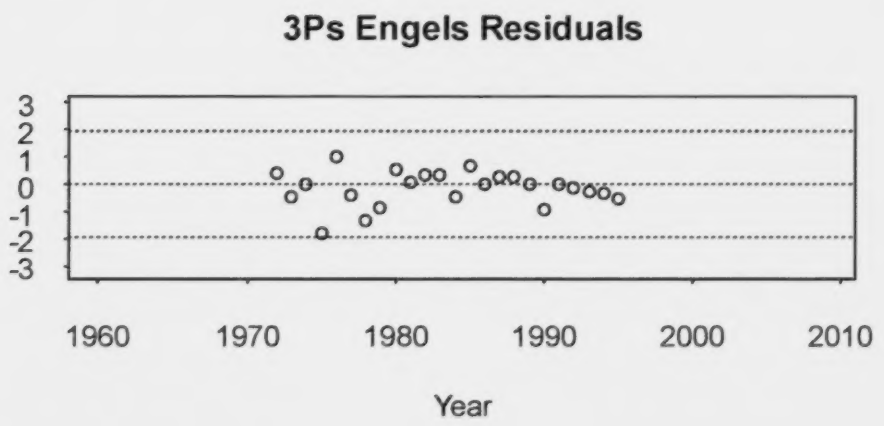

Figure 75b: Canadian Engels trawl series estimates with 95 % credible intervals (top) and standardized residuals (bottom) for 3Ps American plaice. Figures illustrate fit from model 2.

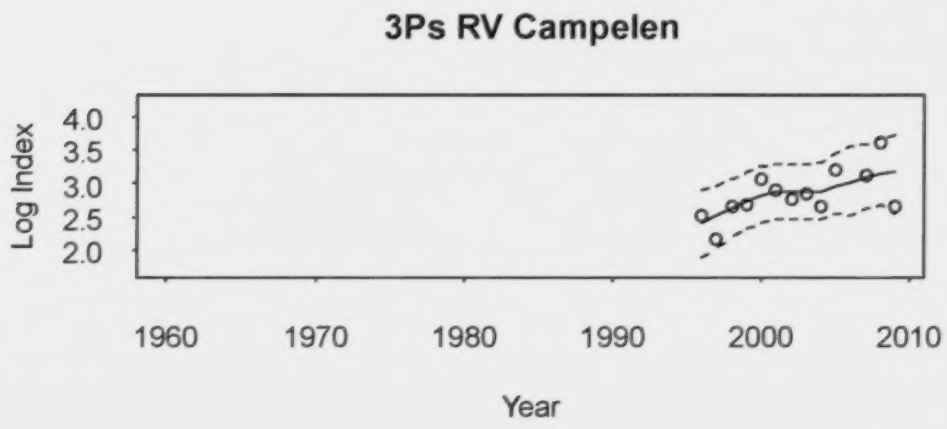

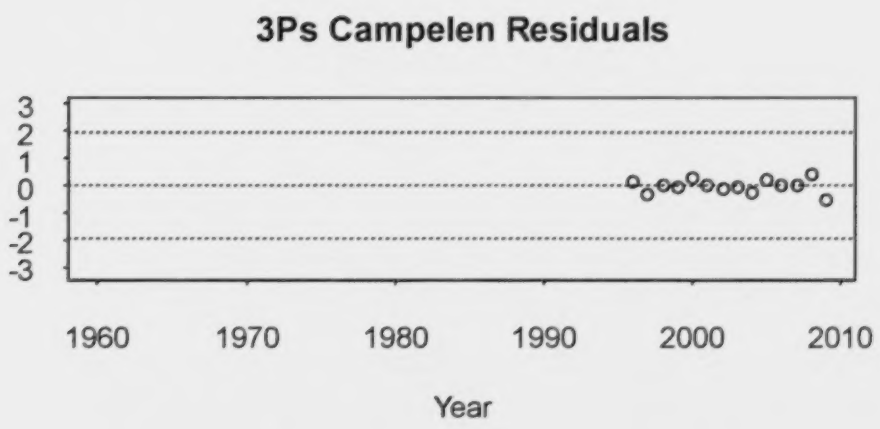

Figure 76a: Canadian Campelen trawl series estimates with 95 % credible intervals (top) and standardized residuals (bottom) for 3Ps American plaice. Figures illustrate fit from model 1.

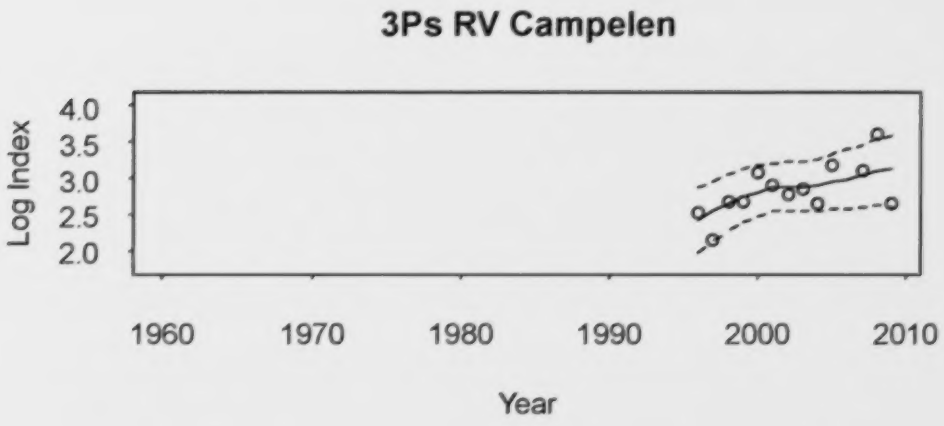

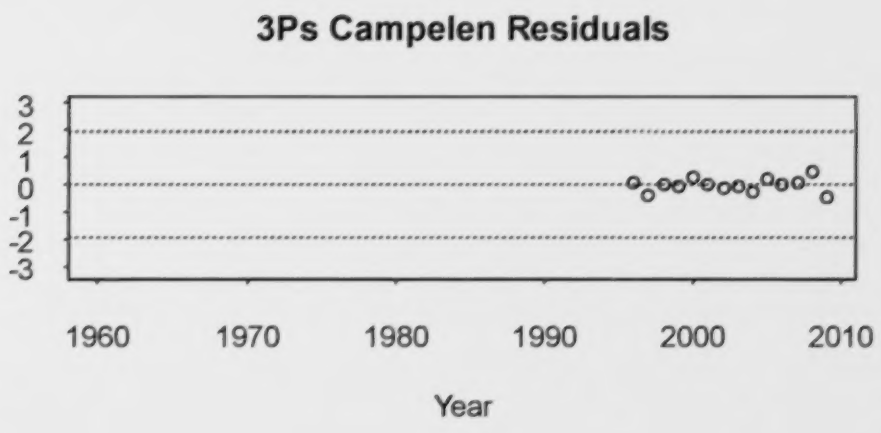

Figure 76b: Canadian Campelen trawl series estimates with 95 % credible intervals (top) and standardized residuals (bottom) for 3Ps American plaice. Figures illustrate fit from model 2.

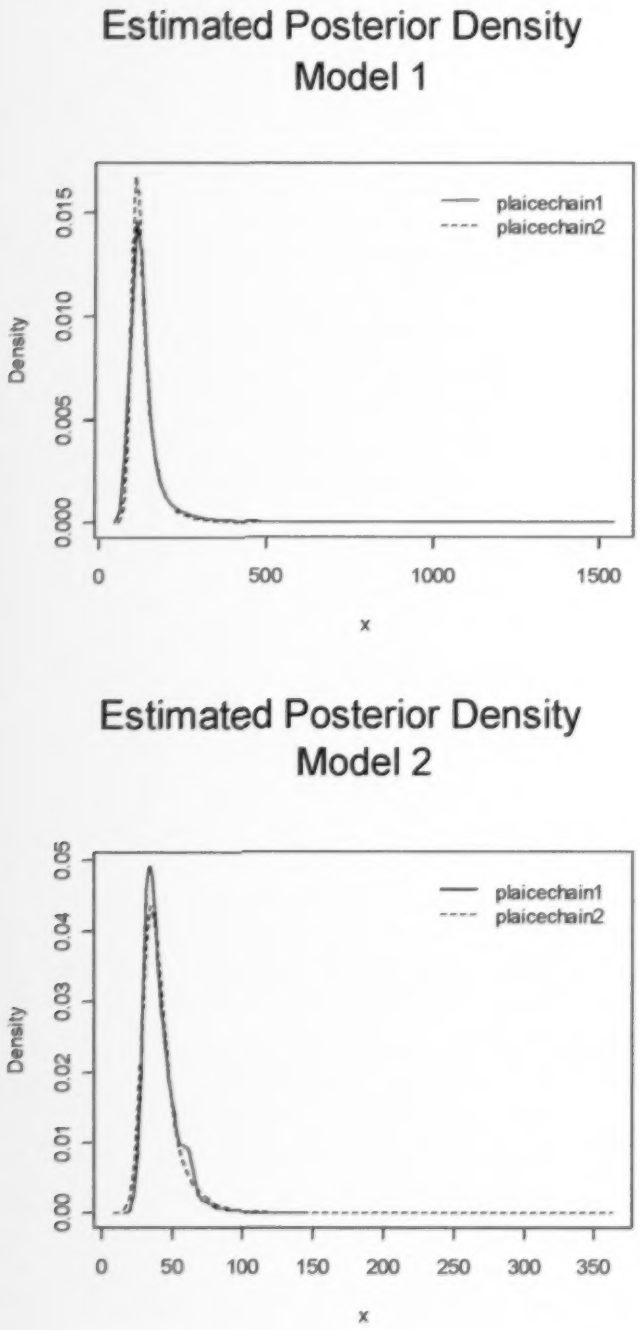

Figure 77: Kernel density estimates of the posterior distribution of K for both chains in models 1 & 2 for 3Ps American plaice.

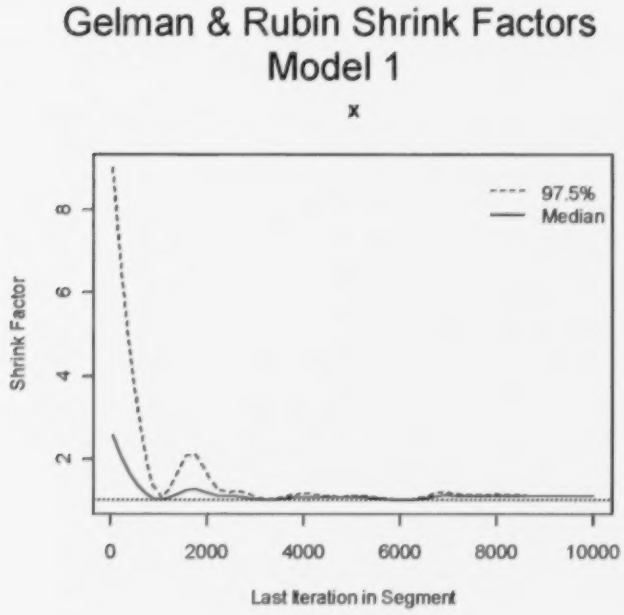

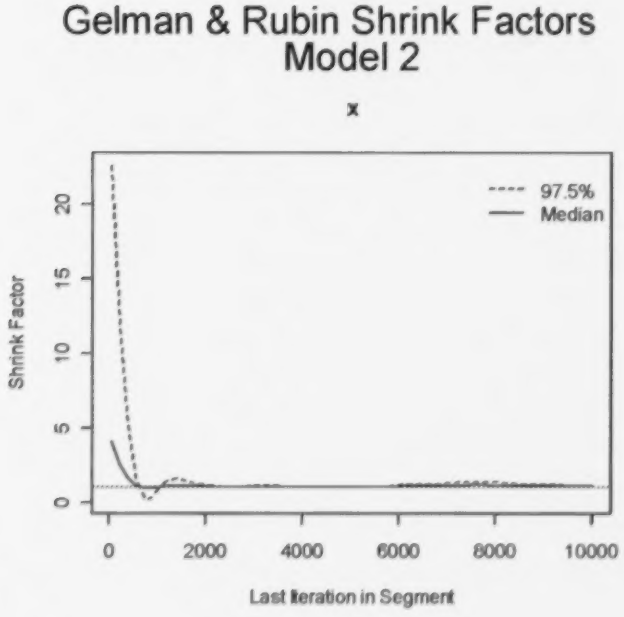

Figure 78: Gelman & Rubin shrink factors for K in models 1 & 2 for 3Ps American plaice. Gelman & Rubin shrink factors examine the reduction in bias in estimation. The shrink factor approaches 1 when the pooled within-chain variance dominates the between-chain variance. At that point, all chains have escaped the influence of their starting points.

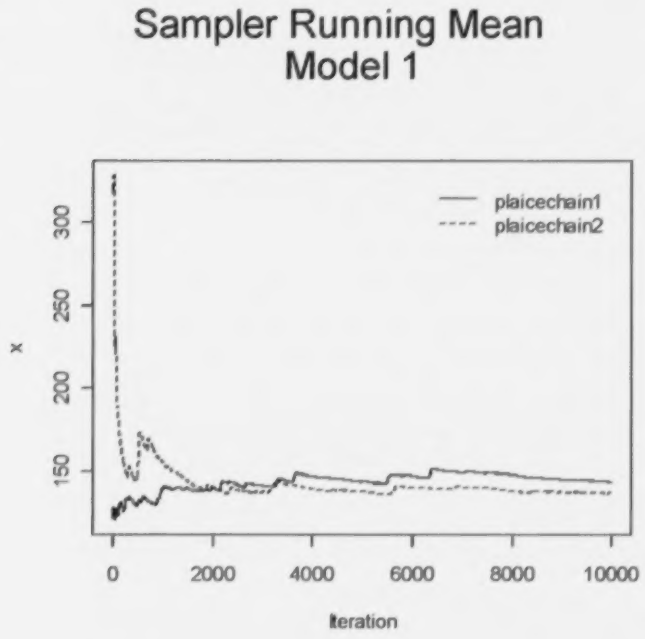

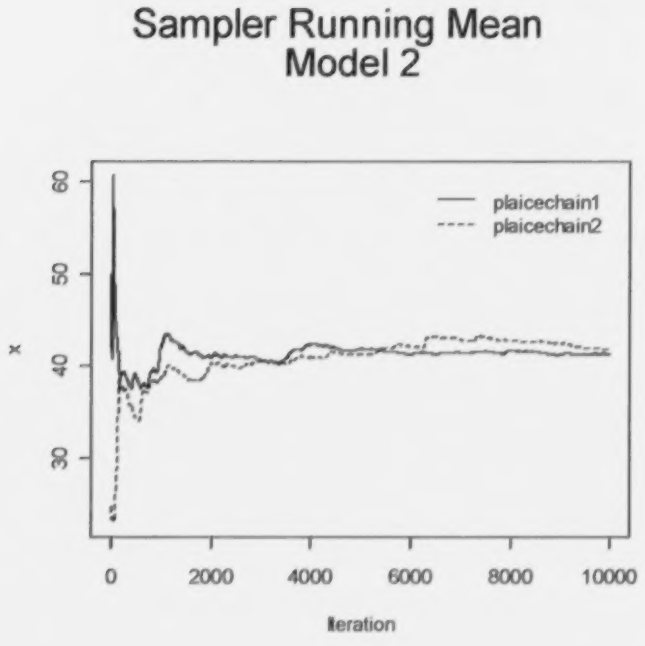

Figure 79: Sampler running mean for both chains of K, carrying capacity, in models 1 & 2 for 3Ps American plaice. Chains are considered to have converged when they overlap.

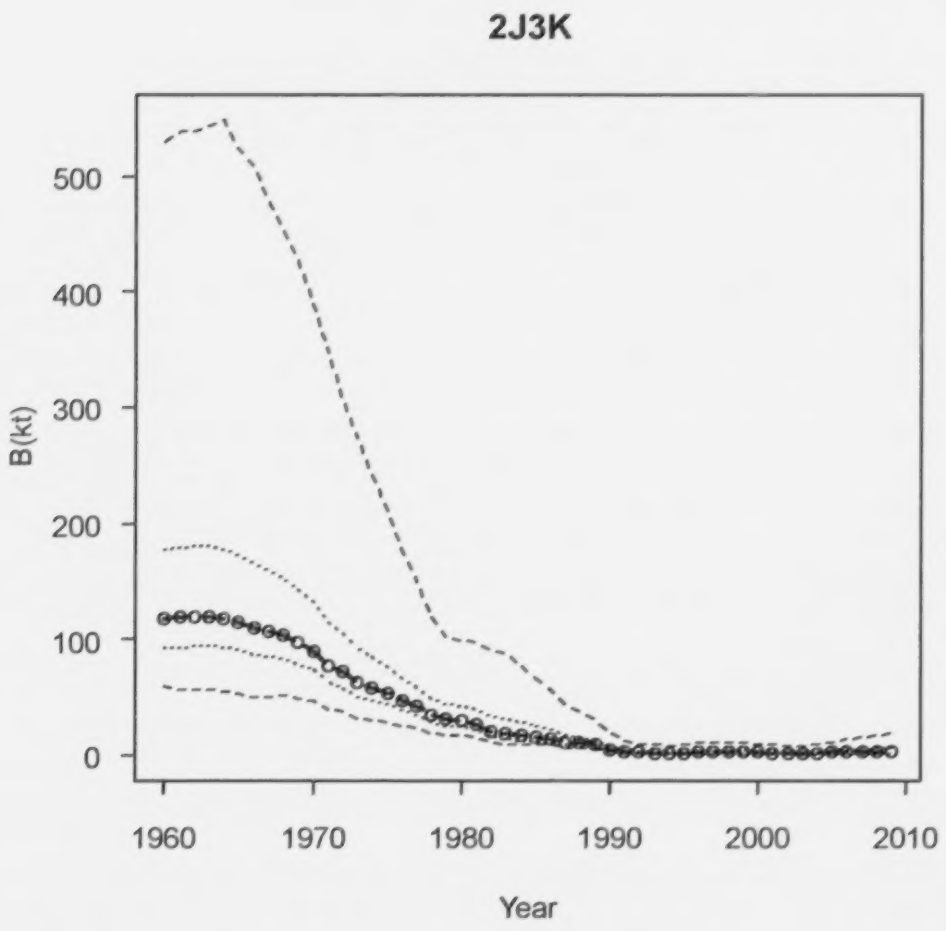

Figure 80a: Schaefer surplus production model 1 of biomass ('000t) from 1960-2009 (dashed line with circles) for 2J3K American plaice. Dotted lines represent 50 % and 95 % credible intervals.

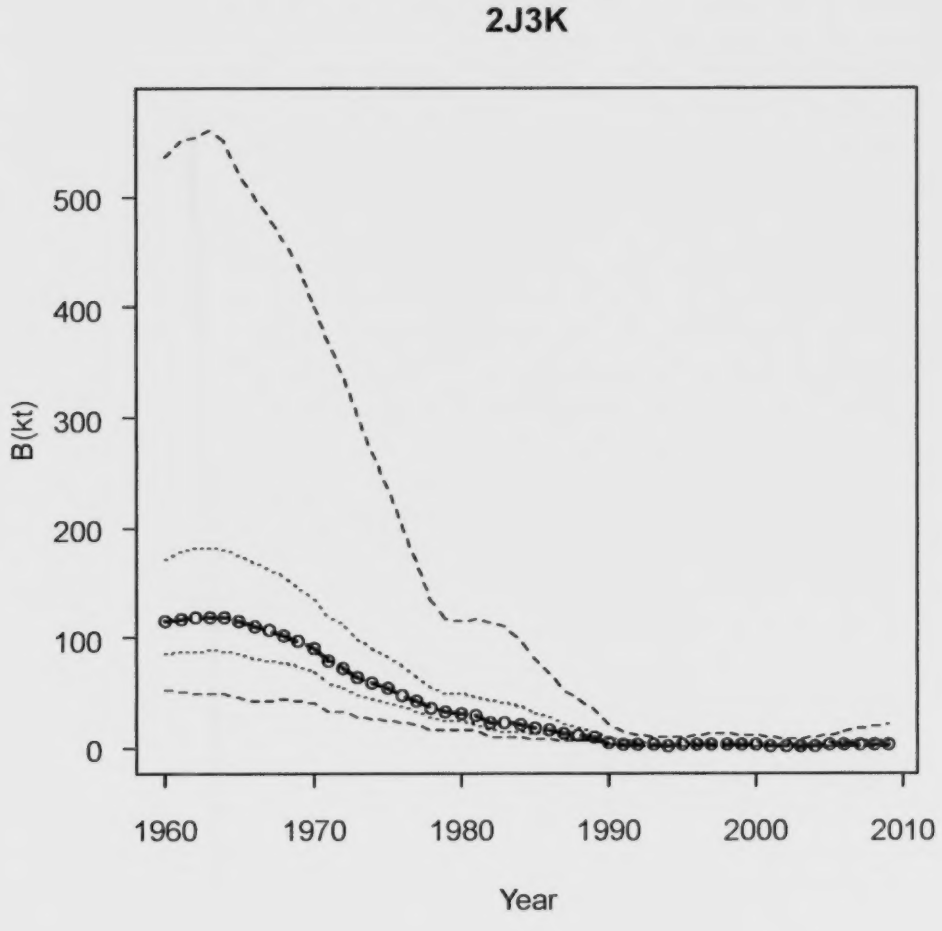

Figure 80b: Schaefer surplus production model 2 of biomass ('000t) from 1960-2009 (dashed line with circles) for 2J3K American plaice. The model divides the series into two periods (1960-1984 & 1985-2009) to estimate two levels of population productivity (r1 & r2 respectively). Dotted lines represent 50 % and 95 % credible intervals.

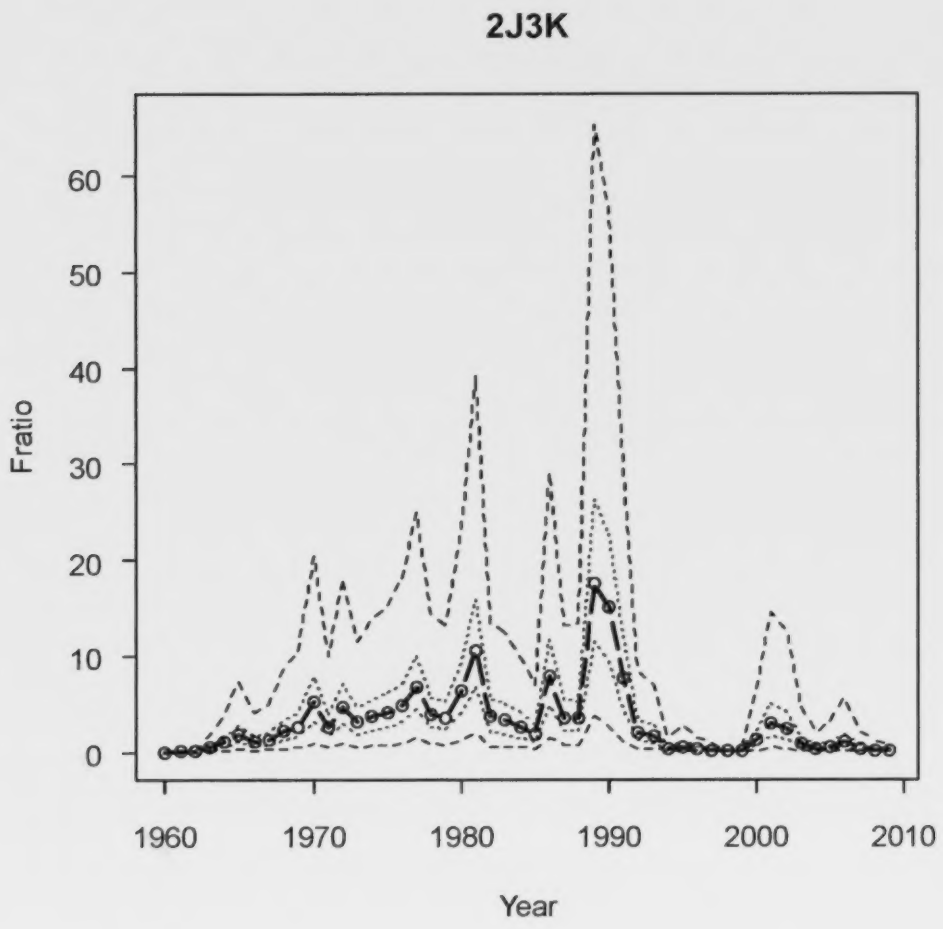

Figure 81a: Model 1 estimates of the F_{ratio}, the ratio of fishing mortality to that estimated for F_{MSY}, from 1960-2009 (dashed line with circles) for 2J3K American plaice. Dotted lines represent 50 % and 95 % credible intervals.

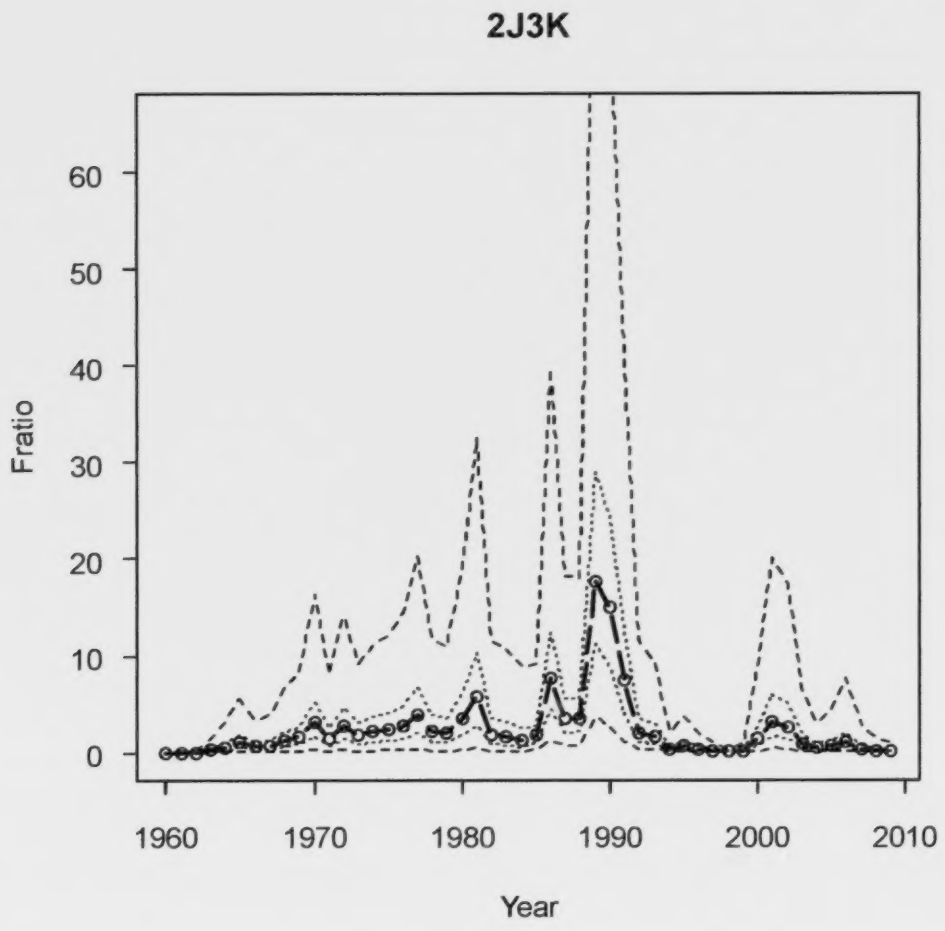

Figure 81b: Model 2 estimates of the F_{ratio}, the ratio of fishing mortality to that estimated for F_{MSY}, from 1960-2009 (dashed line with circles) for 2J3K American plaice. Dotted lines represent 50 % and 95 % credible intervals.

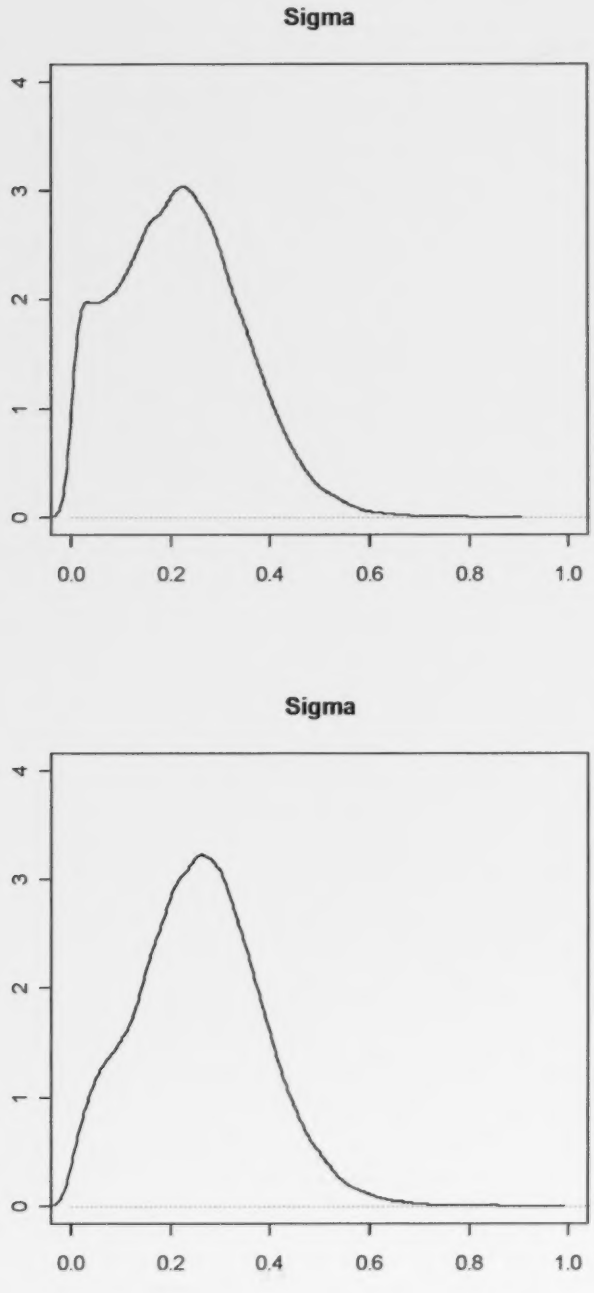

Figure 82: Posterior distributions for process error precision (Sigma) for models 1 & 2 in 2J3K American plaice. Prior distributions are illustrated using red dotted lines.

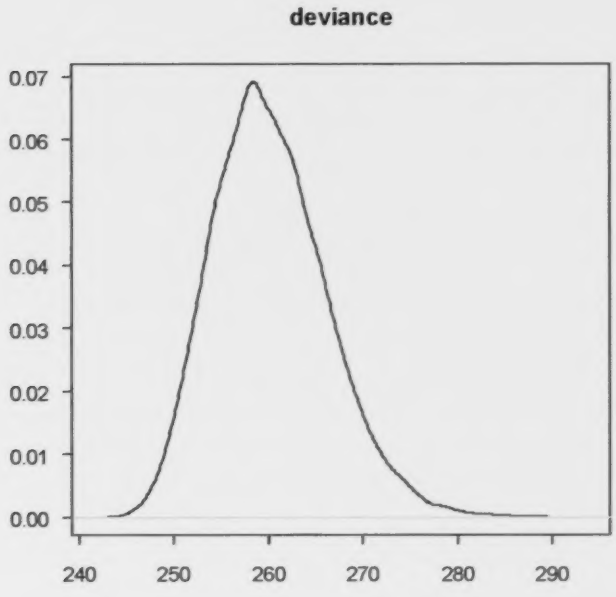

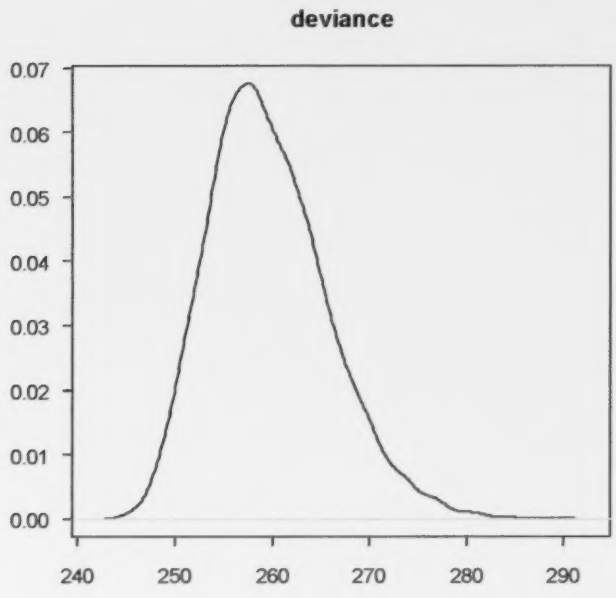

Figure 83: Posterior distributions for deviance in models 1 & 2 for 2J3K American plaice.

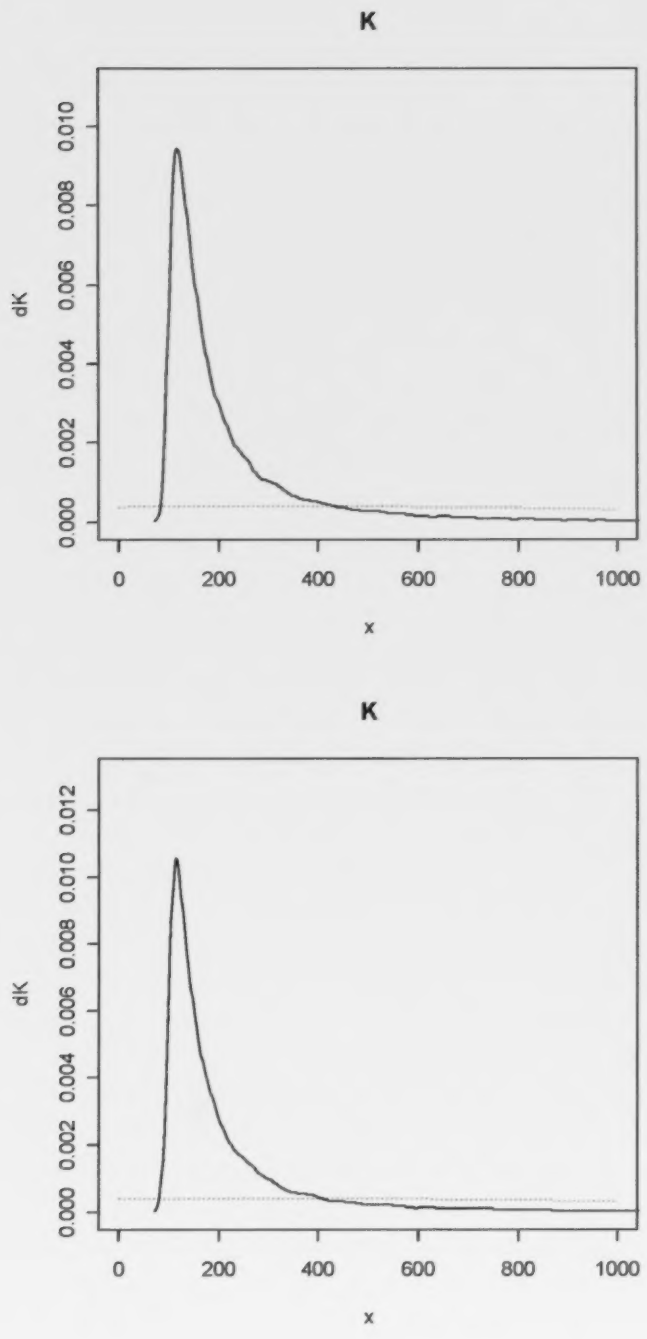

Figure 84: Posterior distributions for K, carrying capacity, for models 1 & 2 in 2J3K American plaice. Prior distributions are illustrated using red dotted lines.

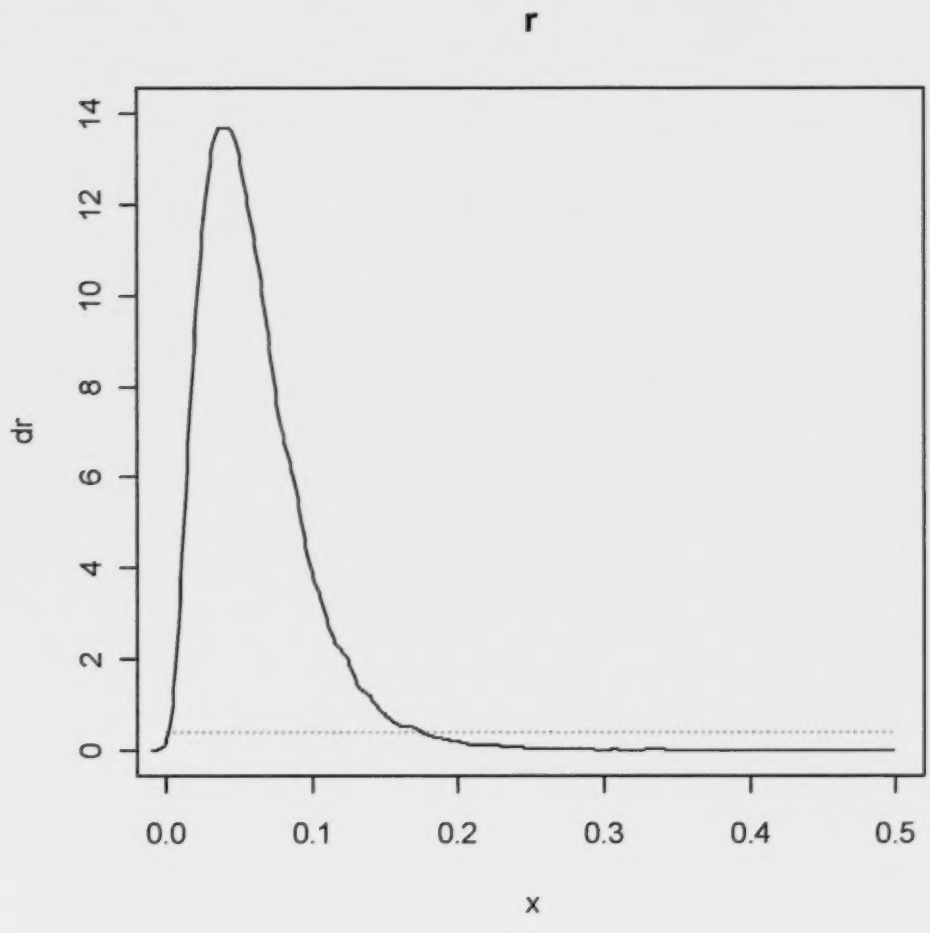

Figure 85: Posterior distribution of r, the intrinsic rate of population growth, for model 1 in 2J3K American plaice. The prior distribution is illustrated using a red dotted line.

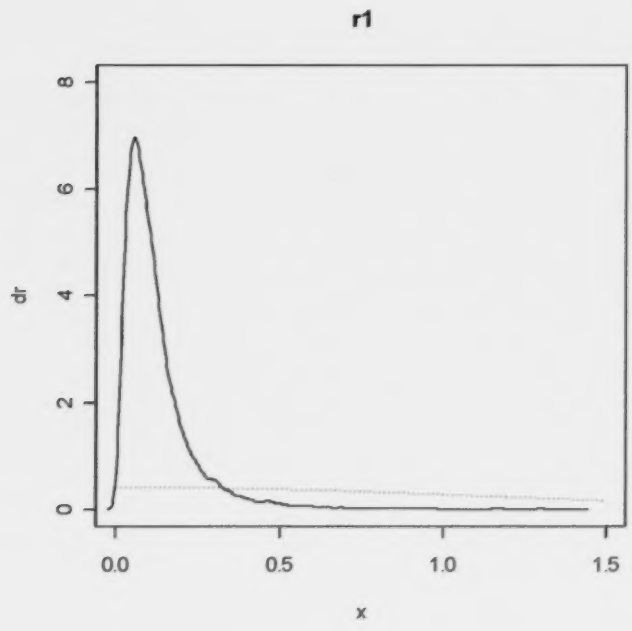

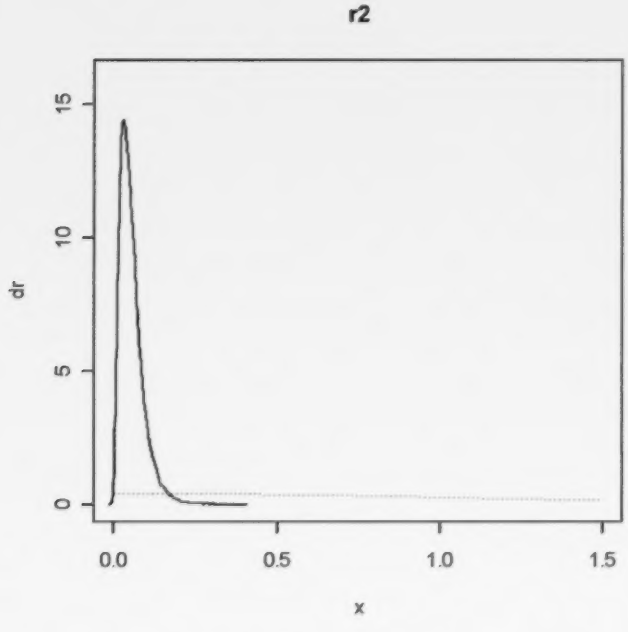

Figure 86: Posterior distributions of r, the intrinsic rate of population growth, for model 2 in 2J3K American plaice. In this model, the series is divided into two periods (1960-1984 & 1985-2009) represented by r1 and r2 respectively. Prior distributions are illustrated using red dotted lines.

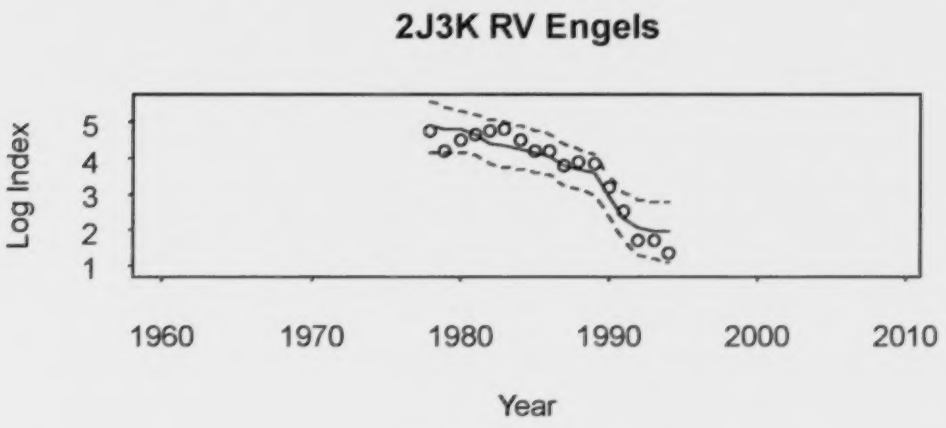

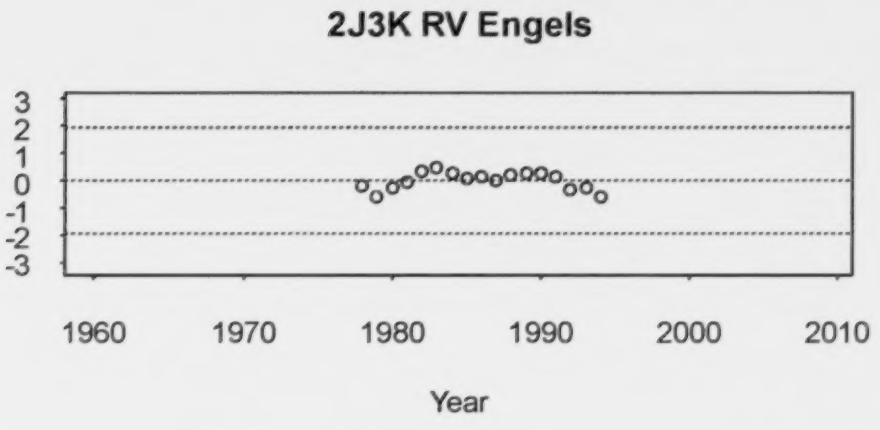

Figure 87a: Canadian Engels trawl series estimates with 95 % credible intervals (top) and standardized residuals (bottom) for 2J3K American plaice. Figures illustrate fit from model 1.

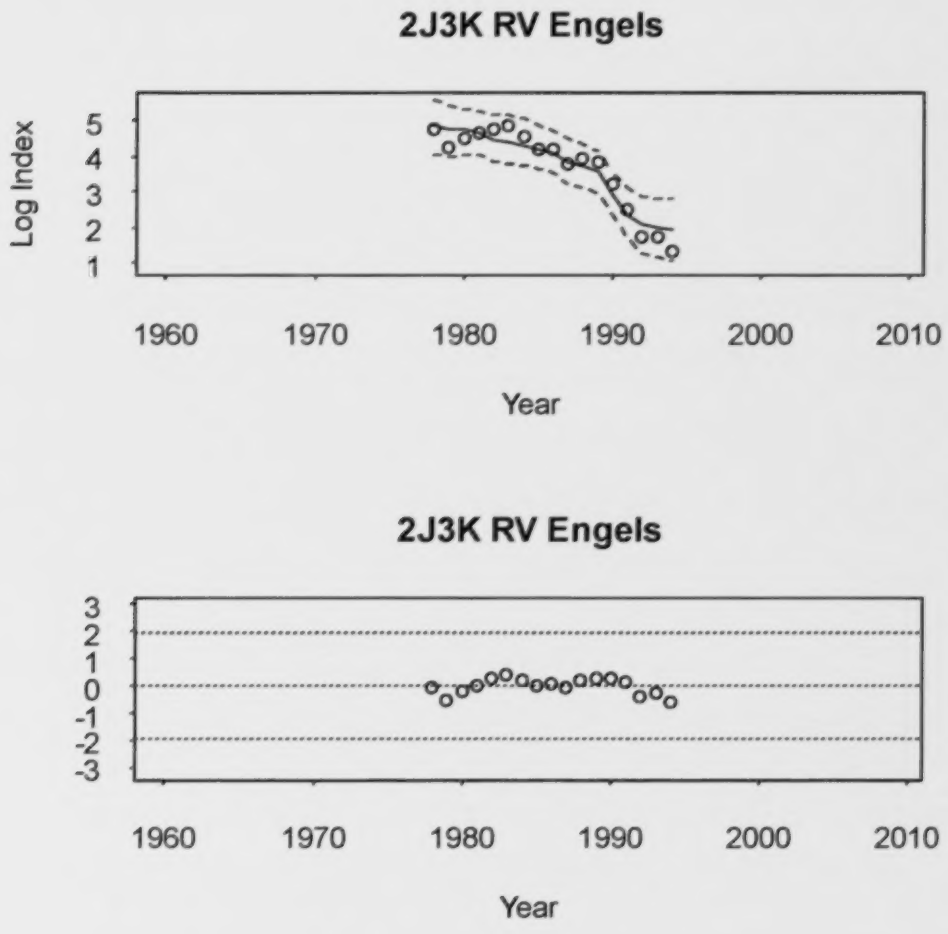

Figure 87b: Canadian Engels trawl series estimates with 95 % credible intervals (top) and standardized residuals (bottom) for 2J3K American plaice. Figures illustrate fit from model 2.

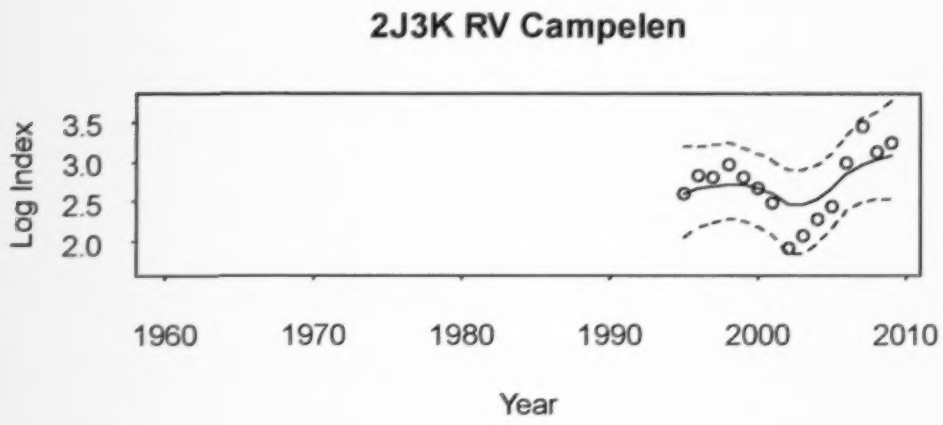

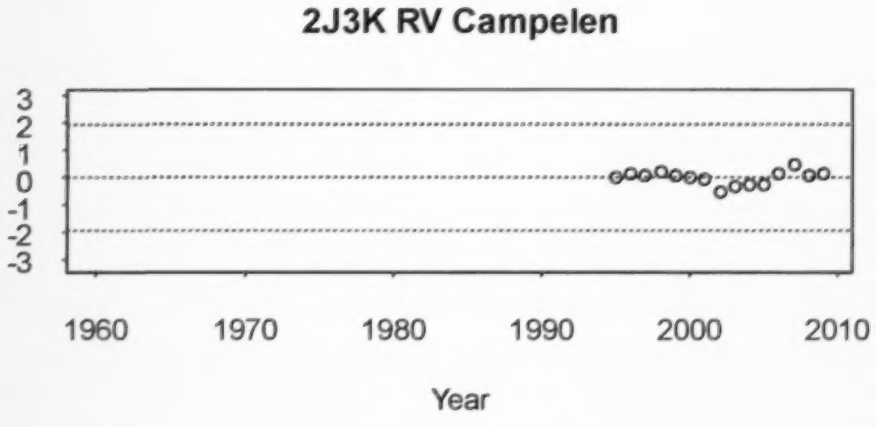

Figure 88a: Canadian Campelen trawl series estimates with 95 % credible intervals (top) and standardized residuals (bottom) for 2J3K American plaice. Figures illustrate fit from model 1.

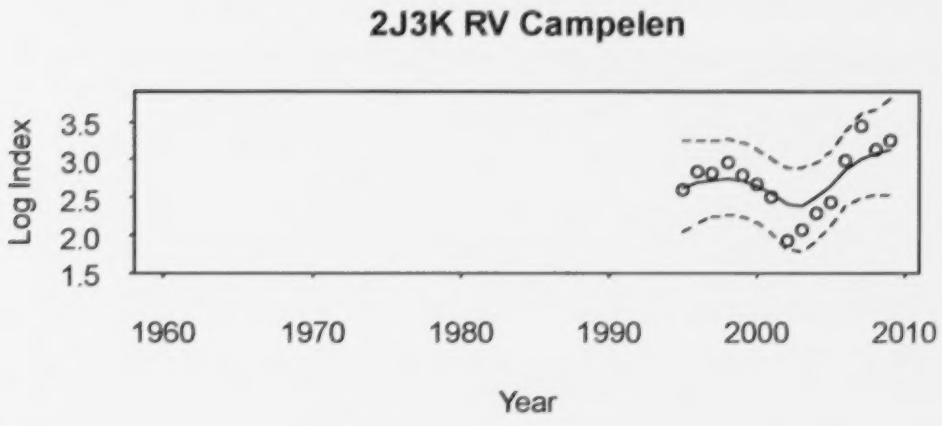

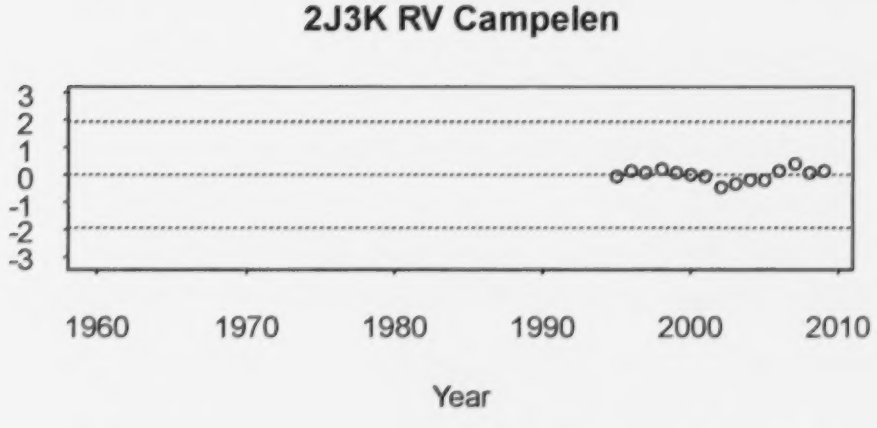

Figure 88b: Canadian Campelen trawl series estimates with 95 % credible intervals (top) and standardized residuals (bottom) for 2J3K American plaice. Figures illustrate fit from model 2.

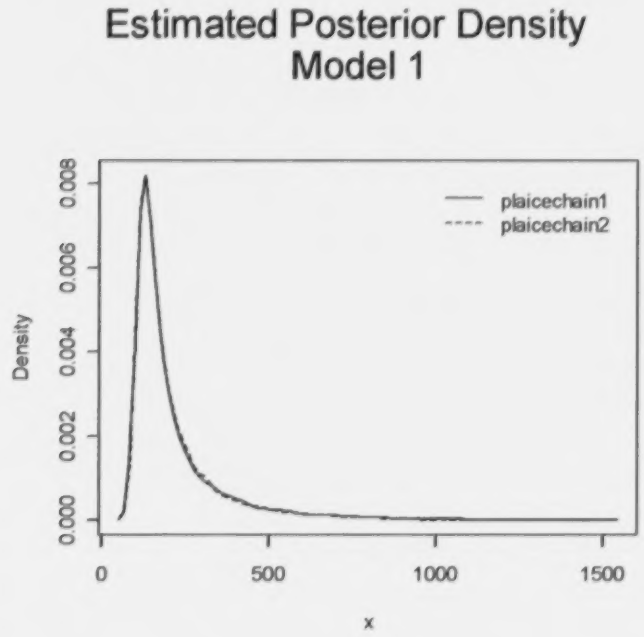

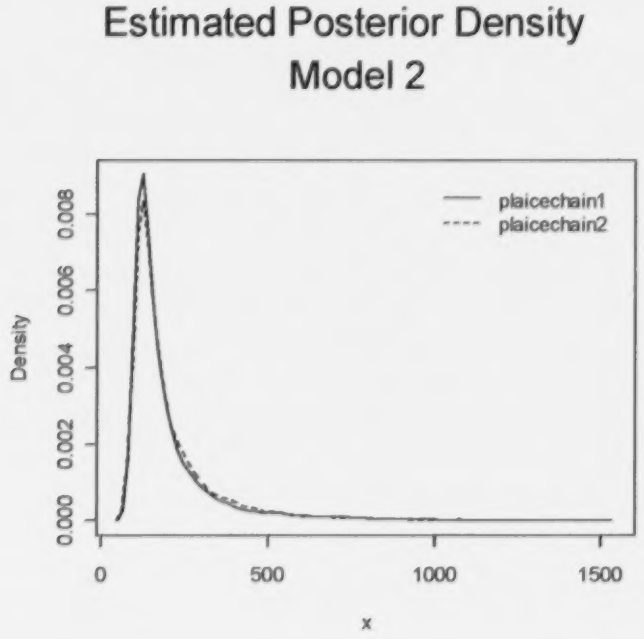

Figure 89: Kernel density estimates of the posterior distribution of K for both chains in models 1 & 2 for 2J3K American plaice.

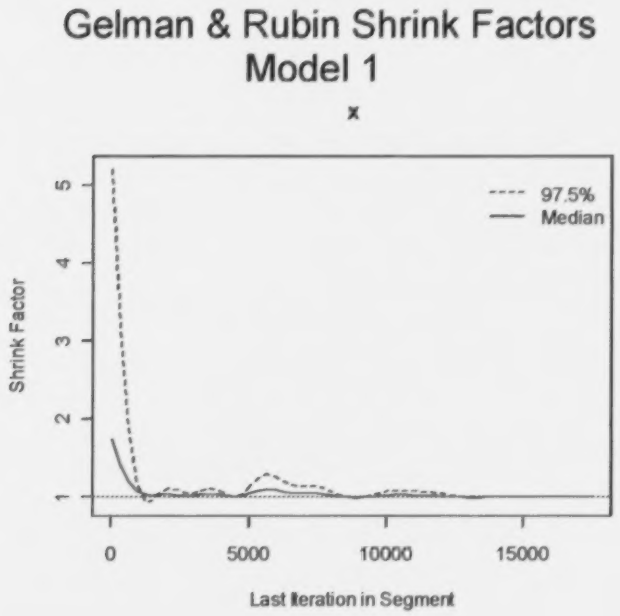

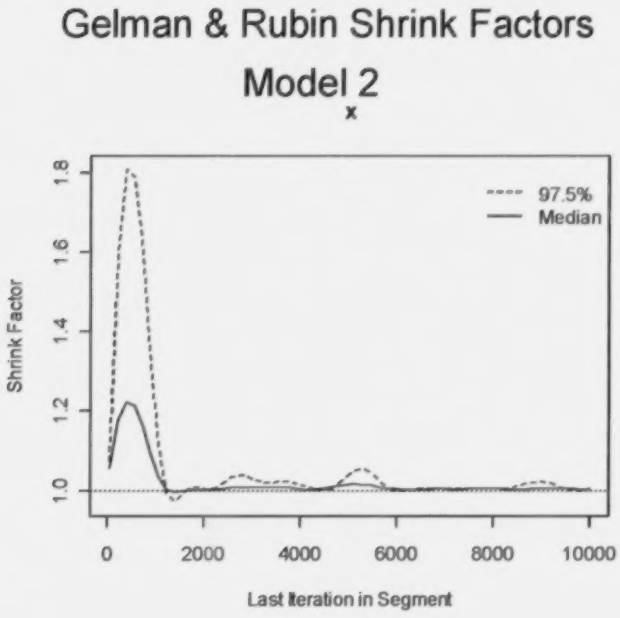

Figure 90: Gelman & Rubin shrink factors for K in models 1 & 2 for 2J3K American plaice. Gelman & Rubin shrink factors examine the reduction in bias in estimation. The shrink factor approaches 1 when the pooled within-chain variance dominates the between-chain variance. At that point, all chains have escaped the influence of their starting points.

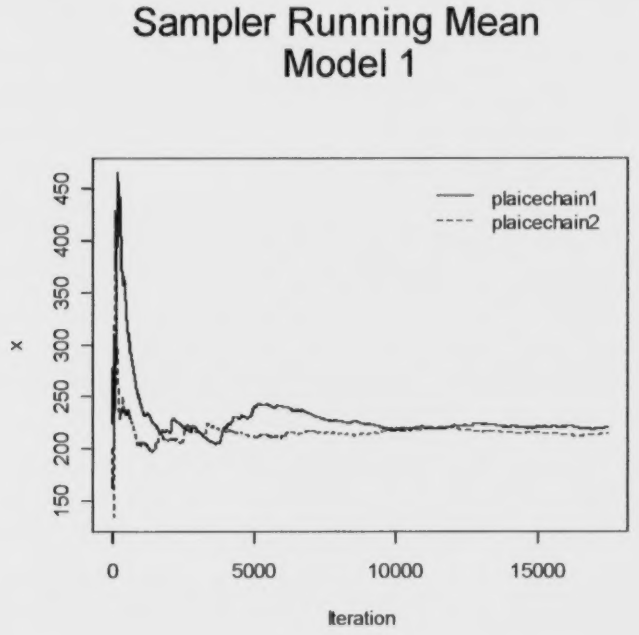

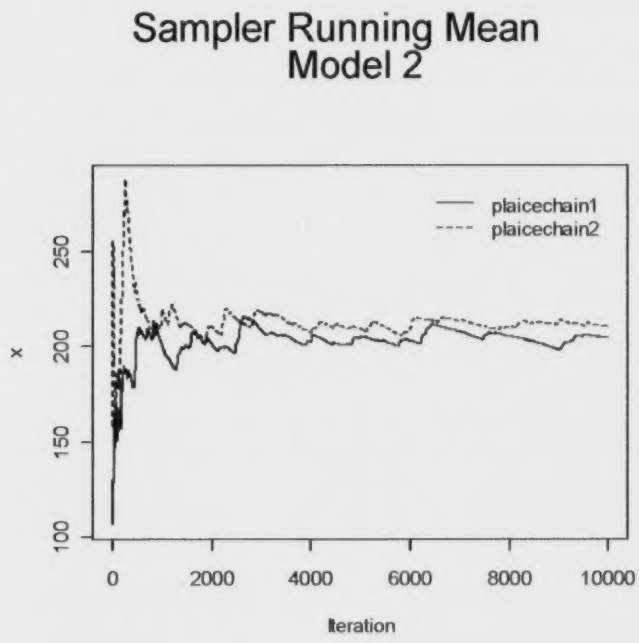

Figure 91: Sampler running mean for both chains of K, carrying capacity, in models 1 & 2 for 2J3K American plaice. Chains are considered to have converged when they overlap.

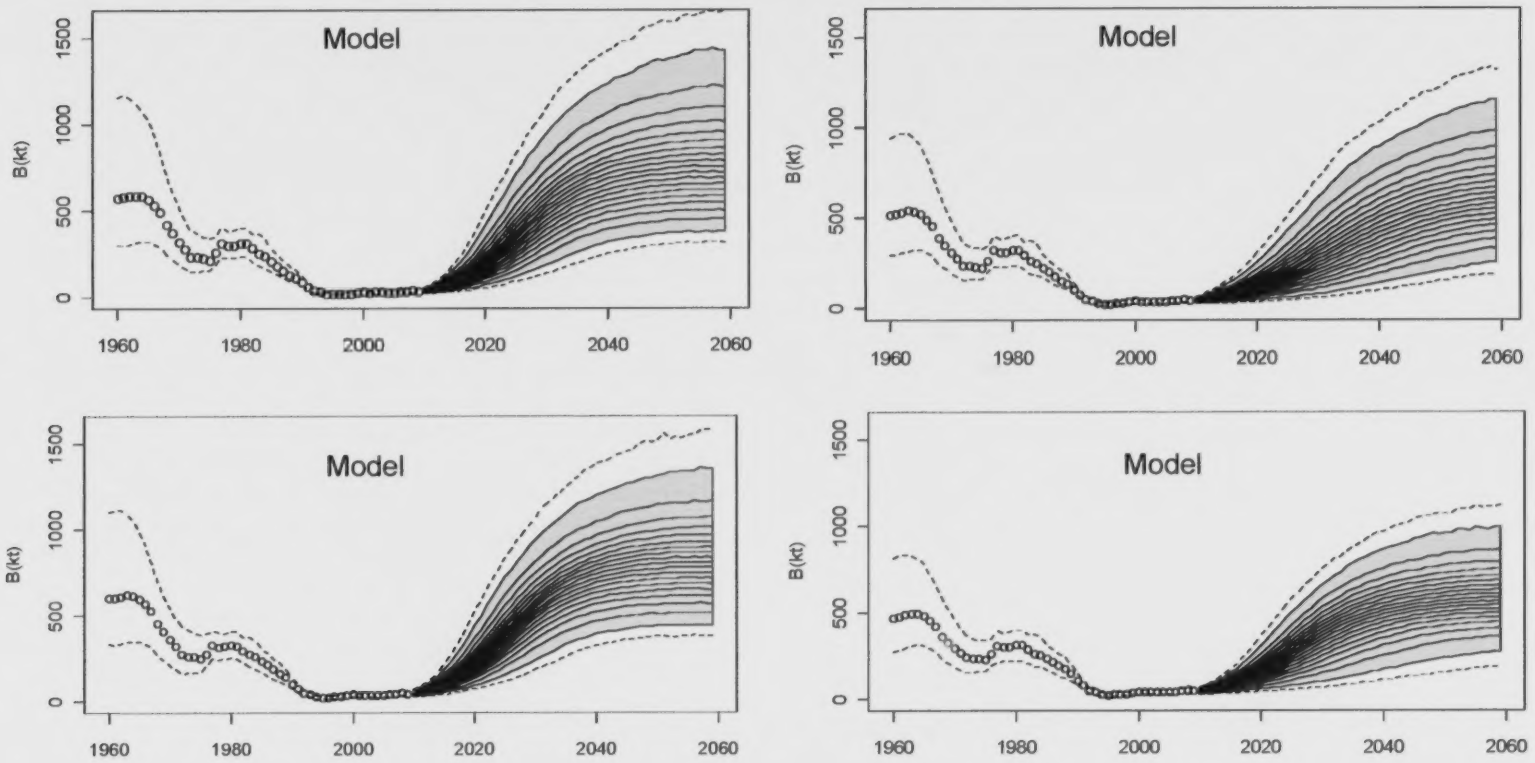

Figure 92: Bayesian surplus-production estimates of historical (1960-2009) and predicted biomass for the next 60 years at F=0.0 in area 3LNO for models 1-4 (see text). Dashed lines encompass the 95 % credible intervals. The lines in the shaded area represent 5 % intervals of the probability distribution for each year and can be read as isolines on a map, with higher line density representing a larger percentage of the distribution.

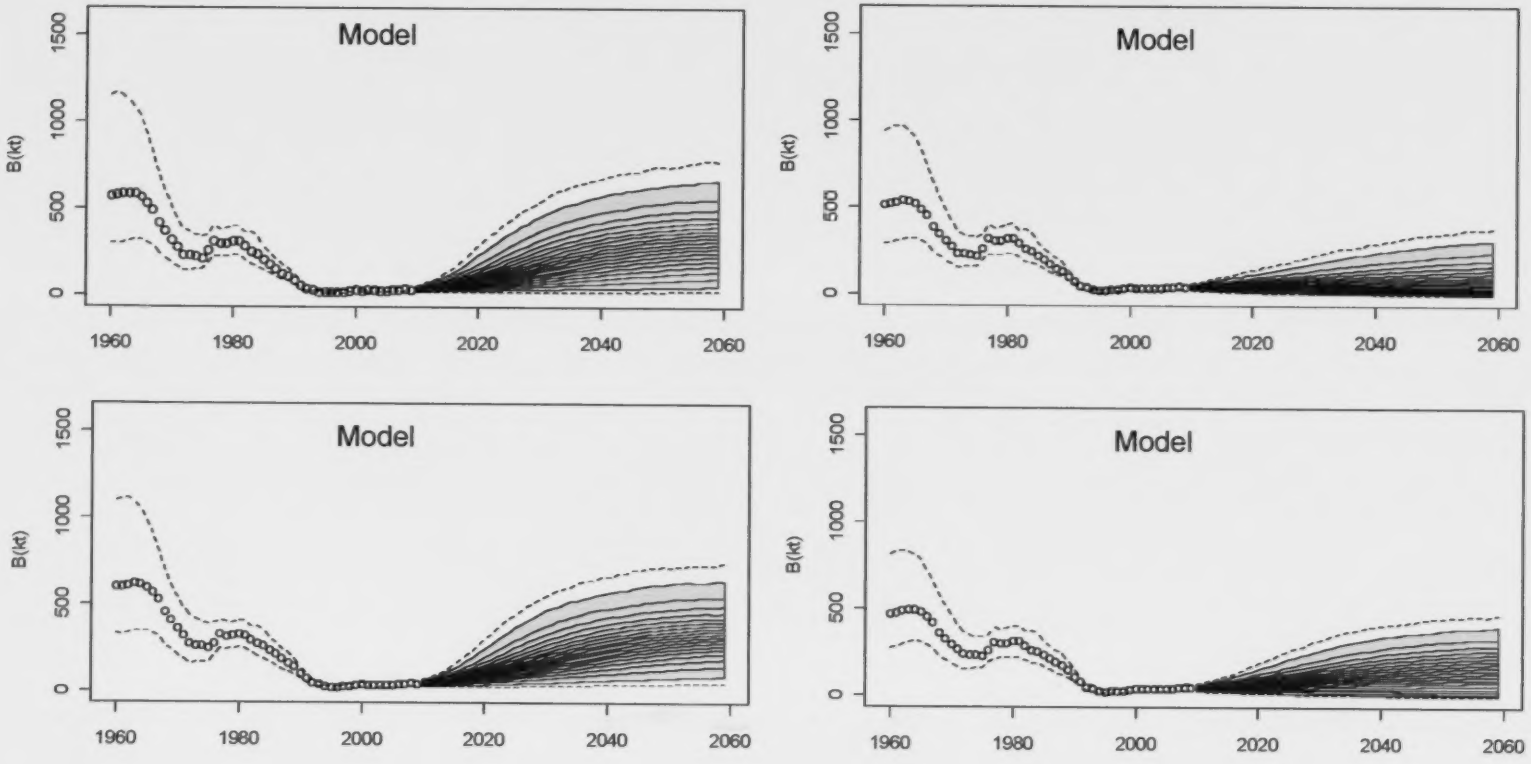

Figure 93: Bayesian surplus-production estimates of historical (1960-2009) and predicted biomass for the next 60 years at F=0.1 in area 3LNO for models 1-4 (see text). Dashed lines encompass the 95 % credible intervals. The lines in the shaded area represent 5 % intervals of the probability distribution for each year and can be read as isolines on a map, with higher line density representing a larger percentage of the distribution.

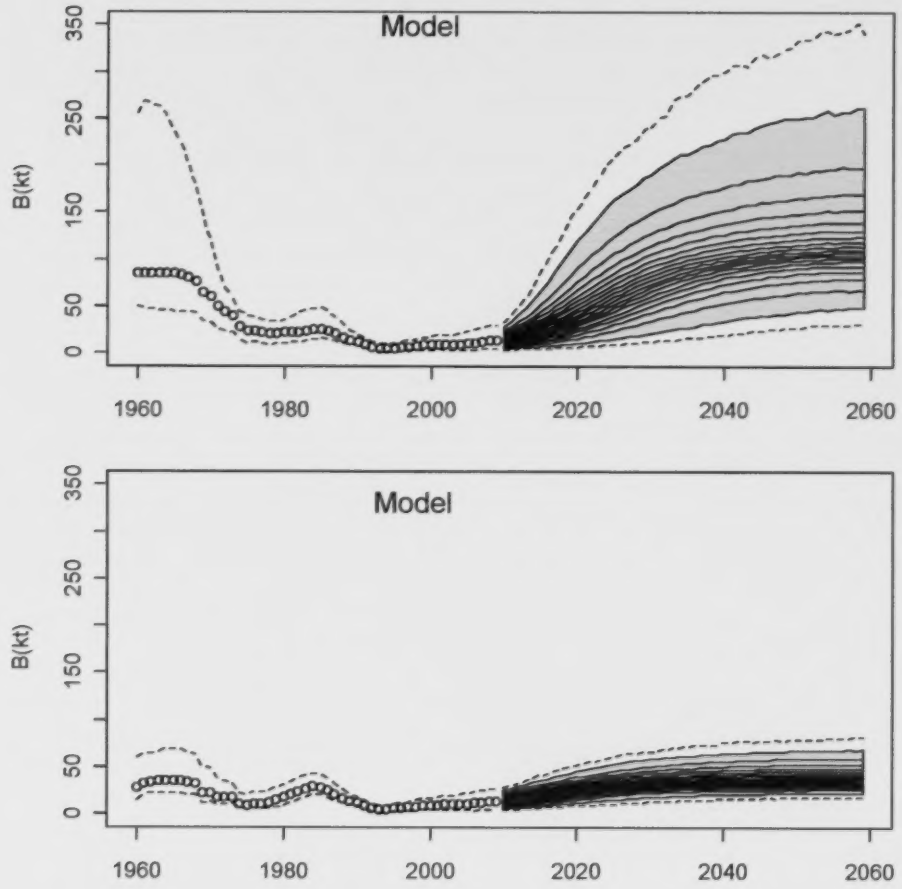

Figure 94: Bayesian surplus-production estimates of historical (1960-2009) and predicted biomass for the next 60 years at F=0.0 in area 3Ps for models 1-2 (see text). Dashed lines encompass the 95 % credible intervals. The lines in the shaded area represent 5 % intervals of the probability distribution for each year and can be read as isolines on a map, with higher line density representing a larger percentage of the distribution.

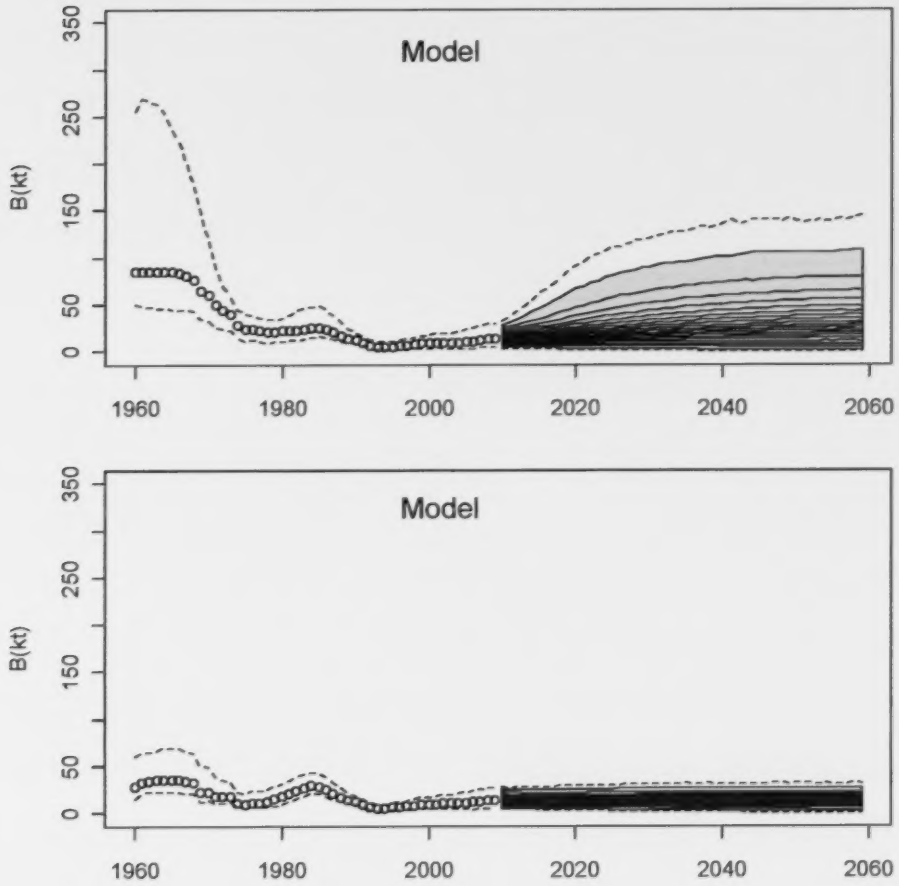

Figure 95: Bayesian surplus-production estimates of historical (1960-2009) and predicted biomass for the next 60 years at F=0.1 in area 3Ps for models 1-2 (see text). Dashed lines encompass the 95 % credible intervals. The lines in the shaded area represent 5 % intervals of the probability distribution for each year and can be read as isolines on a map, with higher line density representing a larger percentage of the distribution.

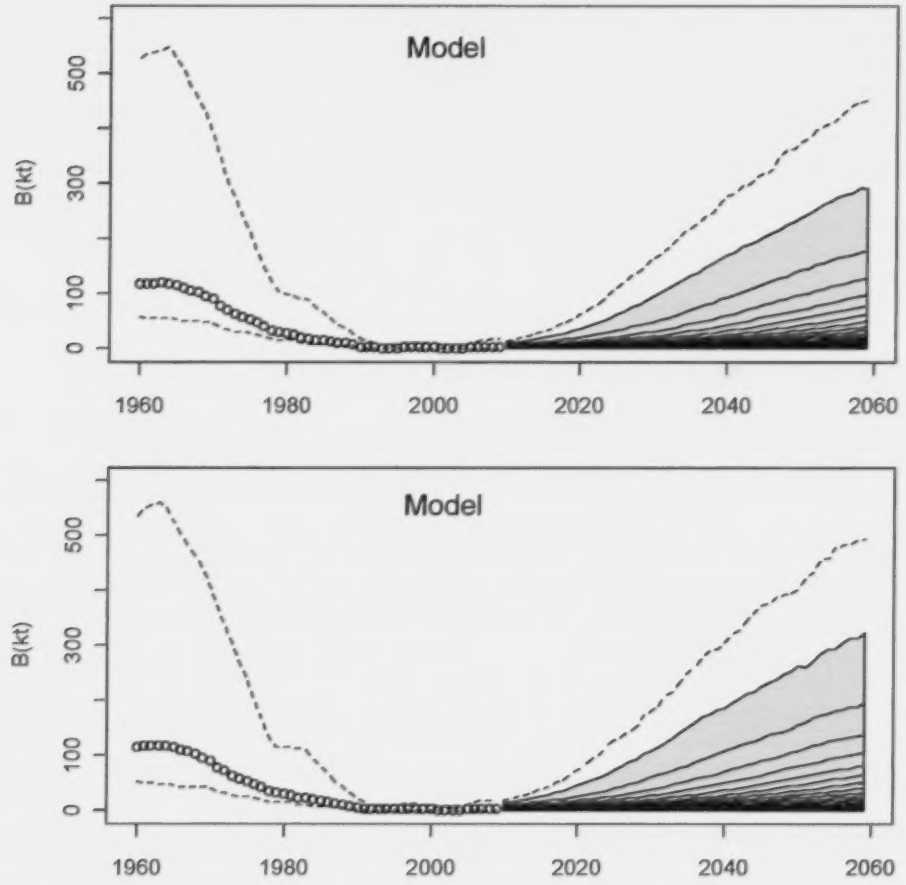

Figure 96: Bayesian surplus-production estimates of historical (1960-2009) and predicted biomass for the next 60 years at F=0.0 in area 2J3K for models 1-2 (see text). Dashed lines encompass the 95 % credible intervals. The lines in the shaded area represent 5 % intervals of the probability distribution for each year and can be read as isolines on a map, with higher line density representing a larger percentage of the distribution.

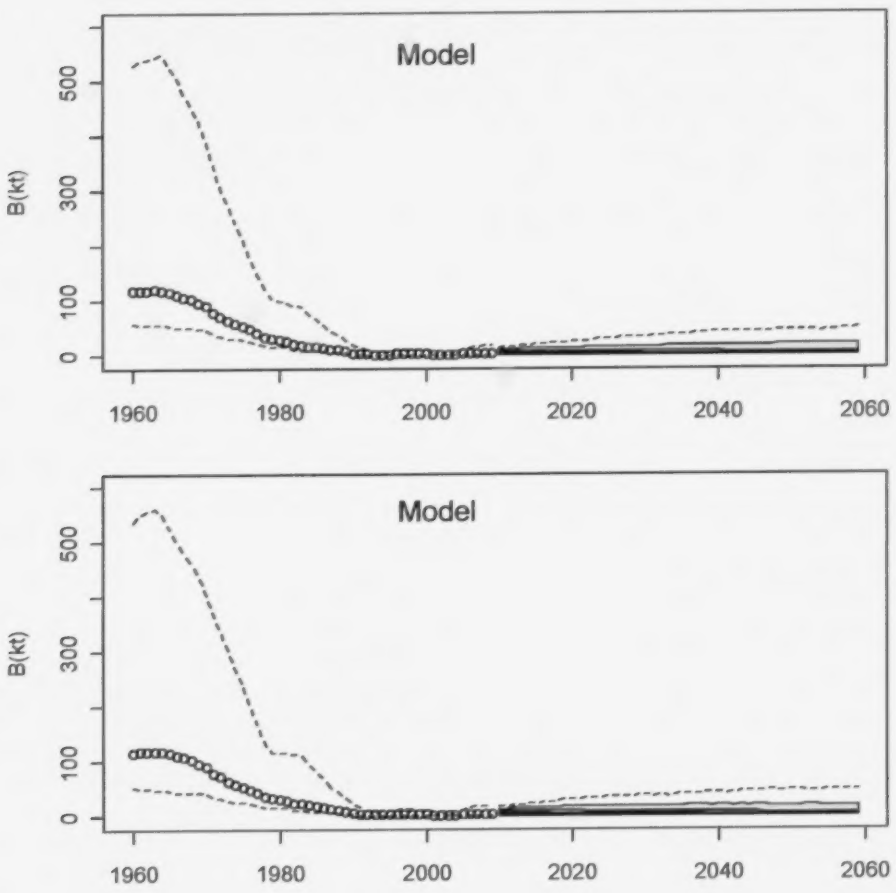

Figure 97: Bayesian surplus-production estimates of historical (1960-2009) and predicted biomass for the next 60 years at F=0.1 in area 2J3K for models 1-2 (see text). Dashed lines encompass the 95 % credible intervals. The lines in the shaded area represent 5 % intervals of the probability distribution for each year and can be read as isolines on a map, with higher line density representing a larger percentage of the distribution.